CHAPTER 4

Plant extract mediated silver nanoparticles: overall toxicity analysis in earthworm-microbes-soil-plant system

4.1. Introduction

Nanotechnology has attained a considerable attention during current time, owing to their versatile application in different aspects of science. Metal nanoparticles are at the top of attraction because of their versatile properties and ease of preparation. Among various engineered nanomaterials, silver nanoparticles have numerous applications [1]. Their antimicrobial and antifungal activity cause them to utilize in various areas such as biomedical [2], food industries [3], and agriculture [4]. It has been estimated that in Europe only, the land surfaces used to receive silver nanomaterials at a rate of about 1581 ng kg^{-1} h^{-1}. The nature of aggregation/dissolution dynamics along with surface charge, dispersibility, and surface area considerably alter soil physico-chemical stability [1,5,6].Widespread use in industrial processes will ultimately cause these nanoparticles to enter into soil environment as a waste generated. This may lead to some influences in soil health then subsequently on plant biota.

There are several reports on positive impacts of nanoparticles (NP) on soil porosity and their interaction with soil organic matter [7,8]. In contrast, few studies reported detrimental effects of NP on soil properties. Silver nanoparticles are reported to alter bacterial community structure in rhizosphere soil thereby greatly pacify soil enzymatic activity and significantly alter carbon use [9]. Moreover, silver nanoparticles suppress soil nitrification rate and greatly affect earthworm health in soil [10,11]. However, reports are available on catalysis of organic pollutants by some nanoparticles in aqueous suspension [12] and thereby deleterious influence on the redox potential of organic matter content present in soil. In contrast, there are reports on beneficial impacts of silver nanoparticles on soil health and crop growth. Despite of such dilemmas in regard to the holistic impacts of silver nanoparticles on soil-plant system limited studies have been done till recent time to recognize the impacts of nanomaterials on soil-plant systems.

Soil is a critical media because the physicochemical characteristics (pH, organic matter, ionic strength, porosity, and moisture contents) of soils greatly alter the behaviour of NPs within soil system and vice-versa [13]. As such, the interaction between the soil environments and silver nanoparticles can transform their chemistry (Agglomeration, dispersion, surface area, charge, surface chemistry etc.) and which may have influence on the stability and transport of silver nanoparticles within soil systems. Plants can also interact with silver nanoparticles and control their transport through biomass accumulation [14]. Although, soil has been a significant pathway in release of silver nanoparticle, realistic on-field research has not been conducted adequately. Rather, more emphasis has been given by the researchers to understand the behaviour of silver nanoparticles in aquatic systems [15-17].

The behaviour of silver nanoparticles in soil-plant systems greatly vary based on soil porosity, water retention capacity, soil chemistry. However, size of the nanoparticles, nature of coating materials and time and level of exposure also play a significant role in behaviour and effects of silver nanoparticles. In general, the responses of plants to silver nanoparticle exposure greatly differ depending on growing media and amount of exposure [1,18,19]. Many workers exhibited significantly greater silver nanoparticle induced toxicity in plants grown in soilless (agar, hydroponic, sand matrix, Hoagland's solution) media as compared to that were grown in soil [18,20,21].

Earthworms are the crucial model to understand soil health and are largely used for environmental toxicology assessment. Significant detrimental effects of silver nanoparticle were observed on earthworm survival, development, and fecundity [22-24]. However, assessment of growth and fecundity of earthworms can't explain properly the internal mechanisms of the body related to stress adjustment.

The prime hypothesis of this study was carried to understand the impacts of silver nanoparticles on soil properties, plant growth metabolism and on earthworm health. As mentioned earlier, very few studies had been conducted till now to identify the efficacy of green silver nanoparticles on microbes-soil-plant system at the same time. And reports on large scale experimentation on food crops are also very scarce. Thereby, to overcome these kinds of research gaps, here silver nanoparticles were synthesized [5,25] and initially applied on soil and grew a short duration winter

vegetables (French bean) to understand short term responses of the nanoparticles. To correlate these effects on soil plant system some indicative short scale experimentations were conducted (metabolic activities, gene expression, and relationship with N-mineralization etc). Afterwards to justify the long term exposure a 72 weeks long soil experiment was conducted. Also the various available reports on toxicity of silver nanoparticles on earthworm model encouraged this researcher to conduct some experimentation with an earthworm species *E. fetida* to identify the toxicity on the specimen model. Our prime aim was to understand the real impacts of AgNPs and is missing in most of the reports on plant growth.

4.2. Materials and methods

4.2.1. Preparation and properties of silver nanomaterials

T. occidentalis leaves were used to prepare the GSNPs following our recently reported protocol [25]. Briefly, *T. occidentalis* leaves (0.2 g) were stirred in 50 mL of distilled water at 50 °C for 2 h. The extract was filtered and added (3 mL) to a 100 mL 0.01 M solution of $AgNO_3$ stabilized by 5 % PEG (w/v). Here, the *Thuja* leaf extract was used to reduce Ag^+ of $AgNO_3$ into Ag^0; while PEG was used to provide steric stabilization of the nanomaterial through electrostatic interaction [25]. Whereas, *Thuja* leaf extract was replaced by $NaBH_4$ as the reducing agent for preparation of the conventional silver nanoparticles (CSNP). The whole process was carried out in neutral condition (pH 7). The formation of silver nanoparticles could be identified by gradual change in colour from black to dark brown irrespective of the synthetic routes and the general properties of both CSNP and GSNP was similar. According to the analytical evidences, silver was present in zero valent form (Ag^0). The sizes of the synthesized materials were recorded between 7 and 14 nm with an average hydrodynamic diameter of 9.8 ± 0.15 nm. The silver concentration in the liquid phase was determined as 2.16 mg mL^{-1} and confirmed through Atomic Absorption Spectrophotometry in both GSNP and CSNP. Stock solutions of both the nanoparticles were serially diluted to obtain desired concentrations for the experimental purpose: 10, 20, 25, 50, and 100 mg kg^{-1}. The concentrations were primarily chosen after preliminary testing and eventually reviewing contemporary and relevant research papers.

4.2.2. Fates of silver nanoparticles in soil-plant environment

4.2.2.1. Preliminary study: silver nanoparticles-soil plant interaction

Dark colored and clay-loam textured soil samples (Typic Endoaquepts) were collected from typical alluvial soil of Sonitpur (Assam, North eastern part of India; 26.7008°N, 92.8303° E). The area is in sub tropical climate with reasonably hot summer and winter spells. The soil samples were obtained from an area with less human interference. Collected soils were air dried, sieved through a 80 mm mesh followed by a 2 mm mesh, and then used for the study. The grain size of the soil is less than 0.002 mm (clay size fraction). CSNP and GSNP solutions of various concentrations were mixed with soil samples in earthen pots of 0.45 m height and 0.25 m diameter (2 L volume); the amount of solution added to each sample was 10% by volume (200 mL). Inherently, the N and P levels in the soil was 314.6 ± 2.2 mg kg^{-1} and 29.6 ± 1.1 mg kg^{-1} respectively; the soil had a pH of 6.5 ± 0.6, bulk density (BD) 1.26 ± 0.2 g cm^{-3}, and water holding capacity (WHC) 52.5 ± 2%; cation exchange capacity and soil organic carbon in the soil was recorded as 4.49 ± 0.22 mmol kg^{-1} and 2.1 ± 0.6% respectively.

Subsequently, seeds of *P. vulgaris* were sown in each vessel, then replicated thrice and cultivated following prescribed management practices [26]. We did not apply any chemical fertilizers to the experimental soil in order to avoid their interactions with silver nanoparticles. However, fresh cow dung was collected and tanned for seven days and used for experimental purpose. The basic properties of the cow dung were: pH - 7.1 ; density – 0.64 g cc^{-1}; TOC – 2.92 %; Mineralizable N – 73 mg kg^{-1}; Available P – 30.56 mg kg^{-1}; Available K- 116 mg kg^{-1}).

Another pot culture study was conducted following randomized block design method by considering tomato (*Lycopersicon esculentum* c.v. Badshah F1 hybrid) as the test crop to assess the effects of GSNP (or AgNP) on plant growth and development. Here, the AgNP was applied only @ 10 mg kg^{-1} because this concentration was least harmful for soil, microbes, and earthworm compared to other concentrations (25 and 50 mg kg^{-1}). Soil samples were collected from the same location used for the previous experiment and uniformly placed in burnt earthen pots of 3 L capacity. Subsequently, nursery grown tomato seedlings were transplanted to such experimental pots.

4.2.2.1.1. Assessment of physico-chemical changes in soil

Samples of control and treated soils (GSNP20, GSNP25, GSNP50, and GSNP100) were collected at harvest maturity, namely after 60 days of cropping. The soil samples were then air-dried, ground in an agate mortar, and sieved (<200 mesh) for physicochemical analysis. The ground soil samples were packed in circular sample holders and subjected to X-ray diffraction analysis (XRD; Rigaku Miniflex) under intense Cu Kα radiation (λ= 1.54 Å) over the range of 10–70° 2θ. The surface morphology and elemental composition of each of the control and treated soil samples (GSNP 25, 50, and 100 mg kg^{-1}) were examined by scanning electron microscopy (SEM; JSM-6390 LV SEM, JEOL) paired with energy dispersive X-ray spectrometry (EDX). Moreover, the BD and WHC of each soil sample were analyzed [27].

The effects of each treatment on soil pH, soil organic C (SOC), easily mineralizable nitrogen, available phosphorus, and CEC were analyzed according to well established methods [27,28]. Urease activity was analyzed in the soil according to the method of Tabatabai and Bremner [29].

Samples from the cropped soil under tomato cultivation were drawn after harvest and analyzed for pH, easily mineralizable-N, available-P, available-K, and soil respiration [27,28]. Moreover, urease and phosphatase activity was also enumerated [29,30].

4.2.2.1.1.1. Bulk density (BD)

Requisites:

1. Apparatus: Metallic core sampler of known volume (around 50 mL)
2. Glassware: 100 mL bottle

Procedure:

1. Core soil sampler was taken and weighed initially (W1).
2. Inserted into the soil surface and taken back.
3. The soil sample inside the sampler was oven dried inside a hot air oven at 105^0C till a constant weight was obtained.
4. Oven dry weight of the sample was taken along with the core sampler (W2 g)

Calculation:

$$\text{Bulk density of soil (g/cc)} = \frac{\text{W2} - \text{W1}}{\text{V}}$$

Where, W1= weight of empty bottle, W2= weight of the bottle with soil,
V = volume of water required to fill the bottle.

4.2.2.1.1.2. Water holding capacity (WHC)

Requisites:

1. Apparatus: circular perforated metallic boxes (keen's box)
2. Petri dish
3. Filter paper

Procedure:

1. Initially the filter paper was cut to the size of the box area of the keen's box and placed to the bottom of the box.
2. Then, weight the box along with filter paper was taken (W_1).
3. Experimental Soil samples were added in small installment with continuous tapping so that it occupies the volume of the box uniformly.
4. Then, the box was kept on a petri dish and filled partially with water so that 1/3 rd of the weight of the box was dipped inside water.
5. Afterwards, it was kept overnight.
6. In the next morning the boxes were taken out of water, the outer surface was wiped with tissue paper and weighed again (W_2).
7. Then, the boxes along with the samples were placed inside a hot air oven (105^oC) for drying till a constant weight was achieved (W_3).
8. After that filter papers of same quantity were cut to the size of the base of the box, soaked in water and weighed again. The taken weight was the average to detect the moist weight of a single filter paper (W_4).

Calculation:

$$\text{Water holding capacity of the soil} = \frac{W_3 - W_2 - W_4}{W_2 - W_1} \times 100\,\%$$

Where,

W_1= weight of the box +filter paper,

W_2=weight of the box+ filter paper+ dry sample,

W_3=weight of the box+ filter paper+ moist paper,

W_4=water absorbed by a single filter paper,

Then, weight of dry soil→ (W_2-W_1) g,

Weight of water absorbed by the soil = (W_3-W_2-W_4) g

4.2.2.1.1.3. pH

Requirements:

1. pH meter
2. Beaker
3. Measuring cylinder
4. Tissue Paper
5. Sample
6. Glass rod
7. Balance

Reagents:

1. De-ionized water
2. pH 7.0 buffer solution
3. pH 4.0 buffer solution

Procedure:

1. About 10 g air-dry soil was weighed (< 2 mm) in an Erlenmeyer flask.
2. 25 mL de-ionized water was added to it using a graduated cylinder or 50 mL volumetric flask to prepare a 1: 2.5 soil suspension.
3. Then mixing was done properly with a glass rod, and allowed to stand about 1 hour.
4. EuTech pH meter (pH 700) was calibrated beforehand and recorded the pH value.

4.2.2.1.1.4. Available Nitrogen

Reagents:

1. 0.32% $KMnO_4$: 3.2 g of $KMnO_4$ was dissolved in distilled water and the volume was made up to 1 L.
2. 2.5 % NaOH: 25 g of NaOH pellets was dissolved in distilled water and made the volume up to 1 L.
3. 0.8 % NaOH: 0.8 g of NaOH pellets was dissolved in 1 L of distilled water.
4. N/50 N H_2SO_4: 550 µL of H_2SO_4 was dissolved in 1 L of distilled water.
5. Methyl red indicator: 0.3 g of bromocresol green and 0.2 g of methyl red was dissolved in 400 mL of 90% ethanol. In case of acidic solution the indicator colour will appear red, however in alkaline or base conditions it will show blue colour.

Procedure:

1. 1 g soil sample was weighed and taken into the Kjeltec distillation tube.
2. Then, 40 mL 0.32% $KMnO_4$, 40 mL 2.5% NaOH, and 20 mL distilled water was added to it with the help of measuring cylinder.
3. After addition of the reagents the distillation tube was fitted properly in Kjeltec^{TM}8100 distillation unit.
4. 20 mL of N/50 N H_2SO_4 was poured into 250 mL Erlenmeyer flasks along with a few drops of methyl red indicator.
5. Then the flask was fitted to the ammonia exhaust pipe and the distillation was started. Almost 100 mL of distillate was collected in 5 minutes of run time of distillation.
6. After distillation the collected ammonia solution was titrated manually with 0.8 % NaOH to original straw yellow colour.
7. Analysis of a blank sample (without soil) was carried out simultaneously following the same procedure.

Calculation:

$$\text{Available N (mg kg}^{-1}) = \frac{(V_b - V_s) \times 0.28 \times 1000}{W}$$

Where,

W = Weight of the sample taken,

V_b = Volume of N/50 NaOH solution consumed in the titration in the blank,

V_s = Volume of N/50 NaOH solution consumed in the titration in the sample.

Weight of soil= 'W' g

Volume of N/50 H_2SO_4 taken = 'a' mL

Volume of N/50 NaOH used= 'b' mL

Volume of N/50 H_2SO_4 used for NH_3 = (a-b)

1 ml of N/50 H_2SO_4=0.00028 g N

Available N (percent)={(a-b) ×0.00028×100}/W

Available N (ppm or mg kg^{-1})= {(a-b) ×0.00028×100×10000}/W

={(a-b) ×0.28×1000}/W

4.2.2.1.1.5. Available Phosphorous

Reagents and standard curve:

1. 0.03 N NH_4F solution: 1.11g of NH_4F was dissolved in distilled water and made the volume up to 1000 mL.
2. 1.5% ammonium molybdate solution: 15g ammonium molybdate $[(NH_4)_6Mo_7O.4H_2O]$ was dissolved in 301 mL concentrated HCl and the volume was made upto 1L with double distilled water in volumetric flask.
3. 5% stannous chloride solution ($SnCl_2$): 2.5g of stannous chloride ($SnCl_2.2H_2O$) was dissolved in 5mL conc. HCl and warm distilled water was added to it slowly to make the volume upto 50 mL.
4. 4N NH_4OH: 27 mL ammonia hydroxide (NH_4OH) solution was added in distilled water and volume was made up to 1000 mL.

5. 4N HCl: 34.5 mL conc. HCl was dissolved in distilled water and made the volume up to 100 mL.
6. 2, 4-Dinitrophenol indicator: A known amount of 2, 4-dinitrophenol was dissolved in distilled water and the volume was made upto 250 mL and filtered with Whatmann no. 42 filter paper and the filtrate was used.
7. Phosphorus free charcoal.
8. Standard P solution: 50 ppm stock solution of P was prepared by dissolving 0.2196 g of potassium orthophosphate (KH_2PO_4) in 400 mL distilled water. Then, 25 mL of 7N H_2SO_4 was added to the solution and volume made up to 1 L. 2 ppm standard P solution was made by taking 20 mL from this stock solution and diluted to 500 mL with distilled water.
9. Preparation of standard curve: Eight different standard solutions were prepared from 2 ppm standard solution by taking 1, 2.5, 5.0, 7.5, 10.0, 12.5, 15.0, and 20.0 mL with glass pipette to individual 50 mL of volumetric flasks. Then, 2-3 drops of 2, 4-dinitrophenol was added to each flask followed by drop wise addition of 4N NH_4OH till appearance of yellow colour. After that, 4N HCl solution was added to each flask until yellow colour disappears and thus pH of each solution was adjusted to 3.Then, 10 mL of $(NH_4)_6MO_7O.4H_2O$ solution followed by 2-3 drops of $SnCl_2$ was added to each flask and volume was made up to the mark. Reading of absorbance was taken in Agilent UV-VIS Spectrophotometer at 660 nm. Then, a standard curve was drawn by plotting the values of the optical density (O.D) of each solution against the standard concentration.

Procedure:

1. 2.5 g of soil sample was weighed and taken in 250 mL Erlenmeyer flask and 25 mL of 0.03 N NH_4F in 0.025 N HCl solution and 1 g of P-free charcoal was added to it.
2. In case of soil sample with higher amount organic matter 1-2 g of charcoal was added, whereas, soil samples with low organic matter addition of charcoal wasn't required. Soils having 1.2% or more oxidizable organic carbon showed a faint yellow colour that disappeared on addition of charcoal.
3. Then the flasks were shaken for 5-10 minutes in a mechanical shaker.
4. After that, the solution was filtered with Whatmann (no. 42) filter paper.

5. From the filtrate 5mL was taken in a 50 mL volumetric flask and mixed well with 2 to 3 drop of 2, 4- dinitophenol, 4N NH_4OH, and 4 N HCl solutions.
6. Afterward, 5 mL of ammonium molybdate followed by 2-3 drops of (5 %) Stannous chloride solution was added to each flask and volume made up to 50 mL with distilled water.
7. Mixing was done properly and absorbance was read at 660 nm in an UV-VIS Spectrophotometer.

Calculation:

$$\text{Available P (mg kg}^{-1}) = \text{P concentration} \times \text{dilution factor}$$

Weight of sample taken=W g

Volume of 0.03 N NH_4F solution taken=25 mL

Taken aliquot of extract=5 mL

Final volume of extract=25 mL (after development of colour)

Reading of spectrophotometer for soil sample=X

Reading of spectrophotometer for blank sample=Y

ppm data for X obtained from graph=A

ppm data for Y obtained from graph=B

$$\text{Available P (mg kg}^{-1}) = (A-B) \times 100 \text{ (dilution factor)}$$

Dilution factor=

$$\frac{\text{Volume of extractant taken}}{\text{Weight of sample}} \times \frac{\text{Final volume of extact}}{\text{Volume of extract taken}}$$

4.2.2.1.1.6. Available K

Reagents and standard curve:

1. Ammonium acetate (1N, pH 7): 77.08 g ammonium acetate was dissolved in 1L of distilled water and mixed properly. Then, the pH was adjusted to 7 with either diluted NH_4OH or HOAc as required.

2. Potassium chloride stock solution: A 1000 ppm of K standard solution was prepared by dissolving 1.908 g of AR grade potassium chloride in distilled water and volume made up to 1L. From this 1000 ppm solution a 100 ppm standard solution was prepared.
3. Standard Curve: 5, 10, 15, and 20 ppm K standard solutions were prepared by diluting the 100 ppm stock solution. Calibration of the instrument was done carefully for every time prior to injection of sample.

Procedure:

1. 2g of soil sample was taken in a 250 mL Erlenmeyer flask.
2. 20 mL of 1N CH_3COONH_4 solution was added to it.
3. Then the flasks were placed upon a mechanical shaker and shaken for 30 minutes.
4. After shaking filtration was done with Whatmann no 42 filter paper and the filtrate was taken and K content was measured by flame photometer.

Calculation:

$$\text{Available K (mg kg}^{-1}) = \text{K concentration} \times \text{dilution factor}$$

Weight of sample taken = 'A' g

Volume of extractant = 'B' mL

Dilution factor = (B/A)

Reading of flame photometer = X

ppm K obtained from standard curve corresponding to X= R

Available K (ppm or mg kg^{-1}) = R× (B/A)

4.2.2.1.1.7. Soil organic carbon (SOC)

Reagents:

1. 1N Potassium dichromate solution ($K_2Cr_2O_7$): 49.04 g of Potassium dichromate was weighed accurately and the volume was made upto 1L with distilled water.

2. 0.5N Ferrous ammonium sulphate solution {$FeSO_4(NH_4)_2SO_4.6H_2O$}: Weighed accurately 196.1 g of Ferrous iron and dissolved in 1L of distilled water followed by 20 mL of conc. H_2SO_4.
3. Diphenylamine indicator: 0.5 g of diphenylamine indicator was dissolved in 20 mL of distilled water by the addition of 100 mL of conc. H_2SO_4.
4. 85% Orthophosphoric acid (H_3PO_4)
5. Conc. Sulphuric acid (H_2SO_4).

Procedure:

1. 1.0 g of soil sample was weighed accurately in 500 mL conical flask.
2. Then, 10 mL of $K_2Cr_2O_7$ solution and 20 mL concentrated H_2SO_4 was added in to it and heated until a few bubble comes.
3. After that, kept it for some time for cooling, followed by dilution of the reaction mixture with distilled water.
4. Then, 10 mL of orthophosphoric acid and 1.5 mL of diphenylamine indicator was added to it.
5. Finally, the solution was titrated with standard 0.5 M Ferrous ammonium sulphate solution to a brilliant green colour.
6. A blank without sample was run simultaneously.

Calculation:

$$\text{Soi organic carbon (\%)} = \frac{\text{Vk}(1 - \frac{\text{Vs}}{\text{Vb}})}{\text{W}} \times \text{Sk} \times 0.3$$

Where,

V_k: Volume of $K_2Cr_2O_7$ solution, V_s: Titrant reading, V_b: Blank reading,

S_k: Strength of $K_2Cr_2O_7$ solution, W: Weight of soil sample,

$0.3 = 3 \times 10^{-3} \times 100$, where 3 is the equivalent weight of C.

4.2.2.1.1.8. Urease activity

Reagents:

1. 40 mM urea: 0.24 g urea was dissolved in 100 mL sodium acetate buffer (pH= 5)
2. 0.3 M NaOH: 12 g NaOH was dissolved in 1000 mL distilled water.
3. Na salicylate solution: 17 g Na salicylate and 120 mg sodium nitroprosside was dissolved in 100 mL distilled water.
4. Mixed solution (freshly prepared): One part 0.3 M NaOH, one part Na salicylate solution, and one part distilled water.
5. Na dichloroisocyanurate solution (freshly prepared): 0.1 g Na dichloroisocyanurate was dissolved in 100 mL of distilled water.
6. Sodium acetate buffer: 54.43 g sodium acetate and 12 mL glacial acetic acid was dissolved in 1988 mL of distilled water and the pH was adjusted to 5 with 10N NaOH.

Procedure:

1. 2g soil sample was blended with 60 mL 50 mM acetate buffer and shaken vigorously.
2. Then, 750 µL suspension and 750 µL of urea solution was taken into a 2 mL centrifuge tube and incubated at room temperature for 2 h.
3. After incubation centrifugation was done @ 10,000 rpm for 1 min.

Ammonium determination*:*

1. 0.5 mL supernatant was pipette into 10 mL culture tubes.
2. Then, 2.5 mL NaOH /Na salicylate solution and 1 mL Na iso cyanurate solution was added.
3. A blank was prepared with acetate buffer instead of supernatant.
4. Optical density (OD) reading was measured @ 690 nm in an Agilent UV-VIS Spectrophotometer.

$$\text{Urease activity } (\mu g\ /g\ /h) = \frac{\text{OD sample} - \text{OD blank}}{\text{Slope} \times t \times \text{weight of sample}}$$

4.2.2.1.1.9. Phosphatase activity

Reagents:

1. Buffer solution (pH 10): This buffer solution was prepared by dissolving 68.045 g of KH_2PO_4 in 500 mL distilled water.
2. 0.5 M $CaCl_2$. $2H_2O$ solution: 18.375 g of $CaCl_2.2H_2O$ was dissolved in 250 mL distilled water.
3. p-nitrophenol phosphate test solution (PNPP solution): PNPP solution was prepared by dissolving 13.91 g of p-nitrophenol in 100 mL phosphate buffer solution.
4. Standard p-nitrophenol solution: 0.1 g p-nitrophenol was dissolved in 100 mL distilled water and stored at 4^0 C.

Calibration curve:

1. 1 mL of standard p-nitrophenol solution was diluted to 100 mL in a volumetric flask. Then, pipette out 0, 1, 2, 3, 4, and 5 mL aliquot of this standard solution in Erlenmeyer flasks (50 mL).
2. Adjusted the volume to 5 mL by addition of distilled water.
3. Then, 5 mL of 0.5 M $CaCl_2$ solution followed by 1 mL of PNPP solution were added into each flask.
4. Mixing was done properly, followed by filtration. After that shaking was done vigorously on a mechanical shaker. Finally, absorbance was measured at 400 nm in an Agilent UV-VIS Spectrophotometer (see Annexure).

Procedure:

1. 2 g of soil sample was taken in a test tube.
2. 5 mL of 0.5 M $CaCl_2$ solution was added and shaken well.
3. A blank was also prepared in absence of soil.
4. 1 mL of PNPP solution was added into each sample tubes and blank.
5. All the tubes were incubated at 37^0C for 1 h.
6. Then, 4 mL of supernatant was taken from each test tube and centrifuged for 5 minutes.

7. After centrifugation 3 mL of clear supernatant was transferred to clean test tubes (recentrifuge if liquid is at all cloudy) and absorbance measured at 440 nm.
8. Enzyme activity was calculated from the calibration curve of known concentration (see Annexure).

Calculation:

$$\text{Phosphatase activity } (\mu g\ /g\ /h) = \frac{(\text{OD sample} - \text{OD blank})}{(\text{slope} \times T \times W)}$$

Where, OD=optical density, T=time for incubation, W=Weight of sample

A calibration curve is generally used to predict an unknown sample's concentration. If a calibration curve is linear then it will fit with the basic equation y=mx+c, where m denotes the slope or gradient. Slope (m) value can be positive, negative and zero. If slope value is positive then the line will gradient upwards, from left to right. If it is negative then the line will slope downwards from left to right. If it is zero then the line will be horizontal.

4.2.2.1.1.10. Soil respiration

Reagents:

1. NaOH (0.1N): 4 g of NaOH was dissolved in 1L of distilled water.
2. HCl (0.05N): At first, 1N HCl was prepared by taking 50 mL of HCl from the stock solution and volume made up to 1L.
3. $BaCl_2$ (0.5M): 122.14 g of $BaCl_2$ was weighed accurately and dissolved in 1L of distilled water.
4. Phenolphthalein indicator: 0.1g of phenolphthalein was diluted to 80 mL of ethanol and the volume was made up to 100 mL.

Procedure:

1. 10 g of moist soil sample was taken into 500 mL conical flask.
2. Then, 1mL of distilled water and 5 mL of 0.1N NaOH was taken in a test tube and put the test tube inside the conical flask in a hanging manner with the help of a rubber stopper.
3. Afterwards, the samples were incubated for 24 hours at 25^0C.

4. Then, after the 24 hours of the incubation the test tubes were taken out from the flask.
5. The solution from the test tube was transferred to a 100 mL conical flask and 5 mL of distilled water was added to it.
6. Then, 5 mL of $BaCl_2$ and 3 drops of phenolphthalein indicator was added to the solution and titrated with 0.05N HCl.
7. The end point was recorded when the solution turned to colourless from pink.

Calculation:

$$CO_2 \text{ mg } g^{-1} \text{ of oven dry soil} = \frac{(Vo - Vt) \times 100 \times 22 \times \delta}{(Mw - Md) \times t}$$

Where, t= Time of incubation,Vo = Blank titrated value, Vt = Sample titrated value, Mw = Weight of the moist soil, Md = Weight of the oven dry soil, δ= Strength of HCl.

4.2.2.1.1.11. Cation exchange capacity (CEC)

Reagents:

1. 1N acetic acid (CH_3COONa) solution: 136 g acetic acid trihydrate was dissolved in 750 mL distilled water and volume made up to 1L. Diluted NaOH was used to adjust the pH to 8.2.
2. Ethyl alcohol (95%)
3. 1N ammonium acetate (CH_3COONH_4) solution: 57 mL of concentrated acetic acid was added in 750 mL distilled water. Then, 68 mL conc. ammonium hydroxide was added and volume made upto 1L. Diluted NH_4OH or CH_3COOH was used to adjust the pH to 8.

Procedure:

1. Soil sample weighed accurately to 5 g was taken in a bottle (250 mL volume) followed by addition of 100 mL of 1 N CH_3COONa solution and then shaken vigorously for 30 minutes in a mechanical shaker.

2. Then, the bottles containing samples were placed on horizontal positions on a tray and kept overnight.
3. On the next day the supernatant contents of the sample was decanted very cautiously to minimize the loss of soil particles.
4. After that 35 mL of ethyl alcohol was added to each bottle and shaken vigorously. Then, the contents were filtered very carefully without unsettling the soil as much as possible.
5. This procedure was continued for three times and all the filtrations were carried out with the same filter paper for the same sample.
6. Then, the filter paper was put inside the bottle with soil sample followed by addition of 100 mL of 1N ammonium acetate solution and shaken for 30 minutes.
7. The solutions of the bottle were filtered in a clean 1000 mL volumetric flask and volume made up to 1000 mL with distilled water.
8. Na ion concentration was determined in flame photometer.

Calculation:

If concentration of Na^+ ions in extracted solution is 'x' ppm then CEC of the soil will be $\frac{20x}{23}$ meq per 100g soil.

Preparation of Na- stock:

1. Dissolve 2.5416 g NaCl in 1L distilled water – 1000 ppm.
2. Dissolve 1.886 g NaCl in 1L distilled water – 1000 ppm.
3. Then make different standard by $S_1V_1=S_2V_2$

4.2.2.1.2. Benefit percentage

Soil physicochemical characteristics (pH, nutrient availability (e.g., N and P), cation exchange capacity (CEC), soil organic C (SOC), WHC, and BD) are strong indicators of soil quality and fertility [31]. Therefore, we derived a formula (Benefit Percentage) to estimate the overall changes in soil fertility in reference to one of our previous

publications [32]. The benefit percentages of different silver nanoparticle solutions with respect to controls for the soil quality variables of WHC, CEC, SOC, pH, and N/P availabilities were computed using the following equation.

$$\text{Benefit \%} = \frac{(\text{Average at 60 d}) - (\text{Average at 0 d})}{(\text{Average 0 d})} \times 100$$

The benefit percentage for BD was computed using a similar formula with an opposite sign, according to the assumption that lower BD represents greater benefit.

$$\text{Benefit \%} = \frac{(\text{Average at 0 d}) - (\text{Average at 60 d})}{(\text{Average at 0 d})} \times 100$$

4.2.2.1.3. GSNP-N interactions

Experiments were conducted to comprehensively assess the impact of selected GSNP concentrations on soil N. Fresh soil samples were collected from the same area, sterilized at 103421.36 kg $m^{-1}.s^{-2}$ pressure for 15 min to avoid the effects of microorganisms on soil N, and distributed into plastic containers at 40 g each. These containers were then inoculated with selected GSNP solutions (25, 50, and 100 mg kg^{-1}) and subjected to laminar air flow for 30 d. The study was replicated thrice; during each study, total Kjeldahl N (TKN) was analyzed at 10 days intervals starting from day 0 [27].

Another experiment was conducted to understand the influence of GSNPs on NO_3^- leaching in soil. Glass columns (300 mm dia.) were packed with 90 g of GSNP-treated soil samples (GSNP25, GSNP50, and GSNP100). For each sample, 100 mL of ultrapure water was passed through the packed soil, and its leachate was collected; this was conducted twice, after 24 and 48 h. Collected leachates were analyzed for nitrate N in a Foss Kjeltec 8100 analyzer following the standard protocol [27].

4.2.2.1.3.1. Total N

Reagents:

1. Concentrated Sulphuric acid (H_2SO_4)
2. Copper Sulphate ($CuSO_4$)

3. Potassium Sulphate (K_2SO_4)
4. 0.1 N H_2SO_4: 2.8 mL H_2SO_4 was added to 1000 mL distilled water.
5. 0.1N NaOH: 4 g NaOH was dissolve in 1000 mL distilled water.
6. Mixed indicator: 0.5 g bromocrescol green and 0.1 g methyl red indicator was mixed well into 100 mL ethanol.

Procedure:

1. 1g sample was taken in a Kjeltec digestion tube and 0.8 g $CuSO_4$, 7 g K_2SO_4 and 12 mL conc. H_2SO_4 was added to it.
2. Then the contents were digested upon FOSS Kjeltec Techtor^{TM} at 420 ^{0} C for 1 h.
3. After the digestion the contents were cooled down and transferred to distillation flask and 80 mL distilled water followed by 50 mL 40% NaOH was added to it until the appearance of black colour.
4. Then, distillation was started and the distillate was collected in an Erlenmeyer flask containing 20 mL 0.1 N H_2SO_4 and 3-4 drops of mixed indicator.
5. Finally the distillate was titrated with 0.1 N NaOH and turquoise blue colour was appeared at the end point of titration.

Calculation:

TKN (%)

$$= \frac{\{(\text{Volume of H2SO4} \times \text{strength}) - (\text{Volume of NaOH consumed} \times \text{strength}) \times 0.014 \times 100\}}{\text{Weight of sample}}$$

0.014= milli equivalent weight of N

If ‘m’ amount of sample is taken for which ‘a’ is the volume of acid used and ‘b’ is the volume of NaOH consumed for titration then for estimation of total N in this case will be

$$\{(a \times 0.1) - (b \times 0.1) \times 0.014 \times 100\}/m$$

4.2.2.1.3.2. Nitrate content

Digestion:

1. For nitrate estimation 50 mL filtrate solution was added into a Kjeltec digestion tube.

2. Then, 5 mL conc. H_2SO_4, 0.2 g Devardas alloy, 2 g K_2SO_4 and 20 glass beads were added into each tube and digested at 350-370 ^{0} C for 1 h. At the end of digestion the solution colour was appeared as light brown to green.

Distillation:

Reagents:

1. 4% Boric acid: 40 g boric acid powder was taken into a 1L volumetric flask. Then, 400-500 mL boiled distilled water was slowly added into it and mixed well till dissolution of the whole amount.

   (a) 10 mg of bromocresol green powder was dissolved in 95% ethanol solution and

   (b) 10 mg of methyl red powder was dissolved in 10 mL 95% ethanol solution.
2. Then, 10 mL from solution (a) and 7 mL from solution (b) was added with the boric acid solution and volume was made upto 1000 mL with distilled water.
3. 0.02 N HCl: From 35% pure conc. HCl solution 1.79 mL was taken into a 1L volumetric flask and volume made up with de-ionized water.
4. Then, 80 mL distilled water and 50 mL of 40% NaOH was added into a Kjeltec distillation tube and fitted into distillation chamber. In an Erlenmeyer flask 25 mL 4% boric acid was taken to collect the distillate. After distillation the distillate was titrated against 0.02 HCl solution.

Calculations:

$$\text{Nitrate (mg/L)} = \frac{(\text{Sample titration}) \times \text{Normality of titrant} \times 14.01 \times 100}{\text{Volume of sample}}$$

Where, 14.01=atomic weight of nitrogen

If ‘a’ is the value of sample titration

‘b’ is the volume of sample taken

Then, Nitrate (mg /L) = (a× Normality of titrant × 14.01×100)/b

4.2.2.1.4. Plant health metabolism: pot culture with French bean and tomato

4.2.2.1.4.1. Pot study with French bean (P. vulgaris)

Periodic changes in leaf number and leaf area index (LAI) along with final crop yield, uptake of nutrients (N and P), crude protein, and yield were analyzed using the procedures of Tandon [33] and Reddy and Reddy [34]. Pod yields (g plant^{-1}) of the harvested products were also measured. Moreover, weight loss after 30 days of storage in ambient conditions was measured to understand each product's storage quality. Chlorophyll content in leaf samples was evaluated by following the procedures of Anderson and Boardman [35], whereas the concentrations of nitrate reductase and proline were enumerated using standardized methods [36,37]. Fresh and dry pod yields of harvested plants were also enumerated on a per plant basis.

4.2.2.1.4.1.1. Leaf number

The measurement of total leaf numbers from each plant was counted in a periodical manner at 15, 45, and 60 days after transplantation.

4.2.2.1.4.1.2 Leaf area index (LAI)

The calculation of leaf area index was done by considering the total area of each leaf in a plant and the ground cover area of the plant by following Mao et al. [38]. The area of individual leaves was calculated by the following formula:

$$\text{Length} \times \text{width} \times 0.83 \text{ [39]}$$

LAI was calculated by multiplying leaf area per plant with actual plant density.

4.2.2.1.4.1.3. Pod yield

Pod yield was calculated by weighing the tomato collected from each plot after harvest.

4.2.2.1.4.1.4. Weight loss per pod

Weight loss per pod was calculated by recording the weight reduction after 30 days of storage condition at room temperature.

4.2.2.1.4.1.5. Uptake of N and P

The detailed procedure for estimation of N uptake was described in section 4.2.2.1.3.1.

For estimation of total P di-acid digestion method was followed [33]. First 1 g of ground leaf/tomato sample was taken in a 50 mL glass beaker and 10 mL of acid mixture solution ($HClO_4$:HNO_3=1:6) was poured into the flask.

1. Then the samples were heated on a hot air oven until red fumes disappeared.
2. After that the digested contents were diluted to 20 mL of distilled water and filtered through Whatmann no. 42 filter paper.
3. The filtrates were taken for analysis of total P.
4. For total P estimation 5 mL of filtrate was taken in a 25 mL volumetric flask then 5 mL of ammonium molybdate solution followed by few drops of stannous chloride was added into each flask, volume was made upto 25 mL with distilled water. Absorbance measurement was taken at 660 nm in an Agilent UV-VIS Spectrophotometer.

4.2.2.1.4.1.6. Chlorophyll

Reagents: 80% ethanol or 80% acetone (v/v) was prepared in distilled water (80 mL ethanol/acetone with 20 mL distilled water).

Procedure:

1. Fresh leaf tissues were weighed accurately to 700 mg and taken in a 10 mL test tube.
2. Then, 80% ethanol or 80% acetone was slowly added in the sample tube so that leaf tissues get immersed properly.
3. Then the sample tubes were kept at -18ºC condition for 3 h.
4. After that, the leaf tissues were crushed properly with a mortar and pester.
5. Membrane filter was used for proper filtration and the filtrate portion was taken for further analysis.
6. Finally, the absorbance measured at 664.2 nm and 648.6 nm for Chlorophyll A and Chlorophyll B.

Calculation: (Unit: mg chlorophyll g^{-1} fresh tissue)

i) Chlorophyll A = (13.36 X $A_{664.2}$)- (519 X $A_{648.6}$)

ii) Chlorophyll B = (27.43 X $A_{648.6}$)- (8.12 X $A_{664.2}$)

iii) Chlorophyll = (5.24 X $A_{664.2}$) + (22.24 X $A_{648.6}$)

4.2.2.1.4.1.7. Proline

Reagents:

1. Acid ninhydrin reagent: 1.25 g of ninhydrin was taken and dissolved in a mixture of 30 mL of glacial acetic acid and 20 mL of 6M phosphoric acid with agitation until it was dissolved completely.
2. 3% aqueous sulphosalicyclic acid: 3 g sulphosalicyclic acid was weighed and dissolved upto 100 mL with distilled water.
3. Glacial acetic acid
4. Toluene
5. Standard proline solution.

Procedure:

1. 0.5 g of leaf sample was weighed accurately and homogenized in 10 mL of 3% aqueous sulphosalicyclic acid and filtered through filter paper. The extraction and filtration procedure was repeated.
2. Then, 2 mL of the filtrate was taken, mixed properly with glacial acetic acid (2 mL) and acid ninhydrin (2 mL).
3. After that, the reaction mixture was kept on a boiling water bath for 1 h.
4. This reaction was terminated by terminate by placing the mixture on ice bath.
5. Then, 4 mL of toluene was added to it and mixed vigorously for 20-30 seconds.
6. The chromophore was expirated (toluene layer) and warm to room temperature.
7. The absorbance was recorded at 520 nm against a reagent blank.
8. The amount of proline was calculated in the sample using a standard curve prepared from pure proline and express on fresh weight basis of the sample (see Annexure).

Calculation:

$$\mu M \text{ of proline per gram fresh leaf} = \frac{\{(\mu \text{ g proline } / mL \times mL \text{ toluene})\}}{115.5} \times (5/\text{g sample})$$

4.2.2.1.4.1.8. Crude protein

Crude protein was estimated by the TKN protocol.

Crude protein content (%) =Total Nitrogen content (%)× 6.25 (on the basis of the supposition that nitrogen constitutes 16% of protein)

The detailed procedure was described in section 4.2.2.1.3.1.

4.2.2.1.4.1.9. Nitrate reductase activity

Reagent:

1. Potassium phosphate buffer (0.1 M, pH= 7.5):
   a. Phosphate A (0.2M dibasic sodium phosphate): Dissolve 35.61 g $Na_2HPO_4.7H_2O$ in distilled water and made the volume up to 1L.
   b. Phosphate B (0.2 M monobasic sodium phosphate): Dissolve 31.21 g $NaH_2PO_4.2H_2O$ in distilled water and made the volume up to 1L.
   c. Phosphate buffer: 61 mL Phosphate A and 39 mL Phosphate B were diluted up to 100 mL distilled water.
2. 0.02 M Potassium nitrate in water
3. 5 % Propanol
4. Chloramphenicol
5. 1 % sulphonilamide in 3M HCl (w/v)
6. 0.02% N-1 napthyl-ethylenediamine HCl (w/v)
7. Standard KNO_3 solution

Procedure:

1. Leaves were rinsed with cold distilled water and slices with a razor.

2. 200 mg of leaf punches were taken in a screw cap vial (25 mL) and 5mL of a medium consisting of 0.1 M phosphate buffer, 0.2 M potassium nitrate, 5% propanol, and 2 drop of chloramphenicol (0.5 mg/mL) was added to it.
3. After that the reaction mixture was kept in dark at 25^0C for desired incubation period.
4. After incubation, 0.4 mL aliquots was taken in a vial and 0.3 mL each of 1% sulphonilamide and 0.02% 4-1 nepthyl ethylenediamine HCl was added to it.
5. Then, the solution was kept for 20 minutes and diluted with 2 mL of water.
6. The absorbance was recorded at 540 nm.
7. Standard curve was drawn with standard potassium nitrate solution in a series of test tubes making up the volume in each 2 mL with water and followed steps 4 to 6. The enzyme activity was expressed as µM of nitrite formed per gram fresh weight of sample per hour.

Calculation:

The enzyme activity was expressed as µM of nitrite formed per gram fresh weight of sample per hour. For the standard curve, the concentration was taken along X-axis and the absorbance was taken along Y-axis.

4.2.2.1.4.1.10. Real-time quantitative PCR: expression of NR and Fd genes

Total RNA was extracted from control and treated leaf samples using TRI reagents (SIGMA-ALDRICH). We observed an overall positive impact of GSNP50 on soil N mineralization and plant growth quality (protein content, NR activity, and chlorophyll content).

Hence, it was imperative to study GSNP50-treated plants to observe the expression of two vital genes related to N assimilation and photosynthesis, namely *NR* and *Fd*. From each total RNA sample, 2 µg was reverse transcribed and subjected to real-time PCR with gene-specific primers in a total volume of 20 µL. The conditions of this qRT-PCR analysis were standardized as follows: initial activation step (95 ^{0}C, 15 min), cycling step (denaturation at 95 ^{0}C, 30 s; annealing at 55 ^{0}C, 30 s; extension at 72 ^{0}C, 30 s, 40 cycles), melt curve analysis (55–60 ^{0}C, 15 s, 40 cycles). A housekeeping gene, GAPDH, was simultaneously amplified in separate reactions and

acted as an internal control; threshold cycle values were corrected using the corresponding threshold cycle values of GAPDH controls. Data from 3 determinations (means ± standard deviation) are used herein to indicate relative expression levels.

Extraction of RNA:

Reagents:

1. TRI Reagent.
2. Chloroform.
3. Isopropanol.
4. Ethanol.
5. DEPC treated water.

Procedure:

1. 50 – 100 mg of tissue was taken in an eppendorf tube.
2. 1mL of TRI reagent was added to it and vortex it properly.
3. Then, the sample was allowed to stand for 5 min at room temperature to ensure complete dissociation of nucleoproteins.
4. 0.2 mL of chloroform was added and shaken vigorously for 15 sec.
5. The reaction mixture was allowed to stand for 15 min at room temperature.
6. Afterwards, centrifugation was done at 12,000 × g for 15 min at 2^0C-8^0C and the upper aqueous phase was transferred to a fresh tube.
7. 0.5 mL of isopropanol was added to it and mixed well, allowed to stand for 10 min at room temperature and centrifuged again at 12,000 × g for 10 min at 2^0C-8^0C.
8. After centrifugation the RNA formed a pellet.
9. Then, the pellet was washed with 75% ethanol. (75% ethanol was prepared in DEPC water) and centrifuged at 10,000 × g for 10 min at 2^0C-8^0C.
10. The pellet was kept in tissue paper for drying at room temperature.
11. Then, the pellet was dissolved in DEPC treated water and kept in 4^0C for 24 h.
12. Next day the RNA was dissolved using vortex. The purity was checked at 260/280 (Ratio 1.6 – 2).

CDNA synthesis:

1. After total RNA isolation, CDNA was synthesized from 2 µg of total RNAs using M-MuLV Reverse Transcriptase (Thermo Scientific), according to manufacturer protocol.
2. The following components were added into a sterile nuclease free PCR tube on ice.
   a. Total RNA-2 µg
   b. Primer (Oligo dT18)-1 µL
   c. DEPC treated water-upto 12.5 µL
3. Then incubation was done for 5 minutes at 65° C, chilled on ice, centrifuged briefly, and placed on ice.
4. 6.5-7 µL of the reaction mixture was added to it containing the following component in each tube.
   a. Ribolock^{TM} RNase inhibitor-0.5 µL
   b. 10mM DNTP mix-2 µL
   c. 5X reaction buffer-4 µL
5. Mixing was done followed by centrifugation.
6. Then again incubated for 5 min at 37°C.
7. After that 1 µL of Revert Aid^{TM} H minus Reverse Transcriptase was added to it.
8. After proper mixing centrifugation was done again.
9. Then, incubated for 60 minutes at 42° C.
10. The reaction was terminated by heating at 70°C for 10 minutes.
11. This reverse transcriptase reaction product can be directly used in PCR or stored at -20°C for further use.

Qualitative PCR for gene expression analysis:

1. After thawing all the solutions were vortexed gently and then centrifuged.
2. Then, a thin walled PCR tube was placed on ice and the following components were added as a PCR Master Mix for each 25 µL reaction
   a. 10x Taq buffer-2.5 µL
   b. 2 mM dNTP mix-2.5 µL
   c. Forward Primer-1µL

d. Reverse Primer-1µL
e. 25 mM $MgCl_2$-1.85 µL
f. Template DNA-2 µL
g. Taq DNA Pol-0.15 µL
h. Nuclease free water-upto 25µL

3. Gently vortexed the sample and spin down
4. The PCR was performed using the recommended thermal cycling conditions mentioned earlier.

4.2.2.1.4.2. Pot study with tomato (L. esculentum)

4.2.2.1.4.2.1 Effect of AgNP on crop growth, photosynthesis, hill activity, nutrient uptake, and Ag accumulation

Ripened tomatoes were harvested at physiological maturity (56–62 days after transplanting) of the crop and yield plant^{-1} along with periodical changes in leaf number and LAI was calculated [38]. The uptake of N, P, K, and Ag in plant biomass was analyzed with the help of Kjeltec N analyzer, UV-VIS spectrophotometer, flame photometer, and AAS respectively [33]. We have also determined the chlorophyll content and Hill activity in leaves [40,41]. In addition, photosynthetic rate was enumerated with the help of a photosynthesis meter (LICOR 6400).

4.2.2.1.4.2.1.1. Leaf number and LAI

The methodology has been described in section 4.2.2.1.4.1.1 and 4.2.2.1.4.1.2.

4.2.2.1.4.2.1.2. Yield

The methodology has been described in section 4.2.2.1.4.1.3.

4.2.2.1.4.2.1.3. N, P, K, and Ag uptake

The methodology has been described in section 4.2.2.1.3.1 and 4.2.2.1.4.1.5.

4.2.2.1.4.2.1.4. Chlorophyll content

The methodology has been described in section 4.2.2.1.4.1.6.

4.2.2.1.4.2.1.5. Photosynthetic rate

A photosynthesis meter (LICOR 6400) was used to enumerate the photosynthetic rate of tomato leaves.

4.2.2.1.4.2.1.6. Hill activity

Reagents:

1. Sucrose-PO_4 buffer (0.5 M sucrose in 0.05 M sodium phosphate buffer, pH 6.2)
2. 0.03% 2-6-dichlorophenol indophenols (DCPIP)

Procedure:

1. Fresh leaf tissues were extracted in sucrose-PO_4 buffer (0.5 M sucrose in 0.05 M sodium phosphate buffer, pH 6.2).
2. Then, centrifuged at 1000 g for 5 minutes (5000 rpm) and collected the supernatant.
3. Again, centrifuged at 5000 rpm for 15 minutes.
4. Then, the pellet containing chloroplasts were suspended in 5 mL of sucrose-PO_4 buffer.
5. The reaction mixture was prepared by taking 1 mL chloroplast suspension, 4 mL sucrose –PO_4 buffer, and 0.5 mL of 0.03% 2-6-dichlorophenol indophenols (DCPIP) in a test tube and mixed well.
6. Then, initial absorbance was recorded at 610 nm.
7. After that the samples were kept in bright sunlight for 30 min.
8. After 30 minutes the OD was measured at 610 nm.
9. The difference in OD was measured and converted from the standard curve using known concentration of DCPIP (see Annexure).

4.2.2.1.4.2.2. Assessment of oxidative stress in AgNP treated plants

A portion of the plant samples were undergone analysis of oxidative stress (catalase, lipid peroxidation, and proline content) posed by AgNP treatments. Catalase activity was indirectly estimated by hydrogen peroxide (H_2O_2) breakdown following Chance

and Maehly [42]. Lipid peroxidation was assessed through enumeration of malondialdehyde production in plant leaves in UV-VIS spectrophotometer [43].Whereas, proline content was estimated following Bates et al. [37].

4.2.2.1.4.2.2.1. Catalase activity

Enzyme extraction:

1g of plant sample was extracted in 10 mL of 0.1 M phosphate buffer solution and centrifuged at 10,000 rpm for 15 min at 4^{o} C in a refrigerated centrifuge.

Reagents:

1. Phosphate buffer (0.1M, pH= 6.8):
    a. Phosphate A: 0.2 M dibasic sodium phosphate-35.61 g $Na_2HPO_4.7H_2O$ was weighed accurately and the volume was made upto 1000 mL with distilled water.
    b. Phosphate B: 0.2 M monobasic sodium phosphate-31.21 g $NaH_2PO_4.2H_2O$ was weighed accurately and the volume was made upto 1000 mL with distilled water.
    c. Phosphate buffer: 51 mL of phosphate A and 49 mL of phosphate B was taken and diluted up to 200 mL with distilled water.
2. 2% Sulphuric acid (H_2SO_4): 2 mL concentrated H_2SO_4 was diluted up to 100 mL with distilled water.
3. 0.01N Potassium permanganate ($KMnO_4$): Take 158.04 mg $KMnO_4$ was dissolved up to 100 mL with distilled water.
4. 0.1M Hydrogen peroxide (H_2O_2): 3.041 mL H_2O_2 (100v/v, 30%) was taken and diluted up to 1000 mL with distilled water.

Procedure:

1. Here, in this procedure the catalase activity was detected by using titration method.
2. The reaction mixture was prepared by mixing 3 mL of phosphate buffer (0.1M, pH =6.8), 1 mL 0.1M H_2O_2, and 1mL enzyme aliquot.

3. Afterwards the reaction mixture was incubated at room temperature for 1min.
4. Then 10 mL 20% H_2SO_4 was added to it in order to stop further reaction.
5. Subsequently, the reaction mixture was titrated against 0.01N $KMnO_4$ to estimate the residual H_2O_2 until a faint pink colour persisted for at least 15secs.
6. The enzyme activity was expressed as amount of enzyme break down by H_2O_2 $min^{-1}g^{-1}$ plant material.

4.2.2.1.4.2.2.2. Proline

The methodology has been described in section 4.2.2.1.4.1.7.

4.2.2.1.4.2.2.3. Lipid peroxidation

Reagents:

1. 20% (v/v) trichloroacetic acid
2. 0.5% (v/v) thiobarbituric acid

Procedure:

Estimation of MDA:

1. 1 mL of extracted sample (0.1-2.0 mg of membrane protein or 0.1-0.2 µM of lipid phosphate) was taken and 2 mL of a reaction solution containing 20% (V/V) trichloroacetic acid (TCA) and 0.5% (V/V) thiobarbituric acid (TBA) was added to it.
2. Then this reaction mixture was placed in a water bath at 95^0 C for 30 min and after that transferred to an ice water bath.
3. Afterwards the solution was centrifuged at 10,000×g for 10 minutes.
4. Reading of the absorbance of the supernatant was recorded at 532 and 600 nm in a UV-VIS Spectrophotometer.

Calculation:

MDA content was calculated using the adjusted absorbance and the extinction coefficient of 155 $Mm^{-1}cm^{-1}$ and the result is expressed as µM g^{-1} dry weight.

$$\text{MDA } (\mu M/g \text{ fresh weight}) = \frac{A532 - A660}{155} \times 103 \times \text{Dilution factor}$$

4.2.2.1.4.2.3. Effect of AgNP exposure on nitrate reductase, glutamine synthetase/ glutamate synthase activity and gene expression in tomato

Nitrate reductase (NR), Glutamine Synthetase (GS), and Glutamate Synthase (GOGAT) are three vital enzymes responsible for N-assimilation and amino acid production in plants. We assessed their activity following Radin [36], Kwinta and Cal [44], and Esposito et al. [45] respectively.

To identify the expression of *GS2* and *GOGAT* genes in plants qRT-PCR was performed with gene specific primers. Initially, total RNA was extracted by using TRI reagent, Isopropanol, and DEPC treated water. Afterwards 2 μL of this extracted RNA was used in qRT-PCR. In each cycle of qRT-PCR standard conditions were maintained like this: initial activation step (95 °C, 15 min), cycling step (denaturation 95 °C, 30 s; annealing 55 °C, 30s; extension 72 °C, 30s, 40 cycles), melt curve analysis (55–60 °C, 15 s, 40 cycles), where GAPDH is served as a house keeping gene.

4.2.2.1.4.2.3.1. Nitrate reductase activity

The methodology has been described in section 4.2.2.1.4.1.9.

4.2.2.1.4.2.3.2. Glutamine synthetase activity

Reagents:

1. 0.1 Tris HCl (pH 7.9)
2. 20 mM $MgCl_2$
3. 1μM β- mercaptoethanol
4. 0.05% Triton X 100
5. 0.2 M L- glutamine
6. 20 mM sodium arsenate
7. 3 mM $MnCl_2$
8. 50 mM Hydroxylamine
9. 1 mM ADP

Procedure:

1. 1g plant material was taken and homogenate was prepared in 0.1M Tris –HCl buffer (pH 7.9) containing 20 mM $MgCl_{2.}$
2. Then, 1mM Mercaptoethanol (2- ME) and 0.05% TRITON X 100 was added to it and centrifuged at 10,000 ×g for 10 min at 4^0C.
3. After centrifugation the supernatant was collected, followed by addition in assay mixture containing 0.2 M of L-glutamine, 20 mM sodium arsenate, 3M $MnCl_2$, 50 mM hydroxylamine, and 1mM ADP.
4. Then, the activity of glutamine synthetase was assessed in spectrometric method at 340 nm.
5. The activity of the investigated enzyme is defined in µM of 4- glutamyl hydroxymate formed in min^{-1} g^{-1} dry weight.

Calculation:

$$\text{Unit/ mL enzyme} = \frac{(\Delta \text{A340nm/ min test} - \Delta \text{A340nm/ min blank}) \times \text{total volume}}{6.22 \times \text{Volume of enzyme used}}$$

4.2.2.1.4.2.3.3. Glutamate synthase activity (GOGAT)

Reagents:

A. Extraction buffer-

1. Phosphate buffer (100 mM, pH 7.5)
2. EDTA (1 mM)
3. DTT (1 mM) (fresh preparation)
4. PVP (1%) (fresh preparation)

B. Assay buffer-

1. Tris HCl buffer (50 mM, pH 7.6)
2. The following reagents were prepared in Tris HCl buffer (50 mM, pH 7.6):
   a) Glutamine (5 mM)
   b) 2-oxalogluterate (5 mM)
   c) NADPH (0.25 mM)

Procedure:

1. 1g of plant sample was taken and extracted in 5 mL buffer constituting of phosphate buffer (100 mM + pH 7.5) + EDTA (1 mM) + Dithio erythritol (DTT-1 mM) + Polyvinyl pyrolidone (PVP-1%).
2. Then, centrifugation was done at 10,000 g for 30 min. After centrifugation the supernatant was taken as the enzyme source.
3. The assay mixture was containing 0.2 mL enzyme extract, 1 mL of Glutamine, 1 mL of 2- oxoglutarate, 1.8 mL of buffer, and 1 mL of NADPH.
4. After that the absorbance reading was recorded at 340 nm.

Calculation:

Activity is expressed as nanomole of NADPH oxidized min^{-1} mg^{-1} protein

$$= \frac{\text{A340} \times \text{Volume of assay solution} \times 1000}{6.22 \times \text{time of incubation (min)} \times \text{mg protein in enzyme extract used}}$$

4.2.2.1.4.2.3.4. qRT-PCR: gene expression of GS2 and GOGAT

The methodology has been described in section 4.2.2.1.4.1.10.

4.2.2.1.5. Estimation of bacterial growth in silver nanoparticle treated soil samples

The bacterial growth was enumerated in soil samples under *P. vulgaris* cultivation. For each soil sample, a 1 g subsample was suspended in a 10 mL of deionized water and mixed thoroughly in a vortex for 15 min. Then, 1 mL aliquots from each mixture were serially diluted from 10^{-1} to 10^{-7}. Subsequently, each diluted sample was used to inoculate Petri dishes using the pour plate technique; for each sample, three plates were prepared containing nutrient agar, Burk's media, or Pikovskaya's media to enumerate total bacterial colonies, N-fixing bacterial colonies (NFB), and P-solubilizing bacterial colonies (PSB), respectively [46]. The Petri dishes containing nutrient agar were inoculated for 24 h at 36 °C, whereas those containing Burk's or Pikovskaya's media were incubated for 48 h at 28 °C. Then, the colonies on the plate

were counted using a colony counter. The whole experiment was replicated thrice, and the number of colony-forming units (CFUs) per mL was computed as follows.

$$\text{Number of bacteria per mL} = \frac{(\text{Number of colonies} \times \text{dilution})}{\text{Volume plated (mL)}}$$

4.2.2.2. In depth and long term study

4.2.2.2.1. Soil spiked by AgNP

A typical alluvial (typic endoaquepts) soil was collected from nearby agricultural fields in Sonitpur, Assam, India (Lat.: 26.7008°N; Long.: 92.8303°E). Collected soil samples were then air dried, ground in an agate mortar, and screened through 2 mm mesh sieve. Subsequently, the whole soil batch was subdivided into 2 kg sub-samples to accommodate all different concentrations and their 5 replicates. Then, three various concentrations (10, 25, and 50 mg kg^{-1} of dry soil) of AgNP in dispersed form was spiked to the soil samples. The AgNP treated soil samples were thoroughly mixed for uniform distribution of the added materials and the incubation was carried out for 72 weeks within an ambient temperature range of 20–35° C. Moisture content was maintained at 45% water holding capacity (WHC) through sprinkling water at 2–3 days interval during the study period. The treatments combinations were as detailed below:

Table 4.1: Treatment combinations for soil and aqueous media

Treatments	Abbreviations
Control	C
AgNP 10 ppm [mg kg^{-1}(soil)/mg L^{-1}(aqueous media)]	$AgNP_{10}$
AgNP 25 ppm [mg kg^{-1}(soil)/mg L^{-1}(aqueous media)]	$AgNP_{25}$
AgNP 50 ppm [mg kg^{-1}(soil)/mg L^{-1}(aqueous media)]	$AgNP_{50}$

Soil samples were periodically drawn at: 0 day, 4, 8, 12, 24, 48, 60, and 72 weeks for analysis of various physico-chemical attributes [pH, easily mineralizable-N (minz. N), available-P (Avl P), available-K (Avl K), microbial biomass carbon (MBC), and

microbial biomass N (MBN)] [27,28,47]. The activity of soil enzymes (urease and phosphatase) was assessed periodically [29,30]. We also measured the total bacterial counts and bacterial biomass in the treated soil samples [46,48]. Moreover, the change in DTPA extractable Ag along with the fractional variations of different bound and labile forms of Ag were enumerated [49,50].

4.2.2.2.1.1. pH

The methodology has been described in section 4.2.2.1.1.3.

4.2.2.2.1.2. Available N

The methodology has been described in section 4.2.2.1.1.4.

4.2.2.2.1.3. Available P

The methodology has been described in section 4.2.2.1.1.5.

4.2.2.2.1.4. Available K

The methodology has been described in section 4.2.2.1.1.6.

4.2.2.2.1.5. Microbial biomass Carbon and Nitrogen (MBC and MBN)

Reagents:

1. Ninhydrin reagent: 0.8 g ninhydrin and 0.12 g hydrindantin were dissolved in 30 mL of dimethyl sulfoxide solution and 10 mL of lithium acetate buffer was added to it. A use of freshly prepared reagents is always recommended.
2. Lithium-acetate buffer: 168 g lithium hydroxide ($LiOH.H_2O$) was mixed in about 500 mL of distilled water. Then, the solution was continuous stirred with a glass rod. When about half of the ingredient was dissolved then 293 mL of glacial acetic acid was added to it and volume made up to 1L. pH was adjusted to 5.2 ± 0.05 with either acetic acid or lithium hydroxide. Then, the solution was allowed to cool overnight in room temperature and then volume made up to 1L.
3. Ethanol-water: 165 mL ethanol (95%) was diluted with distilled water and volume made upto 300 mL.

4. Potassium chloride solution (2M KCl): 149 g of potassium chloride was mixed in distilled water and volume made upto 1L.
5. Chloroform: HPLC grade chloroform stabilized with 0.006%. 2-methyl -2-butane was used.
6. Nitrogen standards: 47 mg of Leucine was dissolved in 2 M KCl and the volume was made upto 50 mL. This contained 100 μg NmL^{-1}. This solution was serially diluted to 0, 2, 4, 8, 16 μg NmL^{-1} with 2 M KCl solution.

Procedure:

1. 10 g soil samples adjusted to 40% WHC was taken for both fumigated and unfumigated and incubated for 15 days in dark condition at 25° C temperature.
2. After 15 days both the two sets of the soil samples were taken out and analyzed for unfumigated and fumigated carbon.
3. The unfumigated samples were taken out in a 250 mL Erlenmeyer flasks, 40 mL 2M KCl solution was added and shaken for 30 min in a mechanical shaker at 200 rpm. After that filtration was done and filtered portion were stored at -15°C.
4. For fumigated set the soil samples were placed in a vacuum desiccators lined with a wet tissue paper and vial containing 10 g soda lime and 25 mL chloroform inside a desiccators which was then evacuated until chloroform boiled for 2 min and kept for 24 hours.
5. After fumigation in the next day the vacuum was released by opening the valve of the desiccators.
6. Then, the fumigated samples were transferred to 250 mL Erlenmeyer flask for extraction with 40 mL 2 M KCl and filtered as mentioned for the unfumigated sample. The extract was used for ninhydrin – N estimation.
7. 1 mL of the filtrate was added into a 50 mL tube along with 0.5 mL Ninhydrin reagent. Then, the tube along with the solution was heated on water bath for some time and after cooling the tubes 9.5 mL ethanol was added to each tube and mixed properly. The absorbance reading was taken in an Agilent UV VIS Spectrophotometer at 570 nm.

Determination of ninhydrin-reactive N:

Calibration:

1. Into 50 mL test tubes, 1 mL of each Leucine standard solution was taken and then 0.5 mL of ninhydrin reagent was added slowly.
2. Then all the standard solutions in duplicate were heated thoroughly on a boiling water bath.
3. After that test tubes were cooled at room temperature and 9.5 mL of ethanol-water was added to each of the test tubes and mixed thoroughly.
4. The absorbance measurement was taken in a spectrophotometer at a wavelength of 570 nm taking KCl solution as a blank.
5. Calibration curve was drawn with the absorbance against N- concentration. Colours of the samples were also developed in the similar fashion. Concentration of the extract solutions was determined with the standard curve (see Annexure).

Calculation:

$$\text{MBC } (\mu g\,/g) \;=\; \frac{[(\text{Fumigated concentration} - \text{Unfumigated concentration}) \times \text{DF}]}{\text{Oven dry soil wt. difference}}$$

Oven dry soil wt difference means, if moist wt was 10 g and oven dry wt = 9.23 g, hence the difference would be 10 – 9.23 = 0.77

Microbial Biomass C (μg g^{-1} oven dry soil) = 31 × ninhydrin N

Microbial Biomass N (μg g^{-1} oven dry soil) = 4.6 × ninhydrin N

4.2.2.2.1.6. Urease activity

The methodology has been described in section 4.2.2.1.1.8.

4.2.2.2.1.7. Phosphatase activity

The methodology has been described in section 4.2.2.1.1.9.

4.2.2.2.1.8. DTPA extractable Ag

Reagents:

DTPA extract:

To prepare DTPA extract solution initially, 1.967 g of DTPA and 1.470 g $CaCl_2.2H_2O$ were taken in a glass beaker and 20–25 mL of double distilled water followed by 13.3 mL of tri ethanol amine (TEA) and 100 mL of distilled water were added. Then, the volume of this solution was made up to 1 L. pH of this solution was adjusted to 7.3 for extraction of different trace elements remained in bio-available forms.

Procedure:

1. 20 g of soil sample was taken in a 250 mL of Erlenmeyer flask.
2. 40 mL of DTPA extract solution was added to it.
3. Then, shaking was done for 2 h in the mechanical shaker and then filtered.
4. The filtrates were then analyzed in Atomic Absorption Spectrophotometer after calibrating the instrument.

4.2.2.2.1.9. Sequential extraction procedures for speciation of particulate trace metal

Reagents:

1. 1M $MgCl_2$ / Mg $(NO_3)_2$ (pH 7.0): 50.51 g in 250 mL of distilled water, adjusting pH at 7.
2. 1M CH_3COONa (pH 5): 98 g of NaOAc salt was dissolved in 1 L distilled water and adjusted the pH to 5 with acetic acid (HOAc).
3. 0.04 M $NH_2OH.HCl$: 2.79 g of $NH_2OH.HCl$ (Hydroxylamine hydrochloride) was dissolved in 1 L 25% (v/v) acetic acid.
4. 0.02 M $HNO_{3:}$ 0.3205 mL of conc. HNO_3 was dissolved in 1 L of distilled water.
5. 30% H_2O_2
6. 3.2 M CH_3COONH_4 (Ammonium Acetate): 61.66 g of CH_3COONH_4 was dissolved in 250 mL 20% (v/v) HNO_3 acid.
7. Conc. HNO_3

Procedure:

1. 1g of soil sample was taken in an Erlenmeyer flask with 20 mL of deionized water and shaken for 30 minutes and then kept overnight.
2. On the next day the contents were filtered and the filtrate was taken for analysis of F_1 (water soluble) fraction. Then, 8 mL of 1 M $MgCl_2$ was added in the residue and vigorous shaking was done for 1h and kept overnight.
3. The contents were filtered and the filtrate was taken for analysis of F_2 (Exch.) fraction. Then, 8 mL of 1 M CH_3COONa was added in the residue, shaken for 1 h and kept overnight.
4. On the next day, filtrate portion was taken for analysis of F_3 (Carbonate) and 20 mL of $NH_2OH.HCl$ was added in the residue and extracted by shaking at 120 rpm for 6 h at $96^0C \pm 3$ and keep it overnight.
5. Again filtrate portion was collected for analysis of F_4 (Fe-Mn oxide) fraction. Then, 3 mL 0.02 M HNO_3 and 5 mL of 30% H_2O_2 was added in the residue (heated at $85^0C \pm 3$ for 2 h initially, a second aliquot of 3 mL 30% H_2O_2 added and heated for another 3 h).
6. After cooling, 5 mL of 3.2 M NH_4COOCH_3 was added and diluted the content to 20 mL and continuously shaken for 30 minutes.
7. Filtrate was taken for analysis of F_5 (organic matter) fraction and in the residue 25 mL conc. HNO_3 was added (kept until content dries at 105^0C, to the dried content 25 mL of deionized water was added). Then, the content was filtered and analyzed for F_6 (Residual) fraction.

4.2.2.2.1.10. Available sulphate and sulphur

Reagents:

1. Sodium acetate-acetic acid buffer (pH 4.8): CH_3COONa weighed accurately to 100 g and mixed with 30 mL glacial CH_3COOH (extra pure) and diluted upto 1L with distilled water.
2. 0.25% Gum acacia solution: 0.25 g Gum acacia was diluted upto 100 mL with distilled water.
3. $BaCl_2$ crystals
4. 100 ppm Standard stock solution: 0.5434 g K_2SO_4 was dissolved in 1 L distilled water.

5. 0.15% $CaCl_2$: 1.5 g $CaCl_2.2H_2O$ was weighed accurately and diluted upto 1L with distilled water.

Procedure:

1. 10 g of soil sample was taken into a 250 mL conical flask and 50 mL of 0.15% $CaCl_2$ solution was added to it and shaken for half an hour in a mechanical shaker.
2. Then filtered through Whatmann no 42 filter paper and 10 mL of the filtrates were taken into a 50 mL volumetric flask.
3. 10 mL acetate buffer and 1 g $BaCl_2$ crystals were added to it and mixed properly. Then, 1mL of 0.25% Gum acacia solution was added to every sample solution as well as the blank flask. Then, mixed properly and the volume was made up to 50 ml.
4. Absorbance readings were recorded at 440 nm using Agilent UV spectrophotometer. Preparation of Standard curve: 0, 0.5, 1.0, 1.5, 2.0, 2.5, 3.0, 3.5, and 4 mL solution was taken from a 100 ppm standard stock solution in nine different volumetric flasks (25 mL). As described in the protocol the required reagents were mixed with it and the absorbance was measured at 420 nm. A standard curve was drawn from absorbance *Vs* concentration and used for unknown concentration (see Annexure).

Calculation:

$$\text{S content in sample (kg/ha)} = \frac{\text{P} \times \text{Vt} \times \text{Ve} \times 2.24}{\text{Vf} \times \text{W}}$$

Soil sample (W) =10 g

Volume of extractant=50 mL

First dilution=5 times

Volume of aliquot taken=10 mL

Final volume=50 mL

Second dilution=5 times

Dilution factor=25

Absorbance reading=X

Against A value the ppm of S recorded= P

ppm value of S in soil sample =P × 25 (dilution factor)

S value in kg ha^{-1}= P × dilution factor × 2.24

4.2.2.2.2. Behaviour of AgNP in aqueous media

4.2.2.2.2.1. AgNP-pH interaction: batch experiment no. 1

Solutions of different pH (4, 7, and 9) were prepared with diluted HCl and NH_4OH. Then, AgNP (10, 25, and 50 mg L^{-1}) were added in such solutions and undergone continuous shaking for 72 h in a mechanical shaker at gentle speed (120 rpm). The shift in pH and Ag^+ availability was recorded at 24, 48, and 72 h.

4.2.2.2.2.1.1. pH

Almost 20-25 mL of the nonacidic filtrate was taken in an Erlenmeyer flask and pH reading was taken with Eutech pH electrode. Calibration was done with buffer solutions before analysis of the samples.

4.2.2.2.2.1.2. Ag content

For analysis of Ag, a portion of filtrate from each sample was taken out and acidified with concentrated HNO_3. Then, the Ag µconcentrations were analyzed in Atomic Absorption Spectroscopy (AAS).

4.2.2.2.2.2. N, P, K, and sulphur (SO_4^{2-} and S^{2-}) release profile and Ag^+ dissolution from AgNP: batch experiment no. 2

Potassium dihydrogen phosphate (KH_2PO_4) was dissolved in milli-Q water (1:10 ratio) in Erlenmeyer flasks and 10, 25, and 50 mg L^{-1} concentrations of AgNP were separately introduced. The solution mixtures were kept under gentle shaking (120 rpm) in mechanical shaker for 21 days. In this experiment, we used KH_2PO_4 to

monitor the P release pattern because of neutral character of the salt. Similar parallel experiment was undertaken with $(NH_4)_2SO_4$ (ammonium sulphate) for navigating the pattern of N release. In both the experiments, dissolution pattern of Ag^+ from AgNP was also monitored along with pH. Moreover, we studied the release profile of SO_4^{2-} and S^{2-} from ammonium sulphate in presence of AgNP. Changes in N (NH_4-N), Available P, Available K, SO_4^{2-}, and S^{2-} were recorded at 1, 2, 7, 14, and 21 days by following standard protocols [27].

4.2.2.2.2.2.1. pH

The methodology has been described in section *4.2.2.2.2.1.1.*

4.2.2.2.2.2.2. Available N

Almost 20-25 mL filtrate was collected at each sampling period and the N content was estimated by the same protocol as mentioned for available N in section 4.2.2.1.1.4.

4.2.2.2.2.2.3. Phosphate

1. From the filtrate solution 5 mL was taken into 25 mL volumetric flaks and 5 mL ammonium molybdate followed by few drops of stannous chloride solution was added into the flask.
2. Volume was made upto 25 mL with distilled water and absorbance was recorded at 660 nm in UV-VIS Spectrophotometer.

4.2.2.2.2.2.4. Potassium

20-25 mL of the filtrate was collected at various time intervals and analyzed the K content in flame photometer.

4.2.2.2.2.2.5. Sulphate and sulphur content

Reagents:

1. Sodium Acetate-Acetic acid buffer (pH 4.8): 100 g CH_3COONa was taken into a 1l volumetric flask and 200 mL distilled water was added into it. Then, 31 mL of Glacial CH_3COOH acid was added and volume made upto to 1L.
2. Gum acacia: 2.5 g of gum acacia was dissolved into 1L distilled water. This solution was kept for overnight and then filtered.
3. $BaCl_2$ crystals

4. K_2SO_4 Standard: 0.5434 g of pure K_2SO_4 was dissolved in 1000 mL distilled water.

Preparation of standard curve:

1. 2.5, 5, 7.5, 10, and 12.5 mL solutions were taken from the standard K_2SO_4 in five volumetric flasks.
2. Then, 10 mL of buffer solution, 1 mL of gum acacia and 1g of $BaCl_2$ crystals was added into each flask and shaken well.
3. After that, volume was made upto 25 mL with distilled water.
4. Absorbance reading was taken at 440 nm in an Agilent UV-VIS Spectrophotometer. The calibration curve is attached in annexure.

Preparation of sample:

1. 5 mL of liquid sample was taken into a 25 mL volumetric flask.
2. 10 mL buffer solution, 1mL gum acacia, and 1g $BaCl_2$ were added into each flask and volume was made upto 25 mL with distilled water.
3. A blank was prepared without sample and following the same procedure.
4. Absorbance reading was measured at 440 nm in UV-VIS Spectrophotometer.

4.2.2.2.2.2.6. Ag content

The methodology has been described in section 4.2.2.2.2.1.2.

4.2.2.2.3. AgNP agglomeration dispersion kinetics through dynamic light scattering (DLS) and UV–VIS spectrum

The agglomeration and dispersion profile of AgNP in soil were appreciated. The soil extracts were prepared and stored according to a previously reported method [51]. The AgNP spiked KH_2PO_4, $(NH_4)_2SO_4$, and pH solutions were bath sonicated for 15 min immediately before DLS and UV measurements. We have carried out DLS analysis for the soil extracts at week 1, 12, 24, 48, and 72 whereas the DLS (Microtrac MN 401, USA) measurements for the aqueous solutions were taken at 24 h, 72 h, and then at 21 days. Simultaneously, the AgNP agglomeration pattern in the above report samples were monitored by scanning the suspension from 200 to 800 nm in a UV-VIS spectrophotometer (Cary 60, Agilent Tech., USA).

4.2.2.2.4. On field trial with tomato

4.2.2.2.4.1. Pilot study-germination test

Prior to large scale study on plant through field experiment small germination test was conducted for all the treatments to determine the germination rate, root and shoot length. The effect of silver nanoparticles on germination of tomato seedlings was evaluated. 0.5 mL of AgNP was mixed in 10 mL deionized water and sonicated for 15 minutes. Meanwhile, 20 seeds of the selected species were placed in tissue papers in sterilized glass petri plates and inoculated with the previously prepared solution mixtures and kept in dark at 25^{o}C for 48 hours. Then, the germination index (GI), relative root growth (RRG), and relative seed germination (RSG) were measured following Das et al. [52], as below:

$$\text{RSG (\%)} = \frac{\text{Number of seeds germinated with treatments}}{\text{Number of seeds germinated in distilled water}} \times 100$$

$$\text{RRG (\%)} = \frac{\text{Mean root length of seeds receiving treated solutions}}{\text{Mean root length of seeds receiving distilled water}} \times 100$$

$$\text{GI(\%)} = \frac{\text{RSG} \times \text{RRG}}{100}$$

4.2.2.2.4.2. Design of experiment- Field trial

After successfully conducting the germination test field experiment was started with in a farmer's field nearby Tezpur university campus which is located approximately 13 km away from Tezpur town, Assam. The average maximum and minimum temperature during the experimental period (June 2015 to April 2017) was 17° to 30°C and humidity recorded as 72 to 85%. The soil samples of this area is generally typical alluvial in nature (typic endoaquept) with sandy loam texture and acidic nature. Completely randomized block design considering seven replicates for each treatment and control were maintained. Total 35 plots were prepared to accommodate all the treatments with 6m^2 each plot size. Short durational winter vegetable Tomato (Badshah *F1 hybrid*) was selected as the test crop for this study. The crop trial was repeated for two consecutive seasons (First season: June 2015-April 2016; second season: June 2016-April 2017).

4.2.2.2.4.3. Nursery, land preparation, and plot size

Initially a nursery land was prepared to maintain the growth of tomato seedlings. Plot preparation in the crop field was also done simultaneously in this period by ploughing. After attainment of some growth stage (after 1 month) seedlings were transplanted to the experimental site.

4.2.2.2.4.4. Treatment combinations

After undergoing various lab scale experimentations on Silver nanoparticles, the treatment combinations for field study were mentioned below:

A. AgNP: 15 and 30 kg ha^{-1}

B. $AgNO_3$: 15 and 30 kg ha^{-1}

C. Control

The main reason behind choosing this range of concentrations is to identify the minimum feasible dose of silver nanoparticles for agricultural application in large scale manner. The recommended dose of NPK for tomato (N: 75 kg ha^{-1}; P_2O_5: 60 kg ha^{-1}; K_2O: 60 kg ha^{-1}) were applied in each treated plot and control. Flooding irrigation system through laid drainage channels alongside the filed boundary was followed for the field experiments.

4.2.2.2.4.5. Soil sampling from the experimental field and physico-chemical assessment of the soil

Soil samples were collected after harvesting of the crop. Then, the collected soil samples were air dried in ambient temperature, removed the pebbles and plant parts, powdered in a wooden mortar and pestle and stored in sample bottles with proper leveling of sample name and collection date.

Various physico-chemical attributes were analyzed from the collected soil samples like bulk density, water holding capacity, pH, available N, available P, available K, soil organic carbon, urease and phosphatase activity following well

established methodologies [27-30]. The yield of tomato under various treatments and shelf life were enumerated in the harvested products.

4.2.2.2.4.5.1. pH

The methodology has been described in section 4.2.2.1.1.3.

4.2.2.2.4.5.2. Bulk density

The methodology has been described in section 4.2.2.1.1.1.

4.2.2.2.4.5.3. Water holding capacity

The methodology has been described in section 4.2.2.1.1.2.

4.2.2.2.4.5.4. Available N

The methodology has been described in section 4.2.2.1.1.4.

4.2.2.2.4.5.5. Available P

The methodology has been described in section 4.2.2.1.1.5.

4.2.2.2.4.5.6. Available K

The methodology has been described in section 4.2.2.1.1.6.

4.2.2.2.4.5.7. Soil organic carbon

The methodology has been described in section 4.2.2.1.1.7.

4.2.2.2.4.5.8. Urease activity

The methodology has been described in section 4.2.2.1.1.8.

4.2.2.2.4.5.9. Phosphatase activity

The methodology has been described in section 4.2.2.1.1.9.

4.2.2.2.4.5.10. Crop yield

After each harvest tomatoes collected from each plot were weighed in kilogram and then converted into ton ha^{-1}.

4.2.2.2.4.5.11. Shelf life in tomato (weight loss in g)

Shelf life is measured based on the temporal weight loss in perishable products in storage (after collection of first harvest).

4.2.2.2.5. Earthworm fecundity, body weight, Ag accumulation, oxidative stress enzymes, and histological analysis

Non-clitellated, juvenile specimens of *Eisenia fetida*, weighing about 300–450 mg were used for the study and undergone gut evacuation. Then, the gut evacuated adult specimens were inoculated into a urine free cow dung based substrates (2 kg) @ 10 worms kg^{-1}. The experiment was conducted for 120 days during spring season. About 40–50% moisture was maintained by sprinkling water at an interval of 2–3 days. Earthworm count and body weight were recorded at an interval of 10 days till 120^{th} day.

The accumulation of Ag in earthworm intestines was measured. Earthworm specimens were collected at 30^{th} days and 120^{th} day. Then, the collected specimens were washed, and kept overnight in a moist filter paper for gut cleaning. The sacrificed earthworms were digested in di-acid mixture [$HClO_4$: HNO_3 (1:6)] and the Ag concentration was determined by Atomic Absorption Spectrophotometry (AAS) (Lab India AA 7000) [53].

Simultaneously, a group of untreated and AgNP (10 mg kg^{-1}) treated earthworms were gut cleaned, killed by freezing, and used for histological assay [54]. Initially, fixation of earthworm tissues were done in Bouin's fluid for a period of 24 h, then the tissues were dehydrated in graded alcohol solution from 30% to 100% and then for 10 min in xylene solutions and embedded in paraffin. Microtome cutter were used to maintain a fine section of 5 μm thickness and mounted in albumin coated slides. Hematoxylin-eosin staining technique was used for slide staining. Finally the prepared slides were observed in high resolution microscope.

In addition, activity of catalase [55], reduced glutathione (GSH) [56], glutathione peroxidase (GPx) [57], glutathione S transferase (GST) [58], and total protein content [59] were determined in both treated and un-treated earthworms.

4.2.2.2.5.1. Catalase assay for animal sample:

Reagents:

1. RIPA buffer
2. 50 mM Tris HCl (pH 8.0)
3. 9 mM H_2O_2
4. 0.25 mM EDTA.

Procedure:

1. Initially a 5% tissue homogenate was prepared in RIPA buffer and then centrifuged at 12,000 g for 30 min at 4^0C. The supernatant was used as sample.
2. Afterwards 20 µL sample was added to 980 µL of assay buffer containing 50mM Tris HCl (pH 8.0), 9 mM H_2O_2, and 0.25 mM EDTA.
3. The decrease in ⊿O. D/min of assay mixture was recorded at 240 nm for 1min.

Calculation:
One international unit of catalase activity is calculated as:

$$= (\text{⊿O. D}/0.071/2) \times (\text{Vc} \times \text{Vx})\ (100/\text{protein in mg})$$

Where,

0.071 is the absorbance of 1mm catalase,

(Vc×Vx) is 1000 µL/20 µL=50 (the dilution level of the sample in the cuvette)

The result is expressed as unit catalase activity/mg protein

(Vc= Total assay volume, Vx = Cell volume)

4.2.2.2.5.2. Reduced Glutathione (GSH)

Reagents:

1. 150 mM KCl solution (ice cold)
2. 10 % TCA solution (Trichloro acetic acid)

Extraction:

1. Initially 150 mM of KCl solution (ice cold) was used to blance the earthworm tissues.
2. After that, 20% homogenate was prepared in distilled deionized water at 4^0 C.
3. Then, 2 mL of the homogenate was mixed with 2 mL of 10% TCA solution (Trichloro acetic acid) and then allowed to stand for 10 min at room temperature.
4. Centrifugation was done at 10,000 rpm for 10 minutes and then the supernatant was taken for further assay.

Assay:

0.5 mL supernatant was mixed with 2.5 mL DTNB solution and then the absorbance was measured at 405 nm in a UV-VIS Spectrophotometer.

Calculation:

GSH of the sample is calculated from standard curve and expressed in terms of microgram GSH/mg protein (see Annexure).

4.2.2.2.5.3. Glutathione Peroxidase (GPx)

Reagents:

1. 2 mM disodium EDTA
2. 1 mM sodium azide
3. 1 mM GSH
4. 0.2 mM NADPH
5. 1 unit of GR in 50 mM Tris HCl

Procedure:

1. The cytosolic sample was incubated at 37 °C with 875 µL of the coupling reagent.

2. The coupling reagent was constituted of 2 mM disodium EDTA, 1 mM sodium azide, 1 mM GSH, 0.2 mM NADPH, and 1 unit of GR in 50 mM Tris HCl.
3. 25 µL H_2O_2 (substrate) was added to the mixture to start the reaction.
4. The decrease in O.D. /min was monitored at 340 nm in an Agilent UV-VIS spectrophotometer.
5. The enzyme activity was expressed as nM H_2O_2 degraded min^{-1} mg^{-1} protein.

4.2.2.2.5.4. Glutathione –S-Transferase (GST)

Reagents:

1. 150 mM KCl (ice cold)
2. 20 mM phosphate buffer solution pH 7.4 (with 0.1M NaCl and 0.25M sucrose)
3. 0.1 M potassium phosphate buffer (pH 6.9)
4. 1mM CDNB

Preparation of Cytosol:

1. 150 mM ice cold KCl solution was used to remove the adherent blood from the tissue sample.
2. 5% homogenate was prepared in 20 mM phosphate buffer solution of pH 7.4 (with 0.1M NaCl and 0.25M sucrose) at 4^0C.
3. After that the homogenate was ultra centrifuged to have cytosolic preparation of GST according to the method of Nimmo et al. [58].

Assay Method Habig et al. [60]:

1. Enzyme activity was assessed maintaining the predetermined optimum condition.
2. CDNB was added in the reaction mixture as its rate of reaction was much greater than GSH.
3. The reaction mixture (3 mL at 25^0C) constituted of 0.1 M potassium phosphate buffer (pH 6.9), 1mM CDNB, and cytosol containing 0.4 mg protein.
4. The reaction was started by adding CDNB and the linear change in O.D was observed after 3 min at 344 nm.

Calculation:

Calculate the enzyme activity from the extinction coefficient 9.6 $mM^{-1} \times cm^{-1}$ for DNPG at 344 nm.

4.2.2.2.5.5. Total Protein content

Reagents:

1. BSA stock solution (1g/mL)
2. Reagent (i):
   a. 2% Na_2CO_3: 2 g Na_2CO_3 was dissolved in 100 mL distilled water.
   b. 0.1N NaOH: 0.4 g NaOH was dissolved in 100 mL distilled water.
   c. 1.56% $CuSO_4$: 1.56 g $CuSO_4$ was dissolved in100 mL distilled water.
   d. 2.37% Na- K tartarate: 2.37 g Na- K tartarate was dissolved in 100 mL distilled water.
   e. Mix 50 mL 2% Na_2CO_3+ 50 mL 0.1N NaOH
   f. Mix 10 mL 1.56% $CuSO_4$+10 mL 2.37% Na –K tartarate
   g. Finally reagent (i) was prepared by mixing 2 mL of (f) with 100 mL of (e)
3. Reagent (ii): Folin phenol reagent (1: 1)- 2 mL FFC + 2 mL distilled water

Extraction:

1. Tissues were homogenized in 5 mL ethanol-H_2O mixture (1:1), centrifuged and the supernatant was discarded.
2. Then, 5 mL 0.1N NaOH was added to it and dissolved for 15 min.
3. 0.2 mL protein standard solutions of different dilutions or samples were taken in test tubes.
4. Subsequently, 2 mL each of alkaline $CuSO_4$ solution and reagent (i) was added to it and mixed well.
5. Afterwards, the samples were incubated at room temperature for 10 min.
6. Then, 0.2 mL reagent (ii) was added and incubated for 30 min.
7. Finally, absorbance was recorded at 660 nm in a spectrophotometer.

Standard:

Different dilutions of BSA solution were prepared by mixing stock BSA soln. (1mg mL^{-1}) and water in a test tube. Final volume was made up to in 5 mL (see Annexure).

4.2.2.2.5.6. Tissue preparation for histological studies

Fixation:

The tissue was washed using physiological saline to remove blood and excess fat bodies and then kept in Bouin's fixative for 18 h.

Prepare the Bouin's fixative:

a. Saturated picric acid solution in distilled water-75 mL
b. Formalin (40% formaldehyde)- 25 mL
c. Glacial acetic acid- 05 mL

Dehydration:

1. Initially the tissue was kept in 70 % alcohol for overnight in order to eliminate the excess picric acid from it.
2. Then it was put in 90% alcohol and kept there in undisturbed condition for 1 h.
3. Afterwards the tissue was placed in absolute alcohol for 1h with two changes each.
4. Finally it was placed in acetone for 1 h.

Clearing:

In cleaning process the desired tissue was placed in clearing reagent (Benzene) and kept in undisturbed condition for 1 h.

Infiltration:

In this process the tissue with clearing reagent was kept in the melted paraffin wax (58 – 60^0C) for 3 h in a thermostatically controlled paraffin oven.

Embedding or casting:

1. The mould was filled with melted paraffin wax very cautiously in order to restrict the entrance of air bubbles.

2. The bottom was allowed to cool; however, application of a warm scalpel prevents the cooling of the upper surface.
3. Afterwards, the tissue was rapidly transferred into the melted paraffin wax of the mould, properly oriented with a warm forceps and allowed to cool.

Trimming:

The solid paraffin blocks were trimmed into the form of a square or rectangle with the help of a scalpel.

Microtomy or sectioning:

The machine with which the solid tissue block is cut is called the microtome machine.

Requirement:

Some other instruments were also required for Microtomy.

1. Hotplate (thermostatically controlled)
2. Scalpel.
3. Needle.
4. Fine pointed forceps
5. Microtome knife.
6. Block holder.
7. Spirit lamp.
8. Absorbent cotton.
9. Xylene
10. Micro slide

Procedure:

1. Initially the tissue block was fitted on a block holder and clumped into the object holder of the microtome. Then, it was fitted in a sharp knife carriage in an angle of 45 by adjusting the screwing.
2. The requisite thickness of tissue sections were cut in the form of a ribbon.
3. Then, two sections were attached due to the heat generated from cutting of sections.
4. Afterwards the ribbon was removed cautiously by using a needle and then it was placed in a card board box.

Affixation:

The tissue sections were stretched on glass slide to fix the tissue. The adhesive on the slide was rubbed carefully before affixation.

Requirement:

1. Mayer's adhesive
   Composition:-
   Egg albumin- 50 mL, Glycerin-50 mL
2. Sodium salicylate
3. Floating medium (distilled water).
4. Micro slide.
5. Dropper.
6. Ribbon of tissue section.

Procedure:

1. Initially cleaning of the slide was done by putting a small drop of adhesive on the upper surface of the slide and then rubbed on the surface with a clean fingertip.

2. Thereafter, few drops of floating medium (distilled water) were put on that surface of the slide.

3. The tissue ribbon was transferred on the slide and stretched it on the hotplate with maintaining the temperature.

4. After stretching, the floating medium was drained away and arranged the sections.

5. Then air dried the slide completely by placing it in inclined position for overnight.

Staining:

Hematoxylin-eosin staining was carried out to determine the histomorphology changes of the tissue after treatment.

Requirement:

1. Mayer's hematoxyline:-

Hemayoxylin	1g
Distilled water	1000 mL
Potassium or ammonium alum	50 g
Sodium iodide	0.2 g
Citric acid	1g
Chloral hydrate AR	30 g

2. Alcoholic eosin:-

90% alcohol	100 mL
Eosin powder	1.5 g
Acetic acid	1-2 drops

3. Coupling jar.
4. Distilled water.
5. Blotting paper
6. Cover slip.
7. Mounting reagent (DPX)
8. Forceps.

Procedure:

1. The sections were deparaffinized in xylene solutions for 10 min.
2. Then hydration of the slides was done through grated alcohol (Dowmgrade) and distilled water by keeping them for 5 min in each grade.
3. After that staining was done in Mayer's hematoxylin for 3 min, washed in running tap until thin section become blue.
4. Bring the slides up to 90% alcohol through upgraded alcohol.
5. Counter stain with Eosin for 3-4 min.
6. Differentiate in 90% alcohol again.
7. Dehydrate completely in absolute alcohol with two changes.
8. Clear in xylene and mounted in DPX.

4.3 Statistical analysis

One way and two way ANOVA was performed in SPSS 16.0 software for all lab scale experiments conducted in soil and aqueous media with four observations per cell at significance level $P < 0.05$. Moreover Fisher's t-test was also performed for various plant parameters (under tomato cultivation in pot scale) to estimate the significance level. Considering treatments as single factors that might have influenced various soil and plant parameters, one-way analysis of variance (ANOVA) was performed (under French bean cultivation) with 3 observations per cell at the significance level of $P < 0.05$. The P values are useful indicators to represent the significance of the treatments given by the ANOVA. The standard error values for the post-hoc analyses of least significant difference (LSD) can also be considered as its gross values [61]. We have also performed Pearson's correlation statistics to confirm the mechanistic hypotheses drawn from soil and other batch experiments in aqueous medium. Sigma Plot 10 and MS Excel were used for graphical presentation of data.

4.4. Results

4.4.1. Preliminary assessment

4.4.1.1. Impact of GSNP on soil Physical composition - SEM, EDX, and XRD analyses

The structures of GSNP (25, 50, and 100 mg kg^{-1}) treated and control soils were ascertained by SEM (Fig. 4.1a–d). From this analysis, it was evident that increasing GSNP concentration led to increased soil porosity. The final silver nanoparticle contents of treated soil samples were determined by EDX. This analysis confirmed that nanoparticles were present in the samples at concentrations ranging from 0.05–0.21 wt% (Fig. 4.1e–h). EDX analysis of the control sample or untreated soil showed that very little amount of silver was already present in the soil. However, the weight percentage of silver was considerably higher in the silver nanoparticle treated soil than that of control.

XRD analysis of the control soil showed peaks attributed to the typical soil minerals (quartz, orthoclase/feldspar, goethite, and calcite) at the 2θ values of 20°, 26°, 50°, 60°, and 70° respectively. The peak intensities indicated that orthoclase feldspar was the major crystalline component of the test soil. Peaks characteristic of silver with an fcc lattice structure were observed at the 2θ values of 38°, 44°, and 54° in soil treated with various doses (25 to 100 mg kg^{-1}) of SNPs (Fig. 4.2).

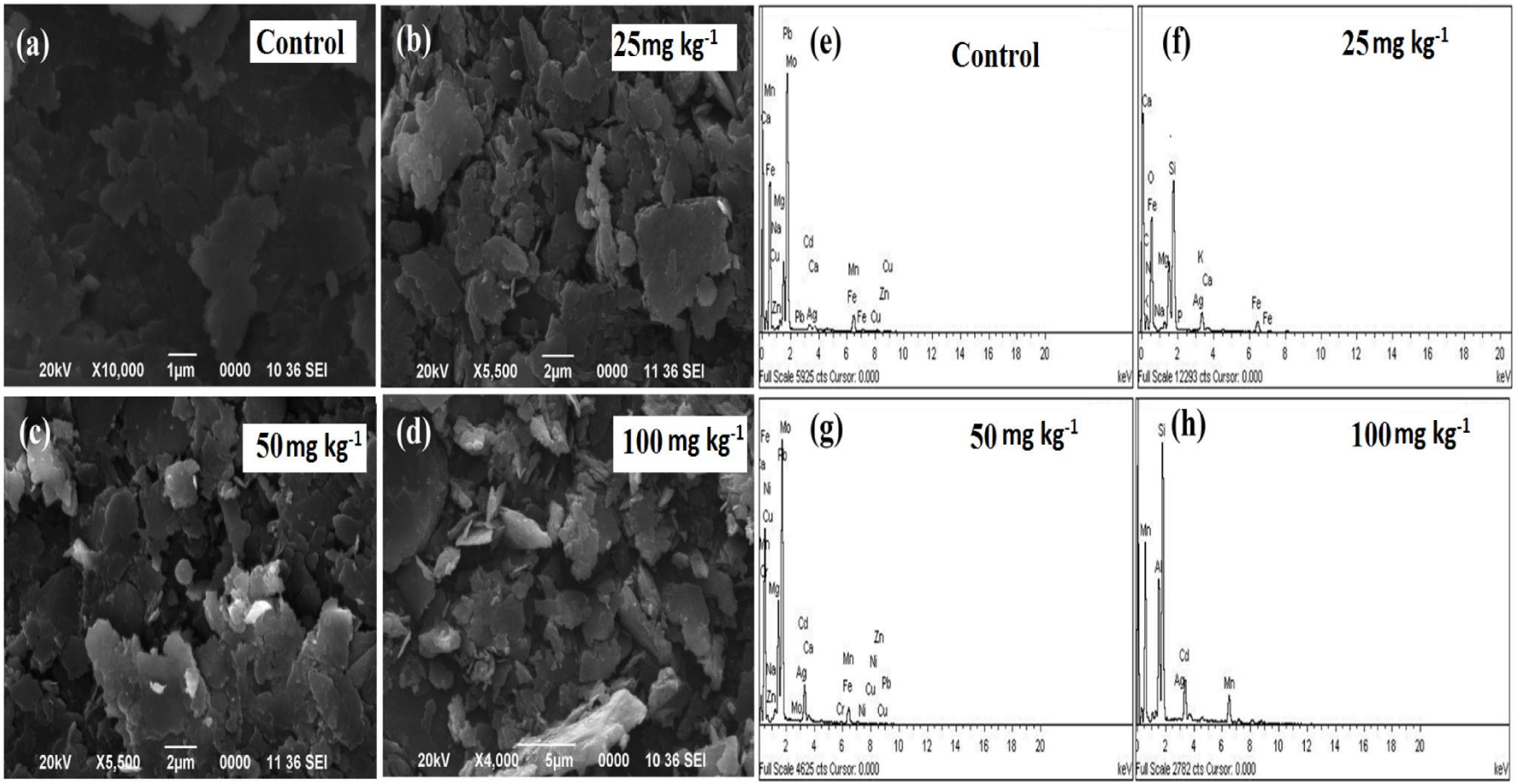

Fig. 4.1: (a–d) SEM micrographs showing the impact of GSNPs on soil texture; (e–h) EDX analysis results of soil composition depicting the impacts of GSNP, source: Das et al. [6]

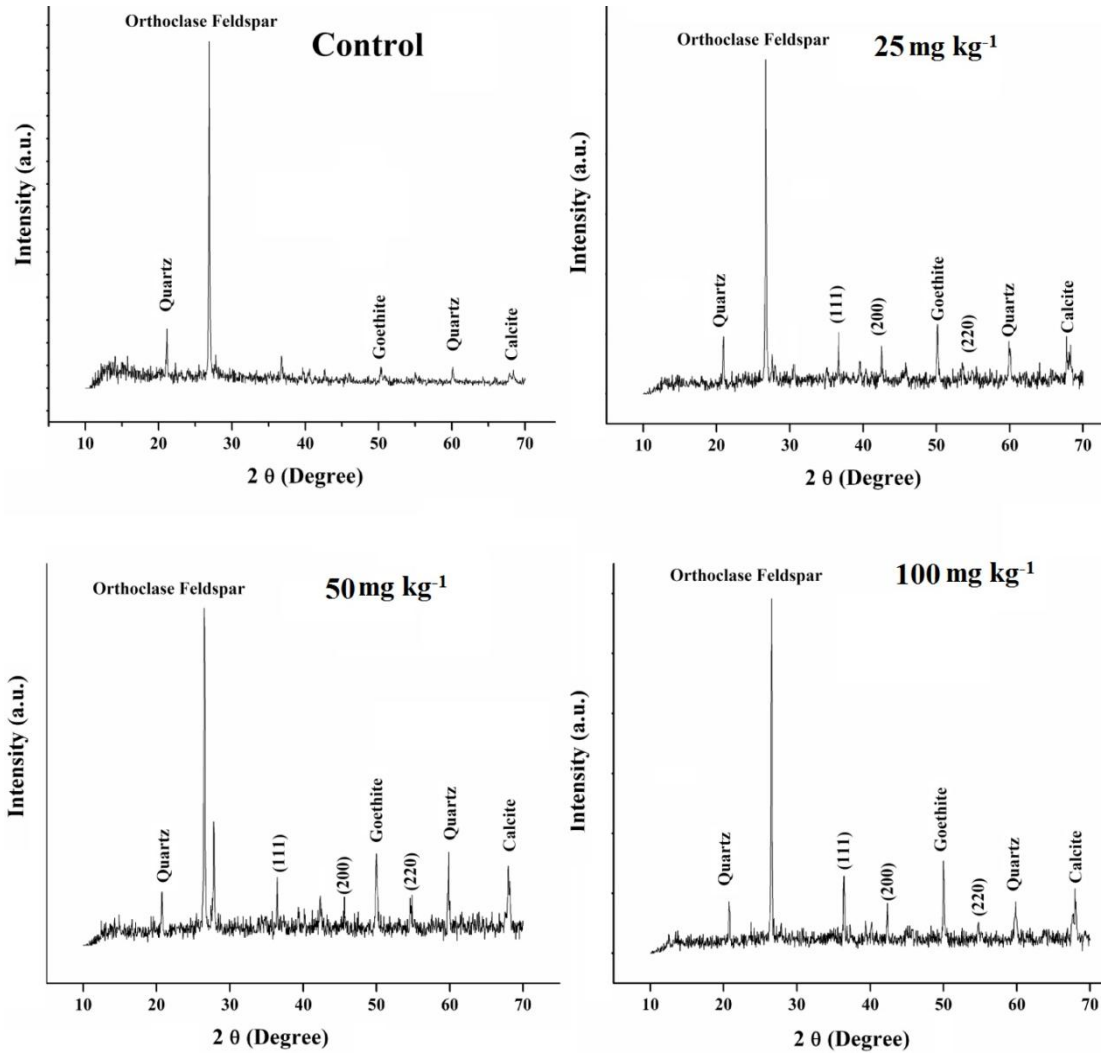

Fig. 4.2: XRD analyses showing the impact of GSNPs on soil structure, source: Das et al. [6]

4.4.1.2. Impact of various concentrations of GSNP and CSNP on soil quality attributes

Inherently, the N and P levels in the soil was 314.6 ± 2.2 mg kg^{-1} and 29.6 ± 1.1 mg kg^{-1} respectively; the soil had a pH of 6.5 ± 0.6, bulk density (BD) 1.26 ± 0.2 g cm^{-3}, and water holding capacity (WHC) 52.5 ± 2%; cation exchange capacity and soil organic carbon in the soil was recorded as 4.49 ± 0.22 mmol kg^{-1} and 2.1 ± 0.6% respectively.

Table 4.2 lists our measured variability of BD, WHC, pH, CEC, SOC, available N, available P, and urease activity in silver nanoparticle treated soil samples. The GSNP20 conditions yielded the greatest reduction in soil BD, followed by GSNP25, GSNP50, CSNP20, and CSNP25 (P = 0.000; LSD = 0.32). The soil WHC was

greatest for the GSNP50 condition, followed by CSNP50, CSNP25, and CSNP20 (P = 0.000; LSD = 1.8).

The soil pH shifted toward neutral range during the study period for all conditions observed. The maximum increment in pH was recorded for GSNP50, followed by GSNP25 (P = 0.000; LSD = 0.15) (Table 4.2). Soil CEC after 70 days of incubation was observed in the following order: GSNP50 > CSNP50 > GSNP100 = CSNP100 > GSNP25 = GSNP20 > CSNP25 = CSNP20 = control (LSD = 2.98).

The original soil was inherently rich in SOC content. However, significant increments in SOC were recorded under various silver nanoparticles treatments, being greatest for GSNP50 (61.9%), followed by GSNP20, GSNP25, and CSNP50 (P = 0.000; LSD = 0.13). GSNP50 and GSNP25 yielded the greatest urease activity, followed by GSNP20 (LSD = 1.53). N availability was highest for GSNP50 and CSNP50, followed by CSNP25 and GSNP25 (LSD = 18.36). P availability was highest for GSNP50 and GSNP25, followed by CSNP50, CSNP25, and CSNP20 (P = 0.000; LSD = 1.61).

4.4.1.3. Benefit percentage

The benefit percentages were computed to assess the overall beneficial impacts of the various silver nanoparticle treatments on soil quality (Fig. 4.3).The benefit percentages for WHC and BD were the highest for GSNP50, followed by GSNP20, GSNP25, and GSNP100. The benefit percentage for CEC was also greatest for GSNP50 (Fig. 4.3). The benefit percentages for N and P availability in soil were also highest for GSNP50.

Table 4.2: Impacts of various concentrations of GSNP and CSNP on soil quality, source: Das et al. [6]

Treatment	pH	Water holding capacity (%)	Bulk density ($Mg\ m^{-3}$)	Total organic C (%)	Available N ($mg\ kg^{-1}$)	Available P ($mg\ kg^{-1}$)	Urease activity ($mg\ kg^{-1}$)	Cation exchange capacity (m mole kg^{-1})
Control	6.7 ± 0.13	51.81 ± 1.6	1.15 ± 0.09	2.1 ± 0.1	318.4 ± 4.0	29.52 ± 2.1	45.76 ± 1.5	2.51 ± 0.2
CSNP 20	7.0 ± 0.10	60.46 ± 2.1	1.08 ± 0.03	2.8 ± 0.3	330.4 ± 4.8	41.56 ± 1.5	47.21 ± 1.6	2.56 ± 0.31
CSNP 25	7.1 ± 0.17	63.29 ± 2.8	1.08 ± 0.04	3.0 ± 0.2	431.2 ± 4.7	43.01 ± 1.5	47.48 ± 1.8	2.77 ± 0.23
CSNP 50	7.1 ± 0.2	65.05 ± 2.5	1.13 ± 0.03	3.1 ± 0.2	451.2 ± 4.3	45.98 ± 2.7	47.34 ± 2.1	8.41 ± 0.21
CSNP 100	7.0 ± 0.17	58.14 ± 2.1	1.19 ± 0.03	2.1 ± 0.1	411.2 ± 3.7	38.98 ± 1.8	46.09 ± 1.4	6.79 ± 0.22
GSNP 20	7.1 ± 0.15	55.85 ± 3.0	1.01 ± 0.05	3.1 ± 0.1	341.6 ± 3.9	36.89 ± 1.5	49.52 ± 1.8	3.20 ± 0.33
GSNP 25	7.2 ± 0.17	57.23 ± 1.4	1.02 ± 0.02	3.1 ± 0.2	418.0 ± 4.7	47.71 ± 2.0	50.11 ± 1.6	3.48 ± 0.32
GSNP 50	7.3 ± 0.26	68.01 ± 2.0	1.06 ± 0.03	3.4 ± 0.1	488.4 ± 4.2	49.21 ± 1.9	50.18 ± 2.2	8.71 ± 0.16
GSNP 100	7.1 ± 0.17	55.69 ± 1.1	1.14 ± 0.03	2.8 ± 0.2	415.6 ± 4.2	34.17 ± 2.1	47.08 ± 2.2	6.79 ± 0.18
P value	0.000	0.000	0.000	0.000	0.000	0.000	0.000	0.000
LSD	0.15	1.8	0.32	0.13	18.36	1.61	1.53	0.298

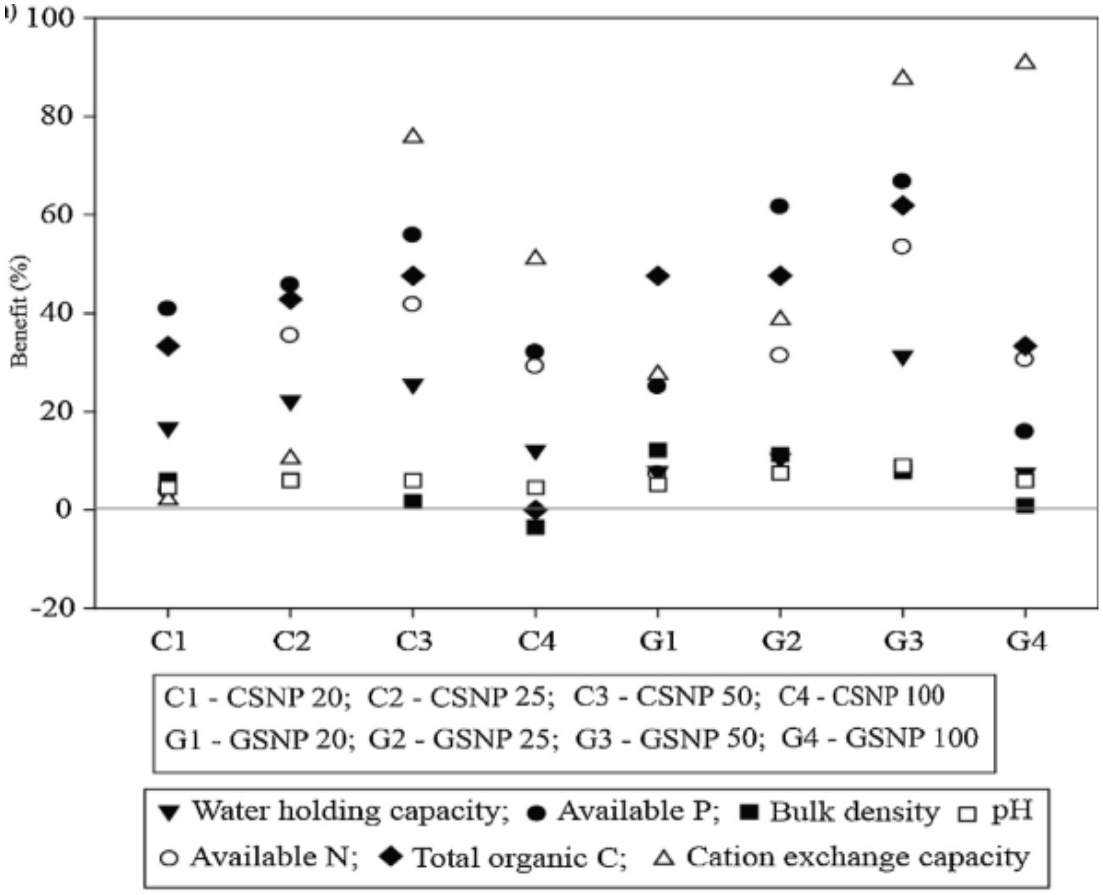

Fig. 4.3: Comparison of the beneficial impacts of green silver nanoparticles (GSNPs) and conventional silver nanoparticles (CSNPs) on soil health [pH, water holding capacity (WHC), cation exchange capacity (CEC), soil total organic carbon (TOC), bulk density (BD), and available N (Av N) and P (Av P)] expressed as benefit percentages, source: Das et al. [6]

4.4.1.4. Lab scale batch experiments: Impact of GSNPs on total N and nitrate leachability in soil

A mechanistic experiment with sterilized soil was carried out to understand the impact of GSNPs on N content in soil (Fig. 4.4). Interestingly, a gradual increase in total Kjeldahl N (TKN) was observed in soils treated under the GSNP25 and GSNP50 conditions. However, high TKN was recorded for GSNP100 over 10 days but then decreased substantially (Fig. 4.4). Inoculation by GSNPs up to 50 mg kg^{-1} had clear positive impacts on soil N content.

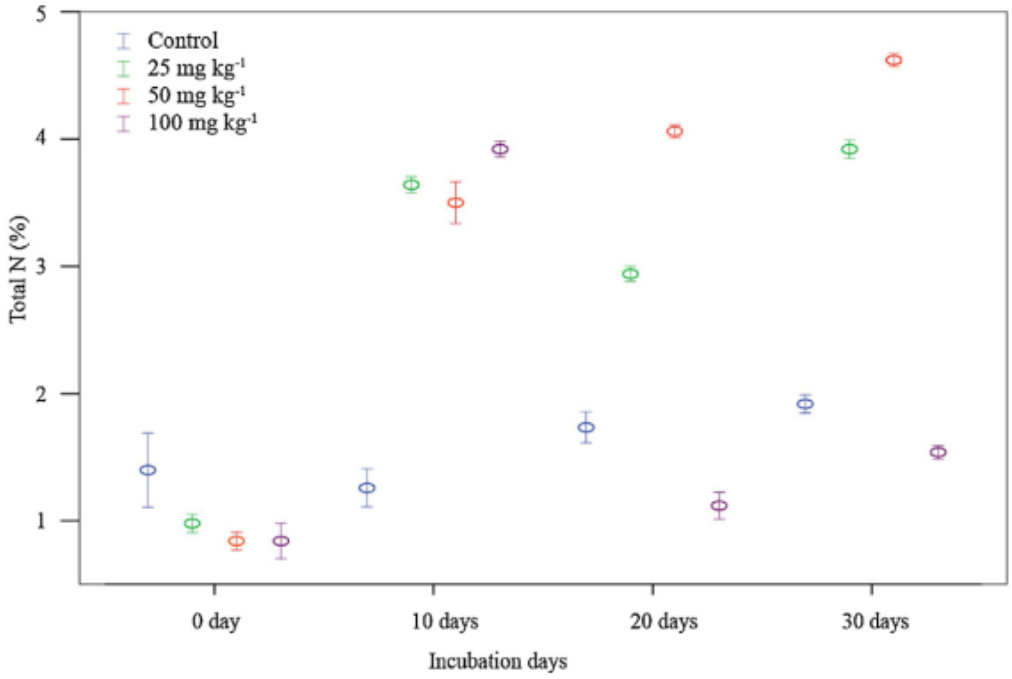

Fig. 4.4: Total Kjeldahl N (TKN) content (%) in sterilized soils treated with GSNPs, source: Das et al. [6]

The effect of GSNP concentration on the leaching of NO_3^- from soil was assessed by means of a column experiment; Table 4.3 summarizes the results. Significant reduction of NO_3^- content in leachates was observed in GSNP25, GSNP50, and GSNP100 inoculated soil samples compared to the control. The NO_3^- concentration was highest in the control at both measurement times (24 and 48 h); the lowest NO_3^- content was recorded for GSNP25, followed by GSNP50, and GSNP100. The rate of NO_3^- leaching was faster at 24 h after the initiation of the experiment than at 48 h.

Table 4.3: Leaching of nitrate from GSNP-treated soils, source: Das et al. [6]

Treatment	NO_3^- in leachate after 24 hr (mg L^{-1})	NO_3^- in leachate after 48 hr (mg L^{-1})
$GSNP_{25}$	44.8 ± 1.1	0.6 ± 0.1
$GSNP_{50}$	63.3 ± 1.5	11.2 ± 0.7
$GSNP_{100}$	74 ± 1.7	19.1 ± 0.9
No treatment	145.4 ± 1.5	56 ± 1.7
P for treatment	0.000	
P for time (hr)	0.000	
P for treatment × hr	0.000	
LSD	1.02	

*The results have been compared on the basis of two-way ANOVA followed by least significant difference (LSD) post-hoc test.

4.4.1.5. Effect of GSNP and CSNP on pod yield, weight loss of pod, leaf number, LAI, and uptake of N, P of P. vulgaris

The impacts of SNPs on health of *P. vulgaris* were assessed in terms of leaf number, LAI, pod yield (g plant^{-1}), pod weight loss over 30 days, and uptake of N and P in French bean (*P. vulgaris*) (Fig. 4.5). The LAI and leaf number of *P. vulgaris* plants cultivated under various treatment conditions were recorded 15 and 45 days after sowing (DAS) and at physiological maturity (60 DAS). Leaves at maturity were most numerous under GSNP50, followed by GSNP25 (P for treatment = 0.000; LSD = 0.34). Moreover, GSNP50 provided the greatest increment in LAI, followed by GSNP25 and CSNP50 (P for treatment = 0.000; LSD = 2.35).

Interestingly, GSNP50 yielded an N uptake up to 4.8 times that of the control (Fig. 4.5); overall, N uptake in pods followed the trend: GSNP50 > CSNP50 = GSNP20 > CSNP20 (P = 0.000; LSD = 0.28). GSNP50 and CSNP50 yielded the highest P uptakes (P = 0.000; LSD = 1.59). Moreover, GSNP50 yielded the lowest pod weight loss, followed by GSNP25, GSNP20, and GSNP100 (P = 0.000; LSD = 1.25) (Fig. 4.5). GSNP50 and CSNP50 treatments gave the highest pod yields, followed by GSNP25, GSNP20, and CSNP100 (P = 0.000; LSD = 1.4).

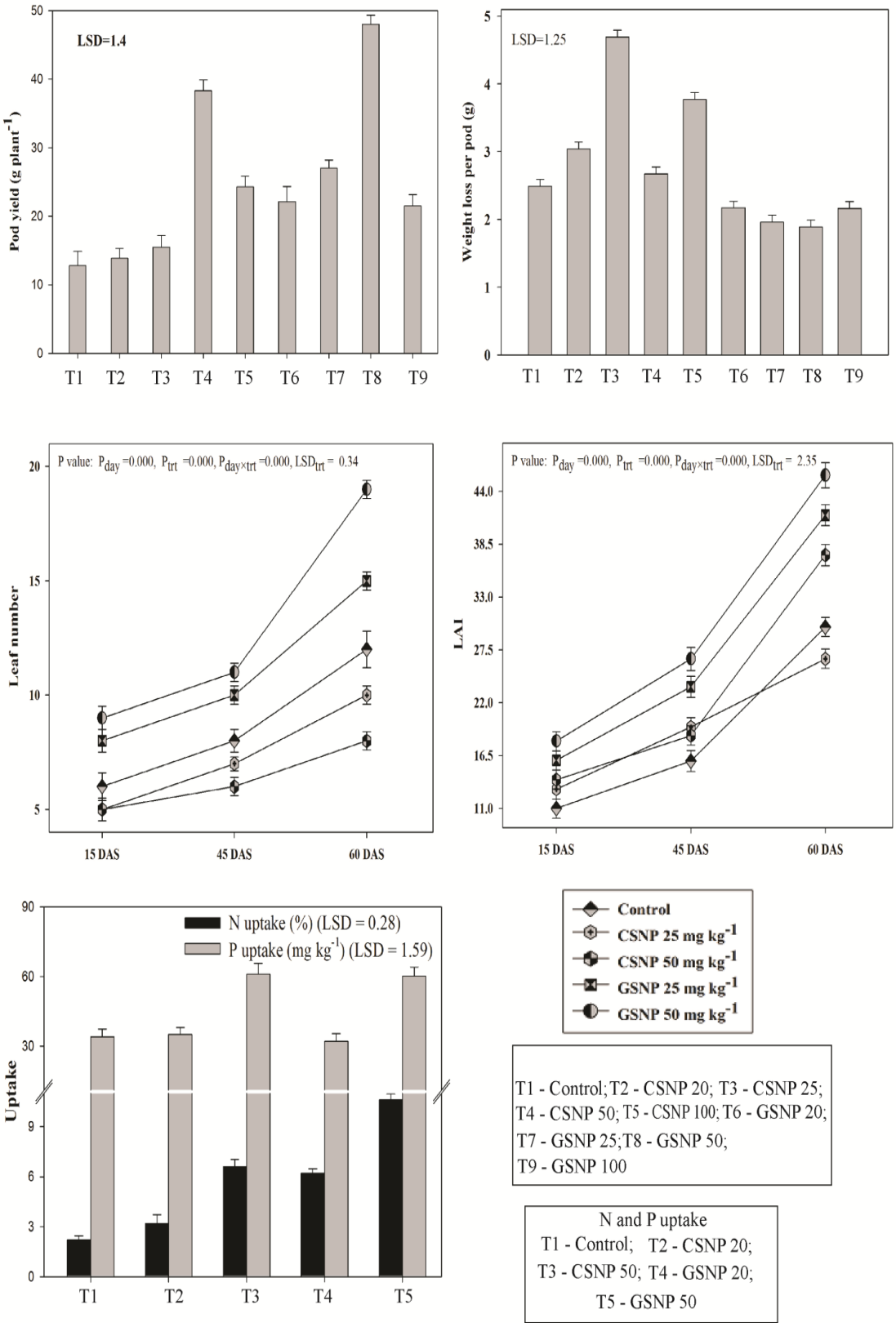

Fig. 4.5: Impacts of GSNPs and CSNPs on leaf number, LAI, pod yield, weight loss per pod, and nutrient uptake (N and P) of *P. vulgaris*, source: Das et al. [6]

4.4.1.6. Impacts of GSNP and CSNP on proline levels, crude protein content, chlorophyll content, activity of nitrate reductase (NR) enzyme, and the expression of mRNA for NR and Fd in leaves of P. vulgaris under various treatments:

Proline expression increases in plants grown under oxidative stress. Therefore, proline levels were measured to assess the internal stress in plants arising from silver nanoparticle exposure (Fig. 4.6).

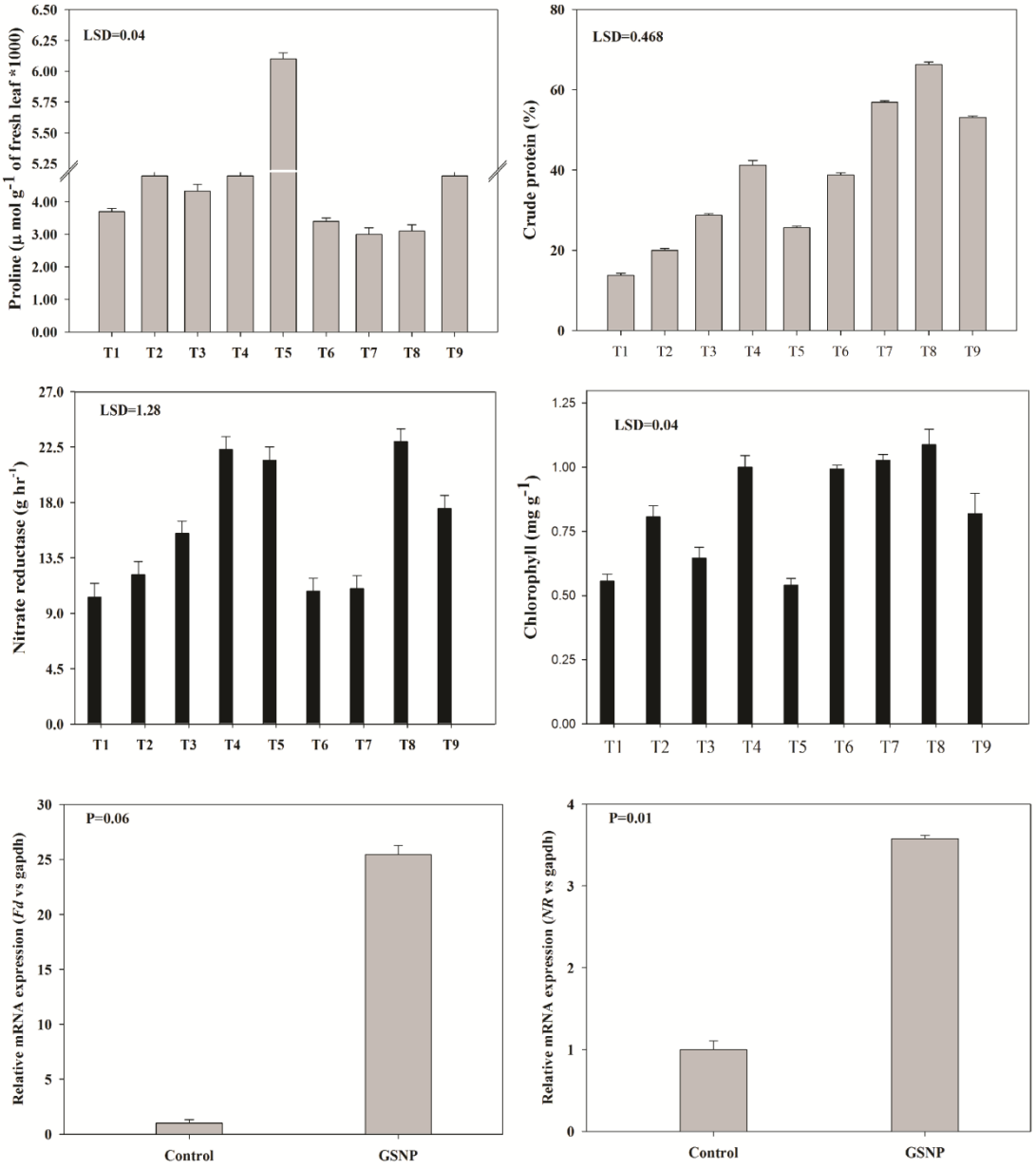

Fig. 4.6 : Impacts of SNPs on proline levels, crude protein content, chlorophyll content, activity of nitrate reductase (NR) enzyme, and the expression of mRNA for *NR* and *Fd* in leaves of *P. vulgaris* under various treatments, source: Das et al. [6]

Proline levels were quite high in plants exposed to CSNP, even at low concentrations (20 and 25 mg kg^{-1}) and increased significantly for the higher CSNP levels of 50 and 100 mg kg^{-1}, suggesting higher oxidative stress on plant metabolisms under higher doses of CSNPs (P = 0.000; LSD = 0.04). Hence, the data of our experiment imply that the threshold of CSNP exposure in *P. vulgaris* should fall between 25 to 50 mg kg^{-1}.

The effects of the various silver nanoparticle treatments on chlorophyll and NR activity in *P. vulgaris* leaves are presented in Fig. 4.6. The highest chlorophyll content was observed under the GSNP50 and GSNP25 conditions, followed by CSNP50 and GSNP20 (P = 0.000; LSD = 0.04) (Fig. 4.6). The highest NR activity was observed for GSNP50, followed by CSNP50 (P = 0.000; LSD = 1.28). Considerably higher protein content in *P. vulgaris* pods was recorded under GSNP treatments compared to CSNP treatments; the overall trend in protein content was GSNP50 > GSNP25 > GSNP100 > CSNP50 > GSNP20 > CSNP25 > CSNP100 > CSNP20 > control (P = 0.000). In light of the positive impacts of GSNP-containing soils with respect to nutrient uptake, NR activity, protein content, chlorophyll content, and the expression of *NR* and *Fd* genes in plants was verified. *NR* gene expression in GSNP-treated plants was 3.58 times that of the control, and *Fd* gene expression of up to 25.46 times that of the control was observed in GSNP-treated plants.

4.4.1.7. Effect of AgNP on pH, available N, P, soil respiration, activity of urease & phosphatase of cropped soil under tomato cultivation

The pH change was insignificant with 10 mg kg^{-1} AgNP exposure in soil under tomato cultivation (Fig. 4.7). N availability was 2.9 folds lower under $AgNP_{10}$ treatment than the control (P < 0.01). Moreover, AgNP incorporation also significantly reduced P availability in soil under tomato cultivation (Fig. 4.7). Almost 1.11–1.66 folds reduction of P availability was recorded under $AgNP_{10}$ treatment compared to the control (Fig. 4.7). However, significantly reduction in soil respiration, urease and phosphatase activity was recorded under AgNP treatments than the control in cropped soil (Fig. 4.7).

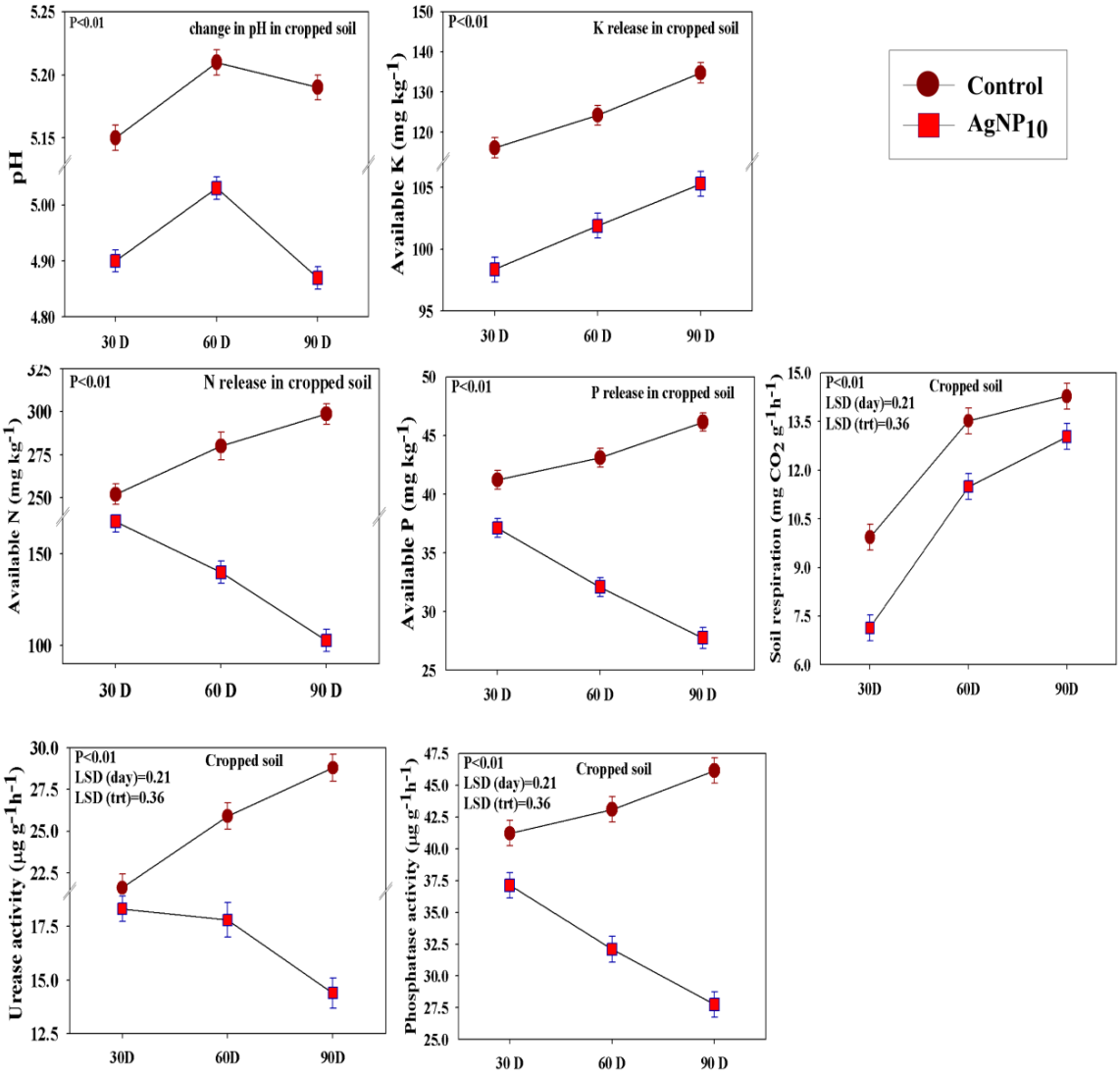

Fig. 4.7: Impact of AgNP on pH, N, P, K availability, soil respiration, urease and phosphatase activity of cropped soil under tomato cultivation, source: Das et al. [5]

4.4.1.8. Growth of tomato plant under AgNP treated soil in pot study

Although, leaf number and leaf area index of tomato was greater in AgNP treated plants than the control, the crop yield was significantly reduced due to AgNP exposure ($P < 0.01$) (Table 4.4, Fig. 4.8). To appreciate the cause plant metabolic activity was also studied.

Table 4.4: Effect of AgNP on leaf number and leaf area index (LAI) in tomato plant, source: Das et al. [5]

Treatment	Leaf number	Leaf area index
	30 Day	30 Day
Control	33±1.7	31.37±0.9
$AgNP_{10}$	37±2	33.9±0.5
P value (<0.01)		

4.4.1.9. Effect of AgNP on uptake of N, P, K, Ag, and yield of tomato seedlings

We recorded poor uptake of N, P, and K (1.29–2.47 times lower than control) in AgNP treated plants whereas, Ag accumulation was significantly greater in treated fruits and leaves than the control ($P < 0.05$) (Fig. 4.8).

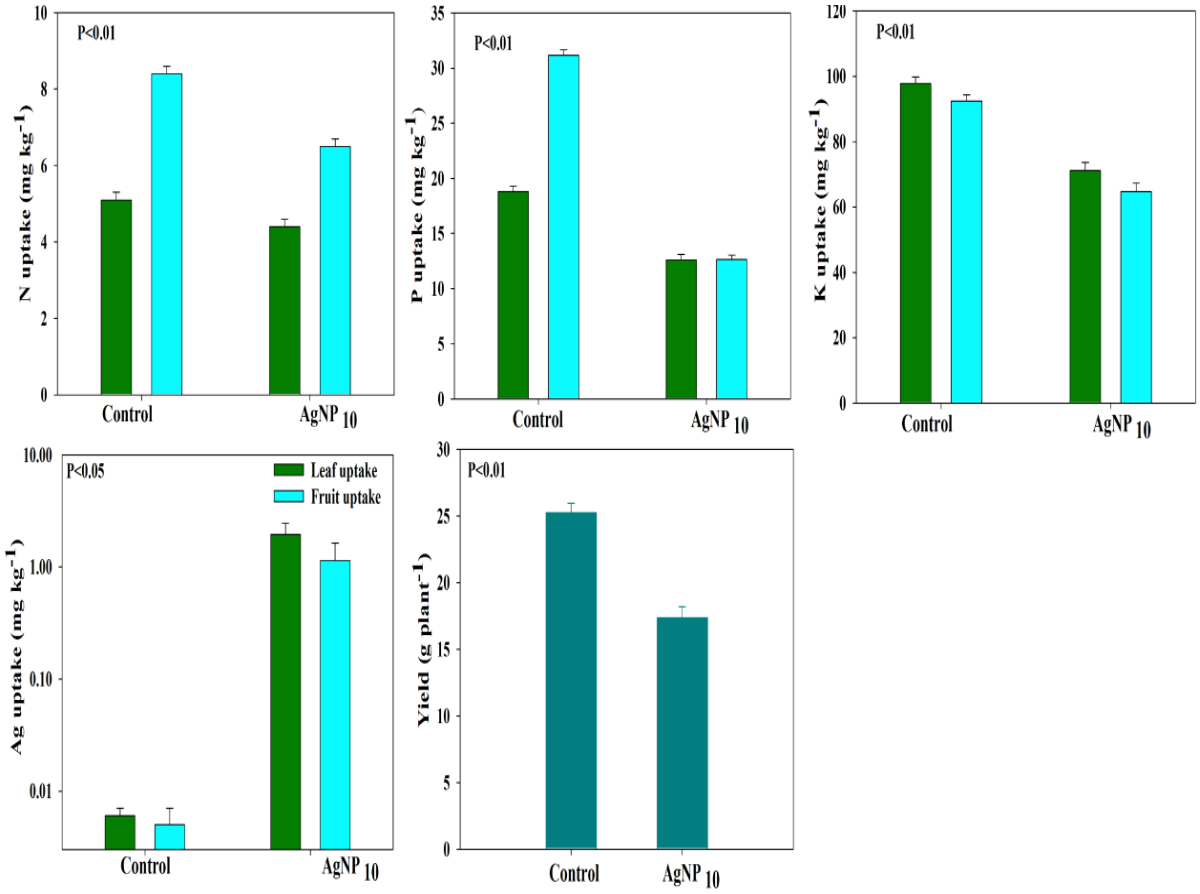

Fig. 4.8: Uptake of N, P, K, Ag, and yield of AgNP treated and untreated tomato (*Lycopersicon esculentum*) (Error bar represent standard deviation), source: Das et al. [5]

4.4.1.10. Activity of glutamine synthetase (GS), glutamate synthase (GOGAT), nitrate reductase (NR), and expression of GS2 and GOGAT gene in leaves of AgNP treated tomato

The low N assimilation in AgNP treated plants was closely related to the activity of GS, GOGAT, and NR enzyme. The activity of NR enzyme was significantly lower in AgNP treated plants than the control ($P < 0.01$). While, the activity of GS and GOGAT enzymes was 1.21 and 1.18 times greater in untreated leaves (control) than the AgNP treated ones ($P < 0.01$) (Fig. 4.9). Such poor activity of these important enzymes probably affected the plant growth due to AgNP exposure. We also confirmed this statement by observing the expression of the respective genes of glutamine synthetase (GS) and glutamate synthase (GOGAT) enzymes in tomato leaves. The *GS1* and *GS2* genes trigger GS activity in cytosol and chloroplast respectively. Hence, we assessed *GS2* expression because the significance of chloroplast is more in leaves than any other plant parts. Eventually, the expression of *GS2* and *GOGAT* genes were significantly retarded in AgNP treated tomato leaves compared to control (Fig. 4.9) ($P < 0.01$).

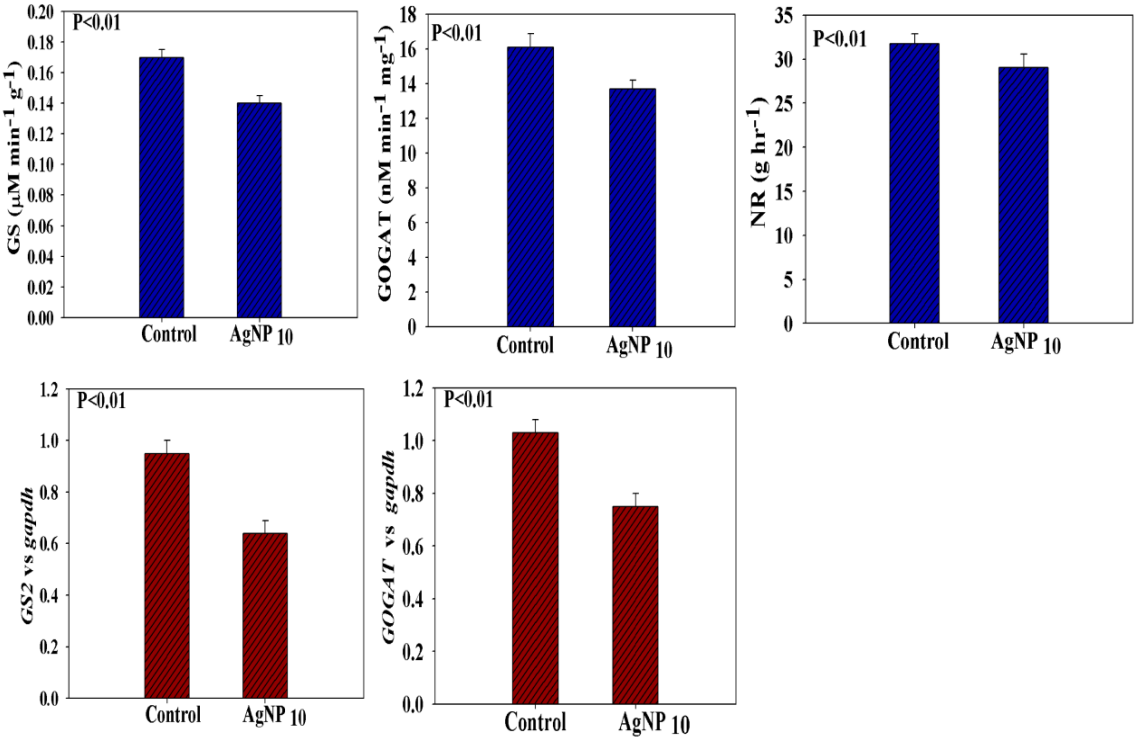

Fig. 4.9: Activity of glutamine synthetase (GS), glutamate synthase (GOGAT), nitrate reductase (NR) and relative mRNA expression of *GS2* and *GOGAT* gene in leaves of AgNP treated tomato (Error bar represent standard deviation), source: Das et al. [5]

4.4.1.11. Oxidative stress, chlorophyll, photosynthetic rate (PS), and hill activity

The oxidative stress in tomato due to AgNP exposure was indirectly measured through lipid peroxidation, proline content, and catalase activity (Table 4.5). Although catalase activity was low in tomato due to AgNP exposure, the lipid peroxidation was significantly greater in plants treated with AgNP than the control ($P < 0.01$). Moreover, proline content was 8.22 folds greater in AgNP treated tomato than control ($P < 0.01$).

The data on chlorophyll content, hill activity, and PS rate were presented in Table 4.5. Chlorophyll content was significantly lower in AgNP treated plants than the control ($P < 0.01$); concurrently, hill activity and the rate of photosynthesis were 1.2 and 1.5 folds lower in AgNP treated tomato than the untreated ones ($P < 0.01$).

Table 4.5: Catalase activity, lipid peroxidation, proline content, photosynthetic rate, chlorophyll content, and hill activity in treated and untreated tomato (mean± standard deviation), source: Das et al. [5]

Treatment	Attributes					
	Catalase (ml min^{-1} g^{-1})	Lipid peroxidation (µM g^{-1})	Proline (µM g^{-1})	Photosynthetic rate (µM CO_2 m^{-2} s^{-1})	Chlorophyll (mg g^{-1})	Hill activity (µM h^{-1})
Control	7.99 ± 4	0.04 ± 0.002	1043.9 ± 12	7.53 ± 0.23	22.68 ± 0.2	4126.67 ± 25.48
$AgNP_{10}$	5.33 ± 2.3	0.08 ± 0.004	8579.6 ± 48	4.99 ± 0.16	16.05 ± 0.2	3533.33 ± 10.21
P value	< 0.01	< 0.01	< 0.01	< 0.01	< 0.01	< 0.01

4.4.1.12. Effects of SNPs on soil microorganisms

The counts of total bacteria, nitrogen fixing (NFB), and phosphate solubilizing (PSB) bacteria have been presented in Table 4.6. The total bacterial count in samples of the soil under French bean cultivation was highest for GSNP50, followed by GSNP25, GSNP20, and CSNP20 (P = 0.000; LSD = 0.18). NFB populations in the soil samples followed the order GSNP50 > GSNP25 > GSNP20 > GSNP100> CSNP25 > CSNP50 > CSNP20 > CSNP100> control (P = 0.000; LSD = 0.11). Similarly, the PSB population was highest for the GSNP50 and GSNP25 treatments, followed by GSNP20 (P = 0.000; LSD = 0.25)

Table 4.6: Impact of GSNPs and CSNPs on total, NFB, and PSB bacterial growth (number of bacteria mL^{-1}), source: Das et al. [6]

	Total count $mL^{-1} \times 10^8$	**NFB count $mL^{-1} \times 10^8$**	**PSB count $mL^{-1} \times 10^8$**
	Mean ± std. dev.	**Mean ± std. dev.**	**Mean ± std. dev.**
Control	4 ± 0.25	3 ± 0.25	3.5 ± 0.25
CSNP 20	5.8 ± 0.26	4 ± 0.26	4.8 ± 0.26
CSNP 25	5.12 ± 0.20	5.1 ± 0.20	4.5 ± 0.20
CSNP50	4.4 ± 0.24	4.6 ± 0.24	4.4 ± 0.24
CSNP 100	4.1 ± 0.14	3.8 ± 0.14	3.7 ± 0.14
GSNP 20	5.8 ± 0.19	5.5 ± 0.19	5 ± 0.19
GSNP25	6 ± 0.26	6.2 ± 0.26	6 ± 0.26
GSNP 50	6.4 ± 0.2	6.8 ± 0.2	6.2 ± 0.2
GSNP100	4 ± 0.27	5.4 ± 0.27	4.1 ± 0.27
P value	0.000	0.000	0.000
LSD	0.18	0.11	0.25

4.4.2. In depth and long term study

Based on the preliminary studies it appeared that the GSNP/AgNP has had some positive impact on soil quality with special emphasis to N availability and plant growth and metabolism. Therefore, it was imperative to understand the impacts of GSNP on soil-plant system through more in depth and long term assessments.

4.4.2.1. AgNP-pH interaction in soil and soil-less medium

The AgNP-pH interaction was studied in soil media (Table 4.7) as well as in aqueous media (Fig. 4.10). In soil, the pH change was at the initial period however decreased significantly from 24^{th} week. The soil pH was least affected by $AgNP_{10}$. In acidic (pH = 4.0) aqueous medium, the AgNP incorporation sharply reduced the pH at early stage and increased slightly at the later (Fig. 4.10). Similarly, considerable reduction in pH of the neutral (pH = 7.0) and the alkaline (pH = 9.0) solutions was evidenced immediately after AgNP incorporation, which slightly increased after 72 h. Overall, the 50 ppm (mg kg^{-1}/mg L^{-1}) concentration was most severe in regard to pH drop in soil and aqueous media.

When AgNP was added in KH_2PO_4 containing solutions, the media pH significantly declined over time and the pH was lowest under $AgNP_{50}$ exposure followed by $AgNP_{25}$ and $AgNP_{10}$ ($P < 0.01$; LSD = 0.02) (Fig. 4.10). In contrast, in presence of $(NH_4)_2SO_4$, the media pH rapidly increased, which may be due to transformation of free NH_4^+ to NH_3; alkalinity of such solution significantly elevated in presence of $AgNP_{50}$ ($P < 0.01$).

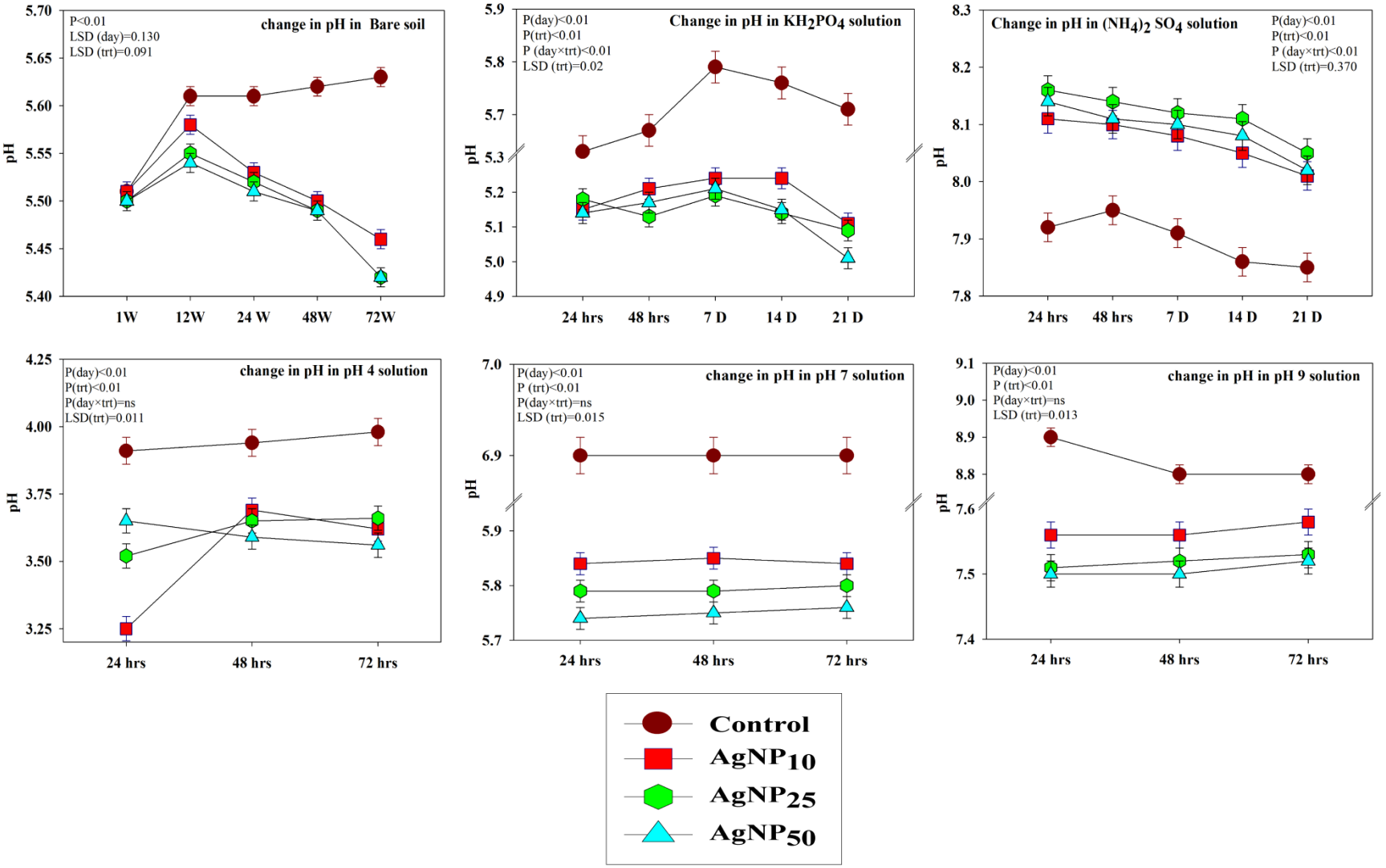

Fig. 4.10: Effect of AgNP on pH in soil and aqueous media (Error bar represent standard deviation), source: Das et al. [5]

Table 4.7: Impact of AgNP on changes in pH, available K, microbial biomass carbon (MBC), microbial biomass nitrogen (MBN) and Ag content in soil (mean± standard deviation), source: Das et al. [5]

Attributes		0 day	4 weeks	8 weeks	12 weeks	24 weeks	48 weeks	60 weeks	72 weeks
pH	T1	5.51±0.17	5.53±0.2	5.57±0.82	5.61±0.10	5.61±0.1	5.62±0.11	5.6±0.02	5.63±0.08
	T2	5.51±0.19	5.53±0.16	5.55±0.13	5.58±0.40	5.53±0.48	5.5±0.28	5.48±0.11	5.46±0.1
	T3	5.5±0.1	5.52±0.02	5.53±0.31	5.55±0.44	5.52±0.5	5.49±0.23	5.45±0.1	5.42±0.12
	T4	5.5±0.17	5.51±0.1	5.52±0.5	5.54±0.63	5.51±0.68	5.49±0.35	5.45±0.11	5.42±0.11
Avl K ($mg\ kg^{-1}$)	T1	115.03±0.4	143.43±2.9	164.53±1.02	175.03±0.5	178.97±0.5	180.8±0.26	181±0.45	182.07±0.2
	T2	112.67±0.8	147.2±1.1	175.63±1.1	174.9±2.8	168.73±1.1	147.03±0.5	126.5±2.8	122±0.38
	T3	110±0.5	146.57±1.3	174.7±1.6	174.1±1.6	166.2±0.75	146.77±4.9	128.37±4.7	118±0.15
	T4	107.13±0.5	146.03±3.3	170.6±0.9	173.83±3.1	163.77±0.25	141.1±0.6	128±0.5	108±1.36
MBC ($\mu g\ g^{-1}$)	T1	41.99±2.7	51.34±1.2	61.89±1.5	66.46±1.4	69.39±1.2	70.48±1.2	75.95±2.2	78.18±1.7
	T2	41.99±1.7	55.09±2.3	72.44±4.9	67.51±1.4	62.36±2.3	51.57±1.1	38.45±0.4	30±0.8
	T3	39.62±3.5	54.04±0.2	69.04±1.9	66.23±1.6	59.54±2.2	48.17±1.1	37.39±1.3	27.55±1.2
	T4	37.82±0.8	52.39±1.3	67.39±2.6	64.94±0.8	55.79±1.4	46.53±1.4	36.92±1.1	22.26±1.3
MBN ($\mu g\ g^{-1}$)	T1	6.53±0.41	7.62±0.18	9.18±0.23	9.86±0.21	10.3±0.18	10.5±0.18	11.27±3.4	11.6±0.3
	T2	6.53±0.26	8.17±0.35	10.75±0.7	10.02±0.21	9.25±0.3	7.65±0.17	5.7±0.1	4.4±0.12
	T3	5.88±0.52	8.02±0.03	10.24±0.3	9.83±1.9	8.84±0.3	7.15±0.18	5.55±0.2	4.1±0.6
	T4	5.61±0.11	7.77±0.2	10±0.4	9.64±0.12	8.28±0.2	6.9±0.2	5.48±0.15	3.9±0.6
Ag ($mg\ kg^{-1}$)	T1	0.01±0.008	0.001±0.01	0.01±0.005	0.007±0.001	0.005±0.001	BDL	BDL	BDL
	T2	0.04±0.01	2.39±0.04	2.26±0.03	2.24±0.04	2.03±0.05	1.85±0.03	1.76±0.01	1.41±0.02
	T3	0.04±0.01	2.89±0.04	2.63±0.03	2.57±0.01	2.67±0.06	2.49±0.01	2.42±0.02	2.15±0.03
	T4	0.07±0.06	2.99±0.06	3.03±0.05	3.12±0.02	3.02±0.04	2.89±0.01	2.79±0.01	2.46±0.01
P value		pH P<0.01		Avl K P<0.01		MBC P<0.01	MBN P<0.01		Ag P<0.01
L.S.D		LSD(d)=0.130 LSD(t)=0.091		LSD(d)=0.074 LSD(t)=0.052		LSD(d)=2.07 LSD(t)=1.46	LSD(d)=0.31 LSD(t)=0.22		LSD(d)=0.012 LSD(t)=0.008

T1=Control, T2=$AgNP_{10}$, T3=$AgNP_{25}$, T4=$AgNP_{50}$ LSD: d = day t = treatment; BDL = Below Detection Limit

4.4.2.2. Effects of AgNP on N, S, P, and K availability in soil and aqueous media

The N availability in soil increased by 17.4–23.9% due to AgNP incorporation in first 12 weeks compared to the initial value (Fig. 4.11, Table 4.8). However, N mineralization progressively reduced in soil after 12 weeks. As such, the N availability in soil was 9–15.7% lower than the initial value due to AgNP application at 72nd week. Finally, the N availability was in the order: C > $AgNP_{10}$ > $AgNP_{25}$ > $AgNP_{50}$ ($P < 0.01$; LSD = 0.87) (Fig. 4.11, Table 4.8).

In aqueous medium NH_4^+ release from $(NH_4)_2SO_4$ significantly reduced due to AgNP exposure. Moreover, NH_4^+ release was significantly reduced under $AgNP_{50}$ as compared to $AgNP_{10}$ and control in aqueous media (Fig. 4.11).

P and K availability in AgNP treated soil significantly increased till 8th week and thereafter sharply decreased at a constant rate till 72nd week. In fact, about 28–32% reduction in soil P was evidenced due to AgNP exposure in various concentrations (Fig. 4.11). The bioavailability of P in soil was lowest under $AgNP_{50}$ followed by $AgNP_{25}$ and $AgNP_{10}$ ($P < 0.01$; LSD = 0.36) (Fig. 4.11). Similarly, the reduction in K availability in soil was maximum with $AgNP_{50}$ exposure followed by the others ($P < 0.01$; LSD =0.052).

Interestingly, the dissolution pattern of P and K in KH_2PO_4 mixed aqueous medium was very similar to that in soil (Fig 4.11). The solubility of P and K increased till 7th day and then sharply declined in presence of AgNP. As usual, the decrease in P and K solubility was significantly greater in presence of $AgNP_{50}$ than $AgNP_{25}$ and $AgNP_{10}$ ($P < 0.01$; LSD: P = 0.09; K = 0.05).

The SO_4^{2-} and S^{2-} contents in soil reduced by 3.30 and 4.9 folds due to 10 and 50 mg kg^{-1} AgNP application after 72 weeks. At 72nd week the order of S^{-2}/SO_4^{-2} availability in soil was: C > $AgNP_{10}$ > $AgNP_{25}$ > $AgNP_{50}$ ($P < 0.01$; LSD: Sulphate = 0.57; Sulphur = 0.22) (Fig. 4.12). Whereas, in aqueous media S^{2-} and SO_4^{2-} release from $(NH_4)_2SO_4$ was 1.2–1.4 times lower in presence of AgNPs than the control.

Table 4.8: Impact of AgNP on changes in available N, available P, urease, phosphatase activity, sulphur and sulphate content in bare soil (mean± standard deviation), source: Das et al. [5]

Attributes		0 day	4 weeks	8 weeks	12 weeks	24 weeks	48 weeks	60 weeks	72 weeks
Avl N	T1	158±1.6	168±1.8	182.93±1.6	203.47±1.1	201.6±2.8	210±2.8	214.67±3.2	220.27±1.6
(mg kg^{-1})	T2	163±1.6	180.13±1.6	190.4±0.8	209.07±1.6	188.53±1.8	167.07±4.3	149.3±1.6	145±1.6
	T3	155±1.6	176.4±1.8	188.53±1.6	197.87±1.6	182.93±1.6	159.6±2.8	144.67±1.6	141±4.3
	T4	150±1.6	174.53±1.6	182±1.8	192.27±1.6	174.53±1.6	158.67±3.2	146.53±1.6	134±2.8
Urease	T1	12.56±0.31	13.97±0.1	15.63±0.1	16.59±0.1	16.64±0.13	16.72±0.2	16.76±0.23	16.04±0.1
(µg $g^{-1}h^{-1}$)	T2	12.11±0.13	13.92±0.1	18.57±0.2	19.94±0.1	19.02±0.2	16.3±0.2	12.98±0.1	11.25±0.02
	T3	12.56±0.11	13.87±0.1	17.17±0.1	19.52±0.1	19.33±0.1	16.04±0.1	12.59±0.1	8.6±0.1
	T4	12.09±0.1	13.68±0.1	17.27±0.99	18.3±1.2	18.02±0.1	14.75±0.04	12.36±0.1	7.1±0.1
Avl P	T1	33.12±0.5	36.73±0.2	39.83±0.5	41.85±0.3	41.71±0.2	42.22±0.3	42.45±0.1	41.81±0.3
(mg kg^{-1})	T2	34.68±0.4	37.19±0.7	41.24±0.3	38.54±0.2	34.16±0.3	32.75±0.3	29.68±0.1	27±0.2
	T3	32.78±0.6	37.06±0.4	40.43±0.2	37.48±0.7	35.02±0.2	32.28±0.2	29.52±0.1	27.09±0.1
	T4	30.95±0.4	36.99±0.2	39.08±0.3	37.05±0.6	30.97±0.2	31.77±0.1	29.14±0.2	22±0.2
Phosphatase	T1	5.89±0.2	6.09±0.04	7.11±0.43	7.25±0.11	7.38±0.11	7.65±0.11	8.86±0.11	8.89±0.11
(µg g^{-1} h^{-1})	T2	5.56±0.49	6.23±0.22	7.21±0.84	7.68±0.09	7.51±0.09	7.11±0.09	5.51±0.02	5.11±0.06
	T3	5.42±0.24	6.2±0.34	7.14±0.07	7.57±0.04	7.48±0.04	7.09±0.04	5.48±0.04	5.01±0.04
	T4	5.79±0.07	6.19±0.09	7.08±1.2	7.45±0.18	7.31±0.18	6.96±0.18	5.44±0.04	4.95±0.05
Sulphate	T1	16.6±0.5	19.1±1.5	22.8±0.7	25.1±0.7	26.1±0.5	27.8±0.5	28.7±0.4	29.3±0.2
(mg kg^{-1})	T2	30±0.2	28.2±0.2	24.9±0.2	18.8±1	16.4±1.4	14.6±0.5	12.2±0.7	8.9±0.5
	T3	29.1±0.4	27.6±0.5	26.5±1	16.7±0.5	15.9±0.5	13.9±0.4	11.5±0.4	6.8±1
	T4	25.2±0.7	22.4±0.5	24.4±0.5	14.1±0.5	13.4±0.7	12.9±0.5	10.4±0.5	6.01±1.2
Sulphur	T1	5.5±0.2	6.4±0.5	7.6±0.2	8.4±0.2	8.7±0.2	9.3±0.2	9.6±0.1	9.7±0.1
(mg kg^{-1})	T2	10±0.1	9.4±0.1	8.3±0.1	6.3±0.3	5.5±0.5	4.8±0.2	4.1±0.2	2.9±0.2
	T3	9.7±0.1	9.2±0.2	8.8±0.3	5.5±0.2	5.3±0.2	4.7±0.2	3.8±0.1	2.3±0.3
	T4	8.4±0.2	7.5±0.2	8.1±0.2	4.7±0.2	4.4±0.2	4.3±0.2	3.5±0.2	2±0.4
		Avl N	Urease	Avl P	Phosphatase	Sulphate	Sulphur		
P value		P<0.01	P<0.01	P<0.01	P<0.01	P<0.01	P<0.01		
LSD		LSD(d)=1.23	LSD(d)=0.12	LSD(d)=0.21	LSD(d)=0.13	LSD(d)=0.81	LSD(d)=0.32		
		LSD(t)=0.87	LSD(t)=0.09	LSD(t)=0.36	LSD(t)=0.09	LSD(t)=0.57	LSD(t)=0.22		

T1=Control, T2=$AgNP_{10}$, T3=$AgNP_{25}$, T4=$AgNP_{50}$; LSD: d = day t = treatment

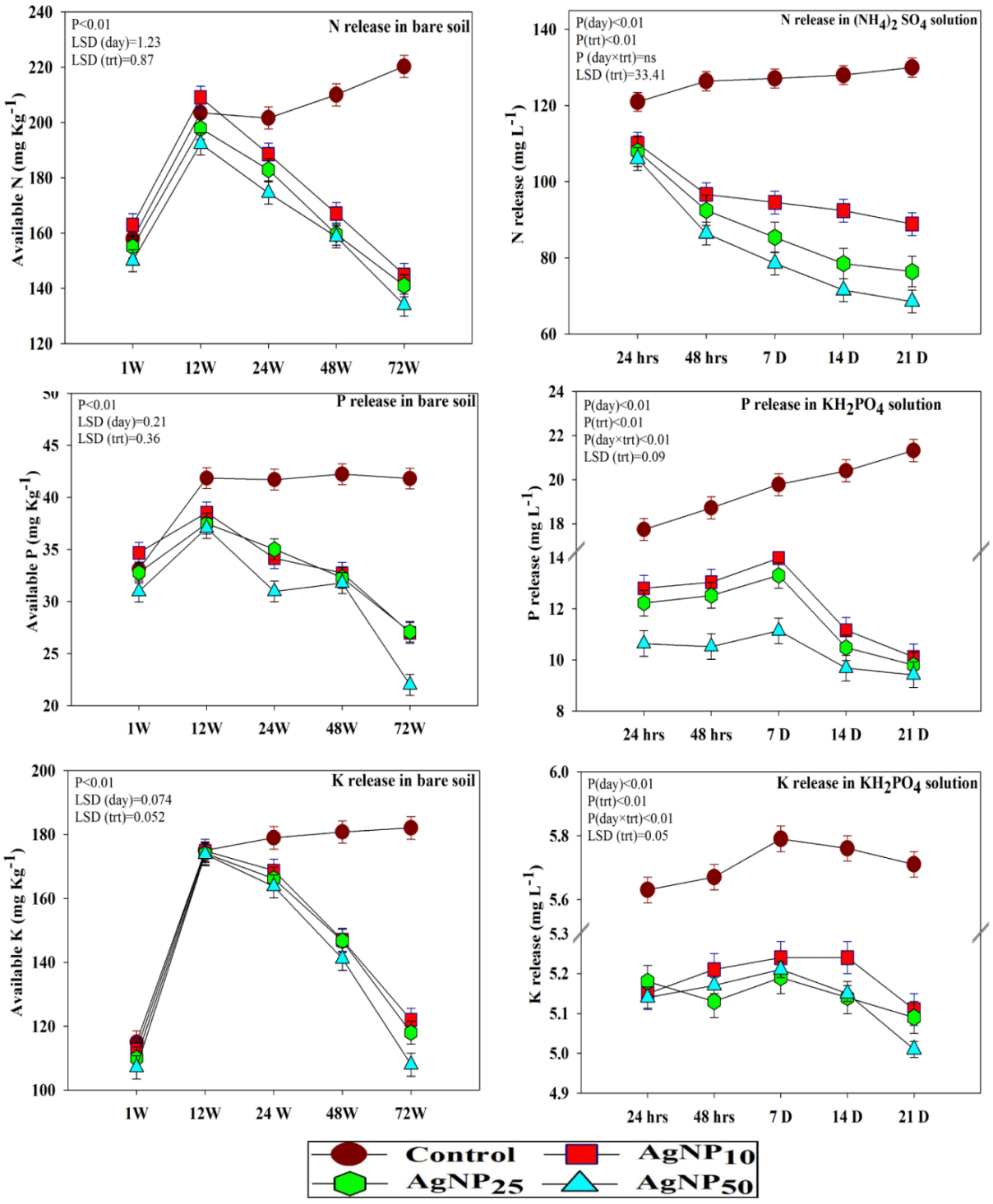

Fig. 4.11: Impacts of AgNP on N, P, and K availability in soil and aqueous media (Error bar represent standard deviation), source: Das et al. [5]

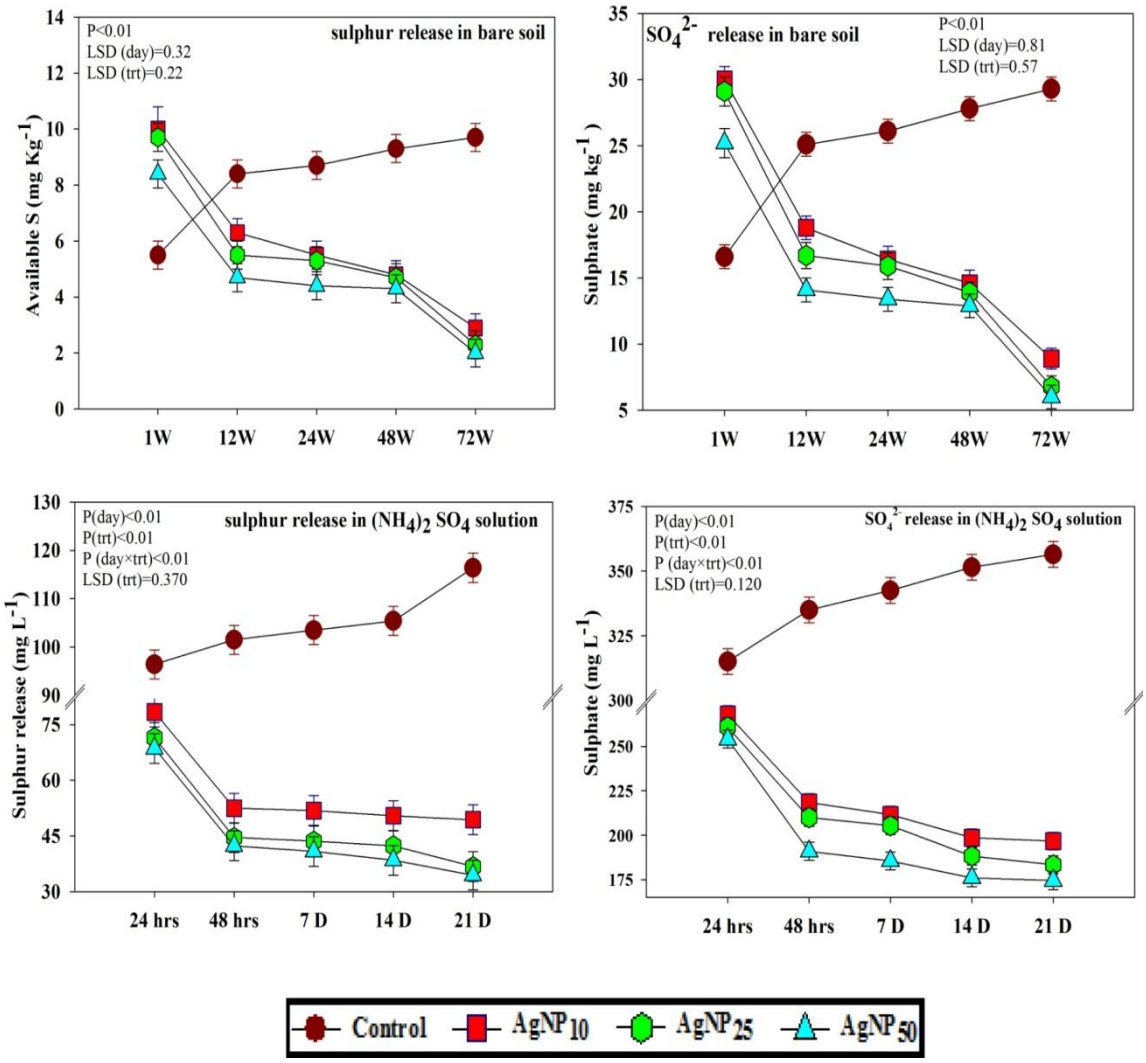

Fig. 4.12: Impacts of AgNP on availability of S in soil and aqueous media (Error bar represent standard deviation), source: Das et al. [5]

4.4.2.3. Silver (Ag^+) release profile, agglomeration/dispersion dynamics, and interactions with other elements in soil and aqueous media (N, P, K, and S): DLS and UV-VIS confirmation

The concentration of soluble Ag^+ sharply increased in soil between 1st to 4th weeks due to AgNP exposure which showed a slight reduction in the later stage (72^{nd} week) (Fig. 4.13, Table 4.7). Overall, Ag^+ concentration in soil was highest under $AgNP_{50}$ followed by $AgNP_{25}$ and $AgNP_{10}$ ($P < 0.01$; LSD = 0.008). This may be due to binding with mineral and organic matter complexes in soil. We recorded 1.54–1.85 times reduction in exchangeable silver fraction in soil; while the residual fraction of silver (Ag^+) enhanced by 4–13 folds between 4^{th} to 72^{nd} week (Table 4.9b).

Conventionally, red shift in UV-VIS spectrum (> 420 nm) for AgNP solution signifies agglomeration while blue shifts (< 420 nm) suggest dissolution. In soil samples, the UV spectrum showed peaks in the range of 450 to 480 nm (i.e., red shift) during 1st to 4th week (Fig. 4.14). However, in the later periods (24–72nd weeks) we recorded clear blue shift (410–350 nm) in UV peaks of the AgNP treated soil samples (Fig. 4.14). This indicates that immediately after incorporation AgNPs rapidly agglomerated in soil; and eventually dispersed into smaller particles in due course. The hydrodynamic diameters and particle size of AgNP treated soil was greater than the untreated soil. Interestingly, particle size substantially reduced after 72nd week as evidenced from the DLS measurements (Table 4.10). Consequently, the calculated specific surface area in such soils also increased over time. Moreover, the particle size was greater in $AgNP_{10}$ treated soil extracts than $AgNP_{50}$, indicating dose dependent agglomeration/dispersion dynamics (Table 4.10).

Ag^{+} release from AgNP was significantly higher at each interval between 1 and 3 days in acidic (pH = 4) solution than neutral (pH = 7) or alkaline (pH = 9) solution. Consequently, we detected lowest hydrodynamic diameter of AgNP in acidic pH (pH = 4). However, the soluble Ag concentration gradually decreased under all the pH (4, 7, and 9). Also, we detected substantial blue shift (380–400 nm) in the UV-VIS peaks of $AgNP_{10}$ added solutions (pH 4, 7, and 9) at day 1; while, at day 3 a distinct red shift (435–460 nm) indicated high agglomeration of AgNP (Fig 4.14). Likewise, we observed temporal increment in hydrodynamic diameter under all pH solutions in DLS assay (Table 4.10).

The Ag release reduced by 150, 73, 7.3 folds respectively in presence of $AgNP_{50}$, $AgNP_{25}$, and $AgNP_{10}$ in Ammonium sulphate solution (Fig. 4.13). However, Ag release from AgNP in solution was greater in KH_2PO_4 than Ammonium sulphate; probably due to reduction in the hydrodynamic diameter by 9–10 folds over 3 days time (Table 4.10). Correspondingly, we detected substantial blue shifts in such solutions in UV–Vis spectrum. However, we observed blue shift (peaks: 350–380 nm) in UV spectrum in presence of $AgNP_{10}$ and $AgNP_{25}$ treatments in both AgNP-KH_2PO_4 and AgNP-$(NH_4)_2SO_4$ solutions, however, considerable red-shift (agglomeration) was evidenced in UV–Vis spectrum when $AgNP_{50}$ was added in AgNP-$(NH_4)_2SO_4$ solutions after 21 days. Likewise, dose dependent agglomeration was distinct in DLS

measurement since the particle size (or hydrodynamic diameter) was substantially greater in $AgNP_{50}$ solutions than that of $AgNP_{10}$.

Table 4.9 a: Changes in water soluble, exchangeable, and carbonate bound fractions of silver in AgNP treated soil (mean± standard deviation), source: Das et al. [5]

Trt	Attributes					
	Water soluble		Exchangeable		Carbonate	
	4 week	72 week	4 week	72 week	4 week	72 week
T1	0.006±0.001	0.003±0.001	0.006±0.001	0.004±0.0005	0.003±0.001	0.002±0.001
T2	1.8±0.1	1±0.05	1.7±0.1	1.1±0.05	1.8±0.1	1.9±0.05
T3	2.2±0.1	1.2±0.05	2.1±0.1	1.2±0.06	1.9±0.1	2.1±0.08
T4	2.5±0.1	1.4±0.05	2.4±0.1	1.3±0.05	2.3±0.1	2.3±0.08
P value	<0.01	<0.01	<0.01	<0.01	<0.01	<0.01
LSD	0.07	0.04	0.07	0.07	0.82	0.82

T1=Control; T2=$AgNP_{10}$; T3=$AgNP_{25}$; T4=$AgNP_{50}$; ns= non significant; BDL = Below Detection Limit; Trt=treatment

Table 4.9 b: Changes in oxide, organic and residual bound fractions of silver in AgNP treated soil (mean± standard deviation), source: Das et al. [5]

Trt	Attributes					
	Oxide bound		Organic		Residual	
	4 week	72 week	4 week	72 week	4 week	72 week
T1	0.004±0.001	0.002±0.0004	0.002±0.001	BDL	BDL	BDL
T2	0.9±0.1	1.6±0.07	0.4±0.1	2.8±0.05	0.3±0.05	4.1±0.07
T3	1.2±0.1	1.8±0.05	0.6±0.1	3.4±0.06	0.4±0.06	3.9±0.1
T4	1.6±0.1	2±0.05	0.8±0.1	3.6±0.05	0.8±0.01	3.8±0.05
P value	<0.01	<0.01	<0.01	<0.01	ns	<0.01
LSD	0.82	0.82	0.82	0.03	0.352	0.05

T1=Control; T2=$AgNP_{10}$; T3=$AgNP_{25}$; T4=$AgNP_{50}$; ns= non significant; BDL = Below Detection Limit; Trt=treatment

Table 4.10: Calculated specific surface area and particle size distribution of AgNP in aqueous media and filtered soil extracts in DLS analysis, source: Das et al. [5]

Soil incubation treatments	Calculated specific Surface area (m^2 cc^{-1})		Size (nm)	
	1^{st} week	72 week	1^{st} week	72 week
Control	12.03±1.2	27.97±2.1	85.2±1.1	67.9±1.0
$AgNP_{10}$	7.84±0.5	9.15±1.1	394±5.4	309±2.3
$AgNP_{50}$	10.4±0.7	15.52±1.3	181.9±2.1	97.9±2.1
Aquatic study treatments	day 1	day 3	day 1	day 3
KH_2PO_4 mixed with $AgNP_{10}$	3.57±0.5	77.64±1.4	596±1.5	43.1±0.4
KH_2PO_4 mixed with $AgNP_{50}$	7.72±0.4	84.98±1.3	745±1.5	81±0.3
$(NH_4)_2SO_4$ mixed with $AgNP_{10}$	70.65±1.3	101.6±1.5	40.1±0.5	39.2±0.2
$(NH_4)_2SO_4$ mixed with $AgNP_{50}$	96.54±1.1	119.4±1.4	60.2±0.4	56±0.1
	24 h	72 h	24 h	72 h
pH 4	64.43±0.1	79.39±1.1	50.1±1.3	58.6±1.2
pH 7	42.38±0.1	48.35±1.2	61.5±1.2	93.4±1.2
pH 9	48.32±0.1	65.62±1.2	54.6±1.1	63.8±1.2

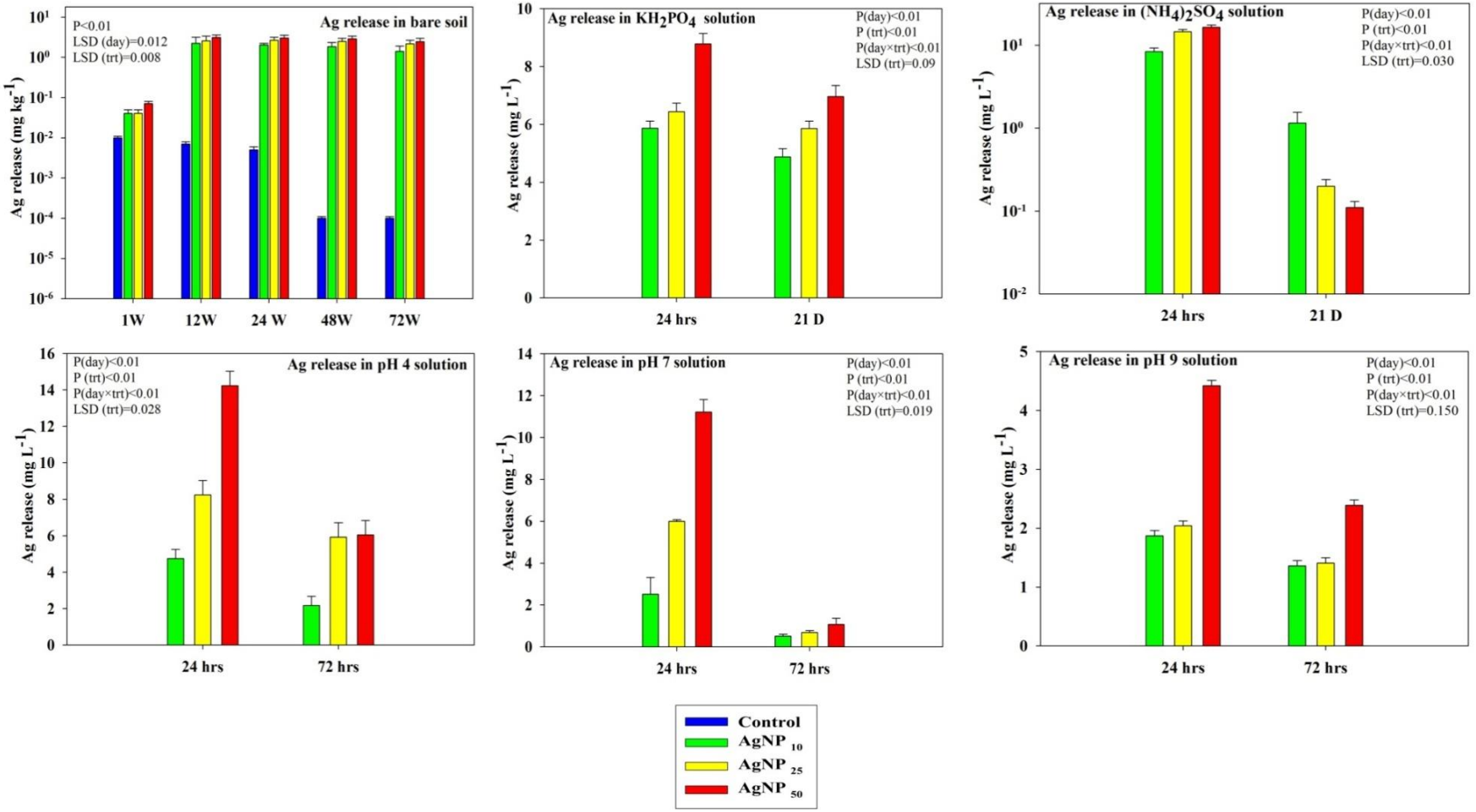

Fig. 4.13: Silver (Ag^{+}) release profile in soil and aqueous media in presence of other elements (N, P, K, and S) (Error bar represent standard deviation), source: Das et al. [5]

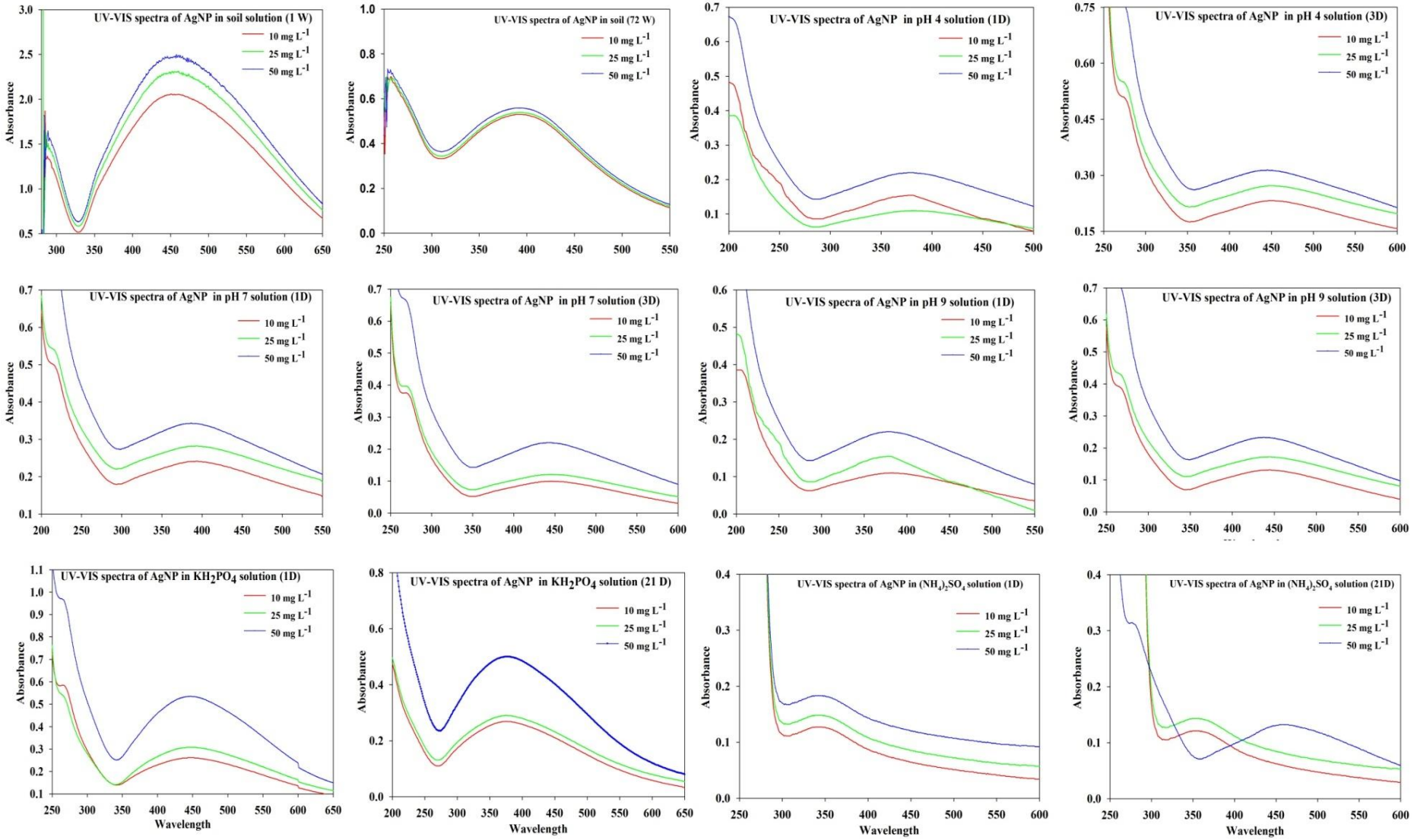

Fig. 4.14: UV-VIS spectra of AgNP under various conditions in filtered soil extracts and aqueous media, source: Das et al. [5]

4.4.2.4. AgNP and microorganisms: biomass, biomass C& N, and enzymes

Initially (till 12th week) the bacterial count and biomass, biomass C (MBC), and biomass N (MBN) were significantly greater in AgNP treated soil than the control (Fig. 4.15, Table 4.7). However, MBC, MBN, urease, and phosphatase activity dramatically reduced after 12 weeks in AgNP treated soil. Likewise, bacterial biomass and count were severely affected in soil due to $AgNP_{50}$ and $AgNP_{25}$ exposure during later stage (Fig. 4.15). Overall, the 50 mg kg^{-1} concentration of AgNP was the most damaging for soil microbial growth and activity.

4.4.2.5. Correlation analysis

The study has been conducted in different phases under varying conditions to assess the behaviour of AgNP in soil and aqueous medium. Hence, the mechanistic hypothesis derived from the results needed to be authenticated with the help of appropriate statistical analysis. Here, correlation statistics was performed for such purpose (Table 4.11). We found strong negative correlation between Ag in soil and MBC, MBN, and bacterial biomass [(MBC: $r = -0.99$, $P < 0.05$); MBN: $r = -0.98$ ($P < 0.05$); bacterial biomass: $r = -0.98$ ($P < 0.01$)]. This approves that abundance of silver in soil was detrimental for microbial communities. Interestingly, the pattern of N and sulphur/sulphate availability in presence of AgNP under different conditions (soil and $(NH_4)_2SO_4$ solution) was strongly correlated with each other (Table 4.11). Moreover, the P and K availability patterns in bare soil, and in KH_2PO_4 solution were strongly correlated ($P < 0.01$) (Table 4.11).

Table 4.11: Co-relation analysis of N, P, K, Ag, and sulphate in various aqueous media and bare soil, source: Das et al. [5]

			Bare soil		
	N	**P**	**K**	**Ag**	**Sulphate**
P study		*0.99***	*0.99***	*ns*	
N-study	*0.99**			*ns*	*0.98***
pH study				*ns*	
			N-study		
	N	**Sulphate**	**Ag**		
pH study			*0.97***		
P study			*0.88**		
Bare soil	*0.99**	*0.98***	*ns*		
			P study		
	P	**K**	**Ag**		
pH study			*0.97***		
Bare soil	*0.99***	*0.99***	*ns*		
			pH study		
	Ag				
Bare soil	*ns*				
N-study	*0.97***				
P-study	*0.97***				
			Bare soil Ag		
	Ag				
Bare soil MBC	*-0.99**				
Bare soil MBN	*-0.98**				
Bacterial biomass	*-0.98***				

= p<0.05; ** = p<0.01, ns=non-significant; MBC: Microbial biomass C; MBN: Microbial biomass N

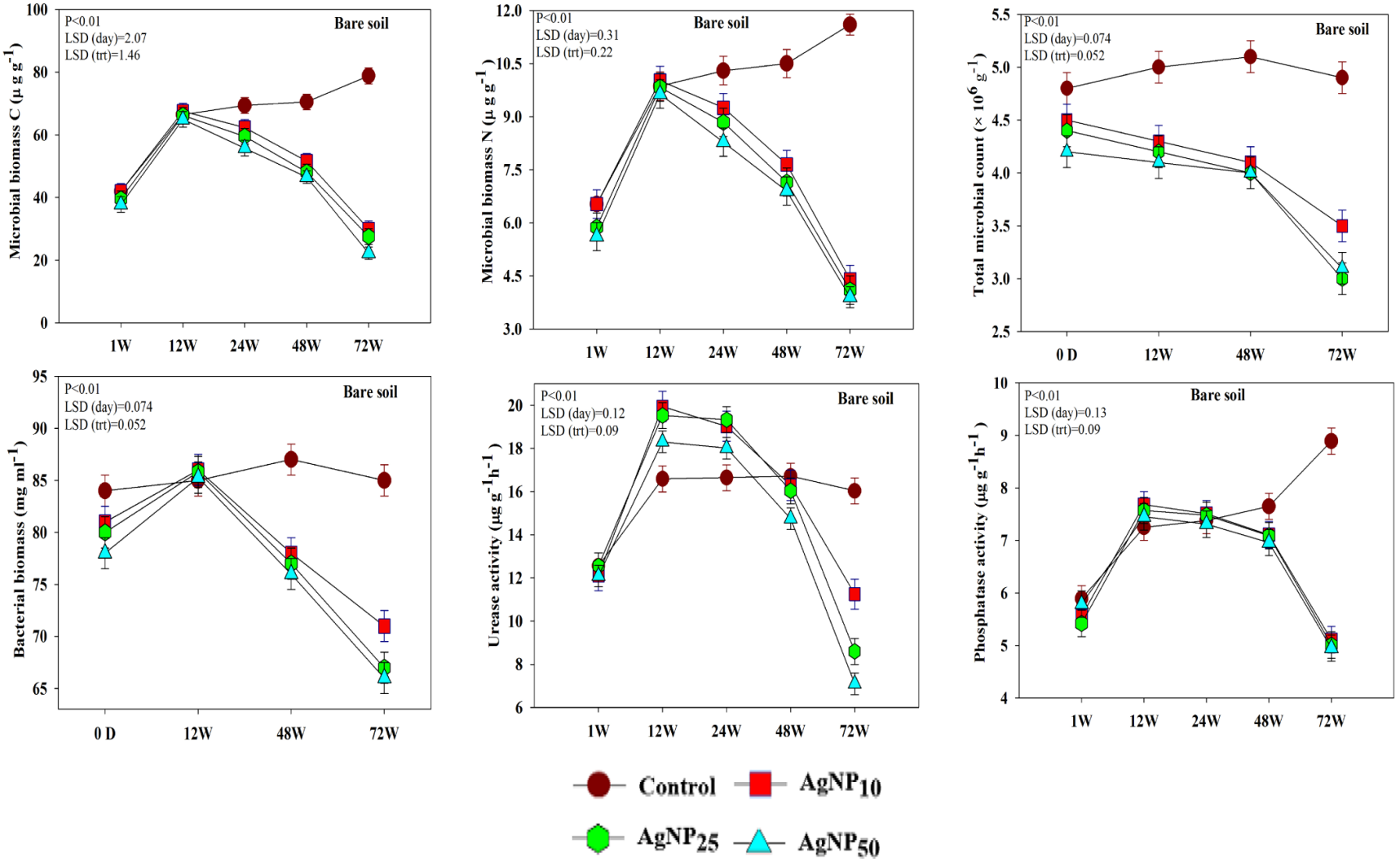

Fig. 4.15: Impacts of AgNP on microbial biomass carbon (MBC), microbial biomass nitrogen (MBN), total bacterial count, bacterial biomass and enzyme activity (urease and phosphatase) (Error bar represent standard deviation), source: Das et al. [5]

4.4.2.6. On field trial with tomato

4.4.2.6.1. Effect on seed germination

So far, the results of this study indicated that although AgNP exposure to soil environment has had no immediate deleterious impact on soil quality in the short run, the harmful effects was conspicuous after 12 weeks of AgNP application in soil. However, these conclusions were drawn from lab based and pot culture studies; and thus a long term field experiment was conducted to validate the previous outcomes. Prior to the field experiment a germination assay with tomato (*Lycopersicon esculentum*) seeds was performed to confirm about the feasibility of large scale on-field trial. The germination index was significantly low (<40%) of both AgNP and $AgNO_3$ treated seeds. However, among the Ag based treatments AgNP-15 kg ha^{-1} dose was appeared to be least inhibitory for the germination of tomato seeds. Similarly, relative shoot and root growths were significantly greater of the untreated (control) seeds followed by AgNP 15 kg ha^{-1}, AgNP 30 kg ha^{-1}, and $AgNO_3$ 15 kg ha^{-1} treatments (Table 4.12).

Table 4.12: Impact of AgNP on germination of tomato seeds

Treatment	Attributes		
	RSG (%)	RRG (%)	GI (%)
AgNP- 15	77.78±2.5	51.16±2	39.79±1.1
AgNP-30	60±2.1	41±1.1	24.65±1
$AgNO_3$-15	60±2	40±1	24.19±1.1
$AgNO_3$-30	55±1.8	39.53±1.1	21.56±1.1
P value	0.000	0.000	0.000
LSD	0.24	0.19	1.78

4.4.2.6.2. Effect on pH, bulk density, water holding capacity, availability of N, P, K, soil organic carbon and enzyme activity of field condition soil

Table 4.13 represent the data on changes of pH, bulk density (BD), and water holding capacity (WHC) in AgNP and $AgNO_3$ treated field soils under tomato cultivation. The soil was inherently acidic in nature and substantial reduction in soil pH was recorded due to application of AgNP and $AgNO_3$ application after two years of tomato cultivation. The drop in pH was more prominent in $AgNO_3$ treated soil than the AgNP treated. After the harvest of the second year crop the soil pH under various treatments

was in the order: Control>AgNP-15 kg ha^{-1}>AgNP-30 kg ha^{-1}>$AgNO_3$-15 kg ha^{-1}>$AgNO_3$-30 kg ha^{-1} (P (trt) <0.01, LSD (trt) =0.12). The BD of the soil increased with substantial reduction in WHC due to AgNP and $AgNO_3$ application. The dose dependent effect was not highly prominent in regard to BD and WHC of the soil.

Table 4.13: Impact of AgNP on pH, bulk density, and water holding capacity of field condition soil

Treatments	pH		Bulk density (g cc^{-1})		Water holding capacity (%)	
	First yr	Second yr	First yr	Second yr	First yr	Second yr
Control	5.23±0.03	5.3±0.02	1.41±0.01	1.40±0.01	61.63±1.02	65.59±1.14
AgNP-15	5.01±0.01	4.96±0.02	1.41±0.01	1.44±0.01	56.24±1.19	53.04±0.98
AgNP-30	4.97±0.02	4.85±0.05	1.42±0.01	1.45±0.01	56.59±0.92	51.76±0.9
$AgNO_3$-15	4.88±0.03	4.75±0.03	1.41±0.01	1.46±0.01	56.43±1.02	51.92±1.5
$AgNO_3$-30	4.75±0.04	4.68±0.03	1.41±0.02	1.45±0.01	56.14±1.09	50.99±1.3
P (yr)	<0.01		<0.01		<0.01	
P (trt)	<0.01		<0.01		<0.01	
P (yr×trt)	<0.01		<0.01		<0.01	
LSD (trt)	0.12		0.008		0.65	

However, the impact of higher dose application was appreciated in regard to soil organic carbon, nutrient (NPK) availability, and enzyme activity. The SOC level of the untreated (control) soil slightly gained after two years of tomato cultivation (Fig. 4.16). In contrast, there was about 7.7-11.3% of reduction in SOC levels of soils under AgNP and $AgNO_3$ treatments. Moreover, the dose effect was significantly prominent in regard to SOC contents. For example, after two years of tomato cultivation the SOC contents were 31.5% and 32.6% lower in AgNP-15 kg ha^{-1} and AgNP-30 kg ha^{-1} treated soils than the control (Fig. 4.16).

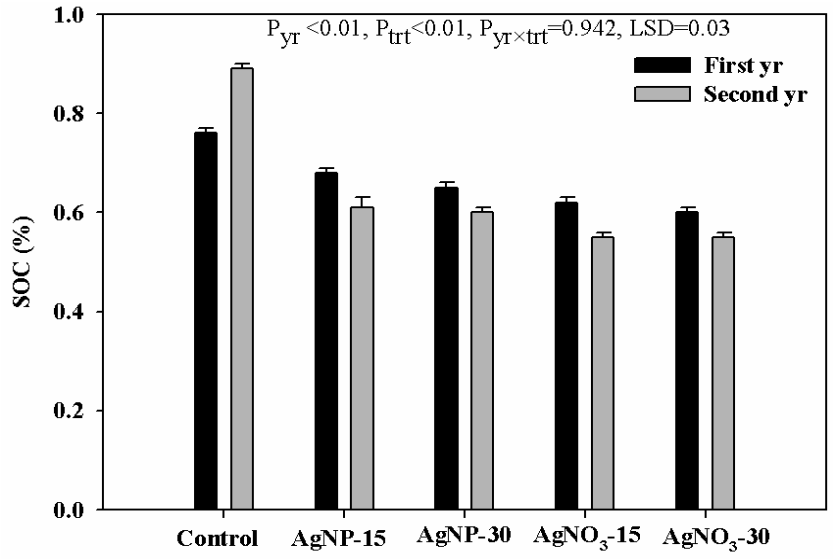

Fig. 4.16: Impact of AgNP on SOC content of field soil under tomato cultivation

The N availability and urease activity in soil drastically decreased due to AgNP-30 and $AgNO_3$-30 application (Table 4.14, 4.15). After two years of tomato cultivation, N availability under various treatments was in the order: Control> AgNP-15 kg ha^{-1}>AgNP-30 kg ha^{-1}> $AgNO_3$-15 kg ha^{-1}> $AgNO_3$-30 kg ha^{-1} (P (trt) = 0.000, LSD (trt) =6.83) (Table 4.14).

Table 4.14: Impact of AgNP on available N, P, and K of field condition soil

Treatments	Available N (mg kg^{-1})		Available P (mg kg^{-1})		Available K (mg kg^{-1})	
	First yr	Second yr	First yr	Second yr	First yr	Second yr
Control	224±14	256.7±18	22.31±1.5	33.06±2.1	41.23±2.2	60.63±2.9
AgNP-15	200.7±14	186.7±12	17.77±1.2	14.79±1.4	30.7±2.0	58.03±2.2
AgNP-30	195.1±12	177.3±11	17.48±1.3	12.67±1.2	29.87±1.8	59.57±2.3
$AgNO_3$ -15	196±14	163.3±12	15.6±1.1	13.49±1.1	29.53±1.6	51.3±2.1
$AgNO_3$-30	186.67±13	149.3±12	14.52±1.1	11.46±1.3	28.9±1.5	49.73±1.9
P (yr)	0.005		<0.01		<0.01	
P (trt)	<0.01		<0.01		<0.01	
P (yr×trt)	<0.01		<0.01		<0.01	
LSD (trt)	6.83		0.46		0.22	

Similarly P availability and phosphatase activity was lowest due to $AgNO_3$-30 application in soil (Available P: P (trt) <0.01, LSD (trt) =0.46; Phosphatase: P (trt) <0.01, LSD (trt) =0.52; Table 4.14, 4.15). However, the K availability in soil substantially increased under all the treatments and the magnitude of increment was greater in AgNP treated soils as compared to $AgNO_3$ and the control (Table 4.14). We

recorded about 1.9 and 2.0 folds increment in K availability in AgNP-15 and AgNP-30 treated soils respectively after the harvest of the second crop.

Table 4.15: Impact of AgNP on urease and phosphatase activity of field condition soil

Treatments	Urease activity ($\mu g\ g^{-1}h^{-1}$)		Phosphatase activity ($\mu g\ g^{-1}h^{-1}$)	
	First yr	Second yr	First yr	Second yr
Control	17.83±1.3	23.93±1.6	21.74±1.1	32.24±1
AgNP-15	16.68±1.3	14.68±1.3	18.43±1.0	16.29±0.8
AgNP-30	15.19±1.1	12.68±1.2	18.38±0.7	16.19±0.9
$AgNO_3$ -15	13.39±1.1	11.92±1.1	17.33±0.5	16.19±0.5
$AgNO_3$-30	11.23±1.0	10.43±1.0	16.12±06	14.26±0.5
P (yr)	<0.01		0.002	
P (trt)	<0.01		<0.01	
P (yr×trt)	<0.01		<0.01	
LSD (trt)	0.07		0.52	

4.4.2.6.3. Impact of AgNP on yield of tomato

The data on yield of tomato is represented in Table 4. 16. Tomato production was reduced under all the treatment combinations of AgNP and $AgNO_3$ over two years. Maximum yield was recorded in untreated (control) plot after two years of crop cultivation. Moreover, after second year of cultivation, crop production was significantly reduced under $AgNO_3$-30 kg ha^{-1} followed by $AgNO_3$-15 kg ha^{-1}, AgNP-30 kg ha^{-1}, and AgNP-15 kg ha^{-1}. The crop yield after the final harvest of second year was in the order: Control>AgNP-15 kg ha^{-1}>AgNP-30 kg ha^{-1}>$AgNO_3$-15 kg ha^{-1}>$AgNO_3$-kg ha^{-1} (P (trt) <0.01; LSD (trt) =1.03).

Table 4.16: Impact of AgNP on yield of tomato crop grown under field condition

Treatments	Yield (tonne ha^{-1})	
	First yr	Second yr
Control	20.8±1.8	21.5±1.8
AgNP-15	18.67±1.8	14.17±0.9
AgNP-30	16.3±1.7	13.83±1.1
$AgNO_3$-15	17.17±1.8	12.67±1
$AgNO_3$-30	15±1.1	11.33±1.8
P (yr)	<0.01	
P (trt)	<0.01	
P (yr×trt)	0.05	
LSD (trt)	1.03	

4.4.2.6.4. Effect of AgNP on shelf life of tomato

Shelf life mainly regarded as the time period, upto which a crop product especially fruit can be stored under ambient condition after harvest. Here in this study, the fresh tomatoes were collected after first harvest of each year and then kept under ambient condition for 60 days. Weight loss was recorded at every 20 days interval. We observed that minimum weight loss was occurred under the tomatoes of untreated sample. However, under AgNP and $AgNO_3$ treatment combinations showed significant weight loss at both first and second year of field study. Maximum weight loss is related to shortage of fresh life of a fruit or crop product. Therefore, from this data we can comprehend that, tomatoes grown under untreated soil can be stored more days in a fresh conditions than the tomatoes under AgNP and $AgNO_3$.

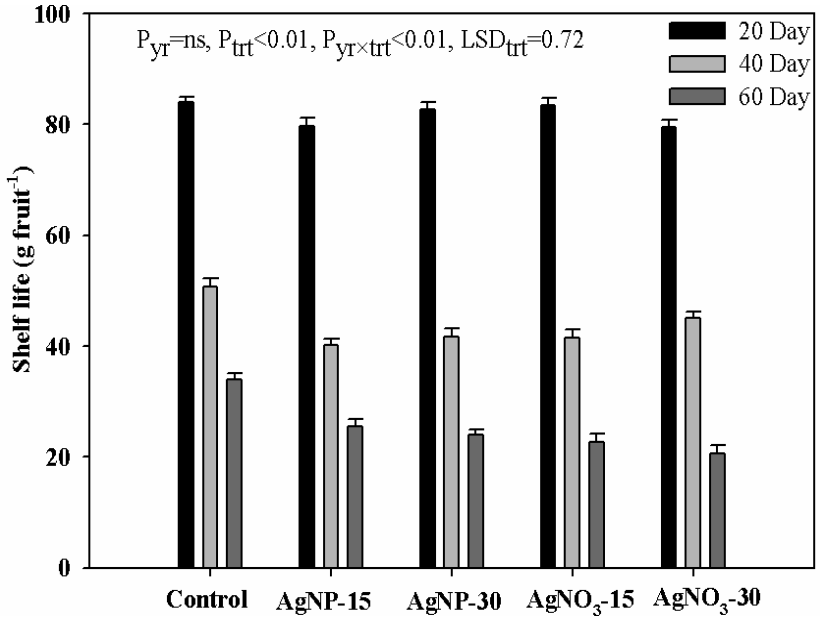

Fig 4.17: Impact of AgNP on shelf life of tomato under field condition

4.4.3. Earthworm response to AgNP

4.4.3.1. Response of earthworm to AgNP exposure: fecundity and body weight

Although AgNP exposure upto 50 mg kg^{-1} level did not produce any apparent lethal effect on earthworms, the rate of increment in body weight and number (i.e., count)

was significantly reduced due to AgNP treatment (Table 4.17). Overall, we recorded about 1.60–1.97 folds reduction in earthworm count in AgNP mixed feedstock. At the end of the incubation period (120 day), the earthworm count under various treatments was in the order: C > $AgNP_{10}$ > $AgNP_{25}$ > $AgNP_{50}$ ($P < 0.01$; LSD = 0.82). Whereas, body weight of $AgNP_{50}$ treated worms was 1.6 times lower than the control worms at 80^{th} day (Table 4.17). The weight of $AgNP_{10}$ and $AgNP_{25}$ treated worms was 1.15 and 1.25 times lesser than the untreated ones during that time.

Table 4.17: Changes in body weight and count of *Eisenia fetida* under AgNP exposure (mean± standard deviation), source: Das et al. [5]

		Duration of the experiment											
	Trt	**10 Day**	**20 Day**	**30 Day**	**40 Day**	**50 Day**	**60 Day**	**70 Day**	**80 Day**	**90 Day**	**100 Day**	**110 Day**	**120 Day**
Body weight	T1	0.63±0.02	0.7±0.01	0.74±0.02	0.79±0.03	0.95±0.2	1.1±0.14	1.3±0.14	1.5±0.14	1.6±0.1	1.7±0.4	1.7±0.1	1.7±0.05
	T2	0.7±0.03	0.8±0.04	0.82±0.03	0.84±0.06	1.1±0.014	1.2±0.2	1.3±0.1	1.3±0.1	1.4±0.3	1.4±0.5	1.4±0.4	1.5±0.14
	T3	0.68±0.02	0.7±0.02	0.71±0.03	0.76±0.07	0.98±0.07	1.1±0.17	1.2±0.1	1.2±0.1	1.2±0.1	1.4±0.4	1.4±0.5	1.4±0.15
	T4	0.6±0.04	0.64±0.03	0.66±0.03	0.69±0.02	0.89±0.03	0.95±0.16	0.9±0.04	0.9±0.1	1.1±0.2	1.1±0.4	1.2±0.4	1.2±0.2
Count	T1	16±1.1	19±1	23±1	30±1.1	34±1	38±1	43±1	54±1	56±1	56±1	57±1	61±1.1
	T2	19±1	21±1	26±1	35±1	41±1	45±1	48±1	59±1	48±1	48±1	43±1	38±1.2
	T3	18±1.1	20±1	24±1	31±1	38±1	42±1	44±1	55±1	46±1	46±1	42±1	36±1
	T4	16.1±1	20±1	21±1.2	24±1	29±1	33±1	32±1	48±1	38±1	38±1	35±1	31±1
P value	Body	<0.01	<0.01	<0.01	<0.01	ns	ns	ns	ns	ns	ns	ns	<0.01
L.S.D	weight	0.023	0.024	0.022	0.041	0.091	0.312	0.308	0.183	0.179	0.27	0.35	0.15
P value		ns	ns	ns	<0.01	<0.01	<0.01	<0.01	<0.01	<0.01	<0.01	<0.01	<0.01
L.S.D	Count	1.023	0.83	2.38	1	0.82	0.82	0.84	0.82	0.82	0.82	1.41	0.82

T1=Control; T2=AgNP$_{10}$; T3=AgNP$_{25}$; T4=AgNP$_{50}$;*ns= non significant, Trt=treatment

4.4.3.2. Responses of earthworms to AgNP exposure: oxidative stress enzymes, Ag accumulation, and histology

The results on earthworm count and body weight indicated that AgNP exposure created metabolic stress to *E. fetida*, which was further confirmed by excessive activity of ROS scavenging stress enzymes (Catalase, GSH, GPx, and GST) in earthworms (Catalase and GST: Fig. 4.18 a; GPx and GSH: Table 4.18). Catalase activity was > 20 folds greater in the AgNP treated specimens than the control, while the GPx, GST, and GSH activity was greater by 2.5–3.25 folds as compared to the untreated specimens ($P < 0.01$). Moreover, $AgNP_{50}$ exposure reduced the total protein content by 3.31 folds in earthworms as compared to the untreated specimens ($P < 0.01$). The histological assessment showed that layers of chloragogenous tissues (CT) were hyperplastic and detached from intestinal wall in AgNP treated worms (Fig. 4.18 b); CT layers were abdominally thick and unevenly distributed throughout the peripheral portion of intestinal lumen. Such abnormalities were absent in the untreated earthworms (Fig. 4.18 b). Interestingly, Ag accumulation was 1.13–2.24 folds greater at 30^{th} day than at 120^{th} day (Fig. 4.18 a). Overall, Ag accumulation was highest in earthworms treated with $AgNP_{50}$ followed by $AgNP_{25}$, $AgNP_{10}$, and control.

Table 4.18: Activity of reduced glutathione (GSH), glutathione peroxidase (GPx), and total protein content in earthworms exposed to AgNP (mean± standard deviation), source: Das et al. [5]

	Attributes		
Treatment	GSH (nM mg^{-1})	GPx (nM mg^{-1} min^{-1})	Total protein (µg μL^{-1})
Control	5632.9±74	205.7±18.48	1.69±0.18
$AgNP_{10}$	7556.1±78	398.7±11	0.45±0.03
$AgNP_{25}$	10562.1±105	489.5±12.6	0.48±0.04
$AgNP_{50}$	17991.3±139	669.4±30.8	0.51±0.04
P value	<0.01	<0.01	<0.01
LSD	515	14.23	0.76

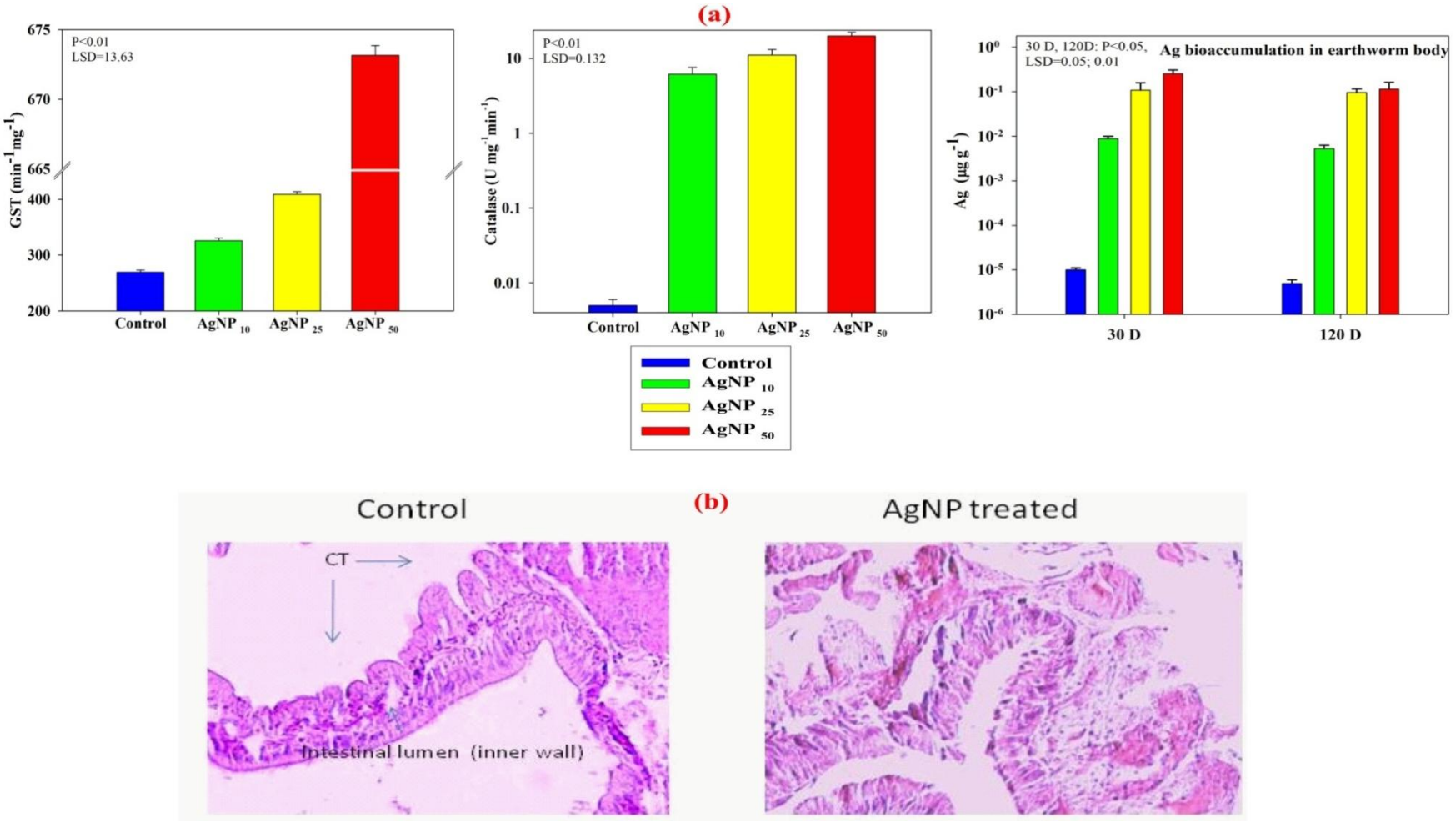

Fig. 4.18: Response of *E. fetida* to AgNP exposure (Error bar represent standard deviation). (a) Activity of Catalase and Glutathione S transferase (GST), and Ag accumulation in AgNP treated and untreated earthworms; (b) Histological evidence of AgNP induced stress in earthworms, source: Das et al. [5]

4.5. Discussions

The experimental results indicated that silver nanoparticles incorporation in soil-plant system has had no apparent harmful effect on soil fertility and plant health in the short run (3-4 months). In fact, some few outcomes of the preliminary experiments were highly encouraging. For example, the soil porosity and WHC improved increasing GSNP concentration; the influence of GSNP was remarkably healthy in regard to N availability in soil; growth, metabolism, and productivity of *P. vulgaris* were benefited when treated with GSNP at various concentrations in the pot culture study. Whereas, silver nanoparticles are known to be toxic to a range of organisms, mammalian cells, and human cells [62-64]. Therefore, long term studies under both laboratory and field conditions were further conducted to ascertain the AgNP-soil plant interactions in a more comprehensive manner.

4.5.1. The effects of SNPs on pH and cation exchange capacity (CEC) of soil

When nanomaterials are introduced into soil systems, they are readily altered due to agglomeration/aggregation, oxidation/reduction, and sorption/desorption [11,65,66]. However, there is considerable uncertainty regarding the true toxicity of SNPs arising from variations in SNP size, shape, and surface properties, as well as the presence of impurities such as reducing and stabilizing agents [64]. Originally, the soil was composed of compact/rounded aggregates, which eventually transformed to crystalline structures after the incorporation of nanoparticles (Fig. 4.1). In general, the very large surface-to-volume ratios of nanoparticles facilitate the formation of stable granular aggregates and regular aggregated flakes in soil [67]. In fact, SNPs can form such stable aggregates in combination with soil particles depending on the ionic strength of the media. In the present work, it is likely that the crystalline structure of the *T. occidentalis*–mediated GSNP greatly increased the internal surface area of the soil, which in turn probably facilitated the formation of stable aggregates in soil [25,68].

Based on the preliminary (short term) experiments, emphasis was placed on quantifying the overall net beneficial impacts of SNPs on soil quality, with the help of benefit percentages. Such evaluation clearly showed the advantage of applying lower concentrations of GSNPs to soil (Fig. 4.3). Most noticeably, GSNP treatment shifted the soil pH toward neutrality; enhanced the CEC of the soil; and considerably

augmented organic C content in soil. Eventually, it was presumed that the neutral state of the GSNP probably contributed to the presently observed changes in soil pH [69,70]. However, the long term study also depicted that the AgNP or GSNP exposure reduced pH in both soil and aqueous media except in $(NH_4)_2SO_4$-AgNP mixture increased over time. The relationship of AgNP and media pH largely depends colloidal stability, background electrolyte composition and capping agents [71,72]. In fact, silver atoms at the NP-surface can greatly scavenge the OH^- in solution [72,73]. CEC is directly dependent on the net negative surface charge of soil solids [74]; while, the net surface charge of a soil is closely related to the total surface area. The occurrence of some impurities of PEG in the GSNPs might have indirectly facilitated the humification process in soil; which in turn increased soil porosity and the gross surface area [6]. In fact, the results of the long term in-depth studies clearly showed that agglomeration of the AgNP was greater during early stage (2-6 weeks), therefore the PEG mediated gain in surface area was prominent in short term study. As a result, GSNPs probably influenced the rate of stabilization of organic matter in soil by increasing soil porosity; this explains the enhancement in CEC that was evident in soil under GSNP50 treatment [7,12]. In addition, GSNPs might have altered the ionization property of the soil by increasing the soil's reactive surface area while also increasing its net negative charge [7].

4.5.2. Bio availability of N, P, K, S, Ag, and microbial health

GSNP treatments yielded remarkable increments in the bioavailability of N in soil during preliminary short term study with *P. vulgaris* (Table 4.2). Among the various concentrations of GSNPs, the 50 mg kg^{-1} dose gave the greatest benefit (Fig. 4.3). Therefore, we specifically addressed the issue of N mineralization through two lab-scale experiments. In the first experiment, we incubated sterilized soil with various concentrations of GSNPs. Sterilization was carried out to avoid the effects of soil microorganisms; under these sterile conditions, a constant increase in total N was observed for $GSNP_{50}$ (Fig. 4.4). In the second experiment, columns were packed with GSNP-incubated soil, and a uniform flow of deionized water was passed through the columns for 48 h. The leachates were collected at 24 and 48 h to measure NO_3^- content (Table 4.3). Note that NH_4^+ and NO_3^- are the two mineralized forms of nitrogen in soil [27]. The ammoniacal form (NH_4^+) generally remains bound in the cation exchange sites of the soil solids, whereas NO_3^--N is leached by percolating

water in the absence of plants [75]. It was interesting to observe that the rate of nitrate leaching from the soil remarkably retarded when GSNP was introduced. As a result, N retention in the root zone soil increased greatly (Table 4.3).

The interaction of nanoparticles with soil is a complicated phenomenon that is highly dependent on variables such as soil physicochemical characteristics, environmental conditions, and the nature of the nanoparticles [12]. Soil organic matter has been reported to promote disaggregation of nanoparticles, thereby promoting their sorption to soil particles [13]. Hence, the sorption potential of SNPs should be closely associated with the retention of NO_3^--N in soil solids (Table 4.3). However, it is worthy to mention that the duration of incubation of both these experiments were short; hence, it was imperative re-confirm the outcomes through long term studies which were performed later. N, P, and K availability greatly depend on the microbial health and redox reactions in soil. The impact of silver nanoparticles on beneficial soil microbes has been reported to be detrimental [76]. Alongside, greater microbial toxicity was found in sandy soils than loamy soils [77].

Short term soil assay with samples from the pot culture experiment did not show any detrimental effects of SNP incorporation. As such, the population of NFBs considerably increased in $GSNP_{25}$ and $GSNP_{50}$ treated soils under *P. vulgaris* cultivation (Table 4.6). As a result, we observed significant urease activity in GSNP-treated soil, which in turn might have facilitated N mineralization in soil (Table 4.2). Moreover, the PSB populations in GSNP-treated soils were quite high (Table 4.6). The observed increments in P availability very likely arose from the greater populations of PSBs. Contrarily, silver nanoparticles were observed to affect the health of microbes by interacting with their cell membranes by many workers [78,79]. However, the tendency of SNPs to agglomerate in soil greatly reduced their size-dependent toxicity [18]. In the short term study, we observed a dose-dependent effect of SNPs on soil bacterial communities, which was in good agreement with a previous finding [76].

When the long term lab as well as field based studies were performed substantial reduction in microbial biomass, retardation in microbe-released enzyme activity was recorded. Although the mechanisms of silver nanoparticle toxicity to microbes is poorly understood, severe damage to cell membranes, DNA, and elevated oxidative stress can be considered as prime causes [80]. Urease is largely responsible for N

mineralization whereas, phosphatase mediate solubilization of insoluble P in soil [52]. Therefore, we recorded significant reduction in N and P availability in soil in the long run. AgNP may readily undergo oxidation followed by dissolution (Ag^+) in soil and aqueous environment. Then, the solubilized Ag^+ may substitute the NH_4^+ from the exchange sites of soil, thereby make the NH_4^+ prone to denitrification loss [81,82]. The UV-VIS spectra and DLS analysis advocated greater dissolution of AgNP in later stage with corresponding reduction in NH_4-N availability. This explanation is applicable for K as this element largely remains in ionic form in soil and aqueous system. On the other hand, P availability in soil is highly pH dependent. As AgNP incorporation led to acidification in both soil and aquatic media, the formation of insoluble orthophosphates was obvious.

We also observed substantial reduction in S^{2-}/SO_4^{2-} contents in both soil and aqueous media that strongly correlated with soluble Ag^+. This indicates formation of insoluble Ag_2S through sulphidation reaction which is a possible phase in natural system [83,84]. Interestingly, in aqueous media the source of sulphur was sulphate in our experiment. However, formation of Ag_2SO_4 is unlikely since the compound is very soluble [84]. Therefore, the S^{2-} was likely the major reactive form of sulphur in soil. In addition, the oxidation of NO_x may significantly accelerate Ag_2S formation in aqueous media [85]. The level of AgNP concentration in aqueous media greatly influenced dissolution/aggregation dynamics in presence of ammonium sulphate. From such results we apprehend that high concentration (50 ppm) exposure led to aggregation thereby drastic reduction in Ag (0) to Ag^+ conversion. Increase in concentration may increase collision efficiency which ensures greater contact, leading to high homo-aggregation [13,82,86].

Overall, the results of the correlation analysis justified that the laboratory based batch experiments could adequately defined the AgNP driven changes in soil quality and nutrient availability. Interestingly, the correlation outputs clearly revealed that the AgNP was not only toxic to microbes in soil but also considerably reduced the P and S bioavailability probably by forming insoluble compounds. In addition, AgNP incorporation strongly acidifies soil. However, the harmful effects on urease activity probably led to reduction in N availability in soil.

4.5.3. Effect of AgNP on plants

As of now, phytotoxicity studies are largely limited to germination test, root growth analysis, and metabolic assay in plants grown in soil less media. In this study, both beneficial and harmful effects of silver nanoparticles were evidenced. In the short term (pot culture) study, the beneficial impacts of GSNPs on *P. vulgaris* growth were evident. Leaf number, leaf area index, and pod yield of French bean enhanced considerably; a substantial benefit in protein content was evident in $GSNP_{50}$-treated plants (Fig. 4.5, 4.6). Although the 100 mg kg^{-1} dose of SNPs induced high proline accumulation, the proline accumulation was negligible with low doses (20, 25, and 50 mg kg^{-1}) of GSNP (Fig. 4.6). Exposure to stressful conditions leads to overproduction of proline in plants, which provides stress tolerance by sustaining cell turgor or membrane stability and protecting the plants from oxidative stress [87]. We also failed to observe any significant retardation in growth of tomato due to AgNP exposure. However, substantial yield loss was evidenced in NP-exposed plants both in pots as well as in field, which could be attributed to failure in nutrient (N and P) uptake mechanism in such plants; while considerable uptake of silver was recorded. Previously, Doshi et al. [88] found failure in nutrient uptake due to Al-nanomaterial exposure; Lee et al. [18] also demonstrated high uptake in NP-exposed plants. However, both these studies reported low bioaccumulation (mass concentration) of Ag in soil system. Whereas, we found that low N and P uptake was substituted by increment in Ag uptake. This indicates that AgNP exposure must have induced significant metabolic alteration in plants.

In French bean significant improvement was observed in nitrate reductase expression and chlorophyll formation under GSNP treatments. Generally, chlorophyll production in plants largely depends on N and Mg translocation from the soil to the plant body. Thus, the increased N uptake under the GSNP concentrations studied probably facilitated chlorophyll activity in *P. vulgaris*; our results are in good agreement with those of a previous report [89]. Interestingly, the expression of *NR* and *Fd* genes was remarkably higher in $GSNP_{50}$-treated plants. In contrast, we detected significant loss in activity of enzymes that regulate N assimilation (GS, GOGAT, and NR) in tomato. Moreover, their respective genes were significantly retarded in AgNP exposed plants. GS is the primary enzyme that catalyses the entry of nitrogen in cellular metabolism. GS triggers the formation of glutamine; which is then utilized by

GOGAT to produce glutamate [90]. In this study we assessed the expression of *GS2* gene because this chloroplastic isoform of GS not only promotes N-metabolism, also detoxify and re-assimilate the elevated ammonium during photorespiration in leaves [90]. Previously, AgNP exposure has been reported to severely affect biosynthesis of lipids, proteins, and structural components in plant cells [91]. Hence, we propose that the AgNP exposure greatly affect the protein synthesis pathway by suppressing the expression of genes responsible for N assimilation in plants. In addition, high level of oxidative stress was also evidenced in AgNP treated plants. Predominance of ROS in bacteria exposed to AgNP has been reported earlier [80]. However, in our knowledge, this report appears to be the first in regard to metabolic stress and gene expressions study for assessing AgNP toxicity in plants.

4.5.4. AgNP stress in earthworms

We recorded concentration dependent retardation in growth (body weight) and fecundity in *E. fetida*. Moreover, highest accumulation of silver was recorded in $AgNP_{50}$ treated worms. These results are in good agreement with some previous studies [11,92]. Few studies also demonstrated significant reproductive failure and tendency of avoidance to AgNP exposure in earthworms [22]. In contrast, we recorded cessation in reproducibility of *E fetida*. However, loss in body weight was a matter of concern in our study. Thus, we detected significant loss in protein content with enhanced activity of ROS scavenging species (catalase, GPx, GST, and GSH) in AgNP exposed earthworms. The activity of the stress enzymes were also closely related to levels of exposure. Moreover, we detected strong positive correlation between Ag accumulation and stress enzyme activity. Although earthworms are capable to detoxify metals by forming organometallic complexes in their intestines [93,94], their efficiency greatly vary depending on the nature and concentration of the metal species and substrate characteristics [95,96]. The authenticity of this hypothesis was further confirmed when the histological assay revealed hyperplastic disruption in chloragogenous tissue layers in treated earthworms.

4.6. Conclusions

The main hypothesis of this chapter was to identify the efficacy of plant extract mediated silver nanomaterials on earthworm-microbes-soil-plant system. According to the short term soil plant pot culture experiment, soil incorporation of GSNP not only improved nutrient availability, also greatly induced activity and proliferation of good soil microbial communities (N-fixing and P-solubilizing bacteria). Total N and nitrate leaching assays demonstrated that GSNP can decrease the nitrate leaching in soil, thereby increasing the total N content in soil. The growth of *P. vulgaris* was benefited in regard to pod yield, protein contents in the pod, and overall vigor of the plant. The uptake of N and P in *P. vulgaris* along with gene (*NR* and *Fd*) expression assays were substantiated the apparent benefits observed in soil and the lab based experiments. Moreover, proline content was significantly lower in plants treated with GSNP below the concentration of 50 mg kg^{-1}. Contrarily, substantial yield loss was evidenced in NP-exposed tomato (*Lycopersicon esculentum*), which could be attributed to failure in nutrient (N and P) uptake mechanism in such plants; while considerable uptake of silver was recorded. Nevertheless, significant losses in activity of enzymes that regulate N assimilation (GS and GOGAT) were recorded. Moreover, their respective genes were significantly retarded in AgNP exposed plants. In depth future study is needed to identify the prime factor of such kind of efficacy of AgNP.

The 72 weeks long soil incubation study revealed that the deterioration in soil quality was greatly dependent on the levels and time of AgNP exposure. We recorded retardation in nutrient availability was greater with 25 and 50 mg kg^{-1} concentrations than the 10 mg kg^{-1} level. Aggregation of AgNP in soil environment was likely to be high during early phase of exposure, while the dissolution of aggregated nanoparticles increased later as evidenced in DLS and UV-VIS analysis. Eventually, bioavailability of essential nutrients (N, P, K, and S) significantly reduced during later stage of the study. However, the earthworms greatly suffered from oxidative stress due to higher levels of AgNP exposure (25 and 50 mg kg^{-1}) as evidenced in elevation of stress enzyme activity (catalase, GPx, GST, and GSH). Moreover, severe damage to chloragogenous tissue layer was detected in AgNP exposed earthworms. Overall, this work strengthened the foundation for future researchers to carry out dedicated studies with soils that are continuously exposed to AgNP contamination over a long period of time.

Bibliography:

[1] Anjum, N. A., Gill, S. S., Duarte, E., Pereira, A. C., and Ahmad, I. Silver nanoparticles in soil–plant systems. *Journal of Nanoparticle Research*, 15:1896–1921, 2013.

[2] Chaloupka, K., Malam, Y., and Seifalian, A. M. Nanosilver as a new generation of nanoproduct in biomedical applications. *Trends in Biotechnology*, 28:580–588, 2010.

[3] Chaudhry, Q. and Castle, L. Food applications of nanotechnologies: an overview of opportunities and challenges for developing countries. *Trends in Food Science & Technology*, 22:595-603, 2011.

[4] Nair, R., Varghese, S. H., Nair, B. G., Maekawa, T., Yoshida, Y., and Sakthi Kumar, D. Nanoparticulate material delivery to plants. *Plant Science*, 179:154–16, 2010.

[5] Das, P., Barua, S., Sarkar, S., Chatterjee, S. K., Mukherjee, S., Goswami, L., Das, S., Bhattacharya, S., Karak, N., and Bhattacharya, S. S. Mechanism of Toxicity and Transformation of Silver Nanoparticles: Inclusive Assessment in Earthworm-Microbe-Soil-Plant System. *Geoderma*, 314:73–84, 2018.

[6] Das, P., Barua, S., Karak, N., Bhattacharyya, P., and Bhattacharya, S. S. Plant extract –mediated green silver nanoparticles: Efficacy as soil conditioner and plant growth promoter, *Journal of Hazardous Materials*, 346:62–72, 2018.

[7] Xie, B., Xu, Z., Guo, W., and Li, Q. Impact of natural organic matter on the physicochemical properties of aqueous C60 nanoparticles. *Environmental Science & Technology*, 42:2853–2859, 2008.

[8] Johnson, R. L., Johnson, G. O., Nurmi, J. T., and Tratnyek, P.G. Natural organic matter enhanced mobility of nano zerovalent iron. *Environmental Science & Technology*, 43:5455–5460, 2009.

[9] Sillen, W. M. A., Thijs, S., Abbamondi, G. R., Janssen, J., Weyens, N., White, J. C., and Vangronsveld, J. Effects of silver nanoparticles on soil microorganisms and maize biomass are linked in the rhizosphere. *Soil Biology and Biochemistry*, 91:14–22, 2015.

[10] Masrahi, A., VandeVoort, A. R., and Arai, Y., Effects of silver nanoparticle on soilnitrification processes. *Archives of Environmental Contamination and Toxicology*, 66:504-513, 2014.

[11] Diez-Ortiz, M., Lahive, E., George, S., Schure, A. T., Van Gestel, C. A. M., Jurkschat, K., Svendsen, C., and Spurgeon, D. Short-term soil bio-assays may not reveal the full toxicity potential for nanomaterials; bioavailability and toxicity of silver ions ($AgNO_3$) and silver nanoparticles to earthworm *Eisenia fetida* in long-term aged soils. *Environmental Pollution*, 203:191–198, 2015.

[12] Ben-Moshe, T., Frenk, S., Dror, I., Minz, D., and Berkowitz, B. Effects of metal oxide nanoparticles on soil properties. *Chemosphere*, 90:640–646, 2013.

[13] Tourinho, P. S., Gestel, C. A. M. V., Lofts, S., Svendsen, C., Soares, A. M. V. M., and Loureiro, S. Metal-based nanoparticles in soil: fate, behavior, and effects on soil invertebrates. *Environmental Toxicology and Chemistry*, 31:1679–1692, 2012.

[14] Rico, C., Hong, J., Morales, M. I., Zhao, L., Barrios, A. C,. Zhang, J. Y., Peralta-Videa, J. R., and Gardea-resdey, J. L. Effect of cerium oxide nanoparticles on rice: a study involving the antioxidant defense system and in vivo fluorescence imaging. *Environmental Science & Technology*, 47:5635–5642, 2013.

[15] Mueller, N. C. and Nowack, B. Exposure modeling of engineered nanoparticles in the environment. *Environmental Science & Technology*, 42:4447–4453, 2008.

[16] Geranio, L., Heuberger, M., and Nowack, B. The behaviour of silver nanoparticles during washing. *Environmental Science & Technology*, 43:8113-8118, 2009.

[17] Liu, J. Y., Sonshine, D. A., Shervani, S., and Hurt, R. H. Controlled release of biologically active silver from nanosilver surfaces. *ACS Nano*, 4:6903–6913, 2010.

[18] Lee, W. M., Kwak, J. I., and An, Y. J. Effect of silver nanoparticles in crop plants *Phaseolus radiatus* and *Sorghum bicolor*: media effect on phytotoxicity. *Chemosphere*, 86:491–499, 2012.

[19] Krishnaraj, C., Jagan, G., Ramachandran, R., Abirami, S. M., Mohan, N., and Kalaichelvan, P. T. Effect of biologically synthesized silver nanoparticles on *Bacopa monnieri L.* Wettst. plant growth metabolism. *Process Biochemistry*, 47:651–658, 2012.

[20] Musante, C. and White, J. C. Toxicity of silver and copper to *Cucurbita pepo*: differential effects of nano and bulk-size particles. *Environmental Toxicology*, 27 (9):510–517, 2012.

[21] Dimkpa, C.O., Mclean, J. E., Martineau, N., Britt, D.W., Haverkamp, R., and Anderson, A. J. Silver nanoparticles disrupt wheat (*Triticum aestivum L.*) growth in a sand matrix. *Environmental Science & Technology*, 47 (2):1082–1090, 2013.

[22] Shoults-Wilson, W., Reinsch, B., Tsyusko, O., Bertsch, P., Lowry, G., and Unrine, J. Role of particle size and soil type in toxicity of silver nanoparticles to earthworms. *Soil Science Society of America Journal*, 75:1–13, 2011.

[23] Shoults-Wilson, W. A., Reinsch, B. C., Tsyusko, O. V., Bertsch, P. M., Lowry, G.V., and Unrine, J. M. Effect of silver nanoparticle surface coating on bioaccumulation and reproductive toxicity in earthworms (*Eisenia fetida*). *Nanotoxicology*, 5 (3):432–444, 2011.

[24] Heckmann, L. H., Hovgaard, M. B., Sutherland, D. S., Autrup, H., Besenbacher, F., and ScottFordsmand, J. J. Limit-test toxicity screening of selected inorganic nanoparticles to the earthworm *Eisenia fetida*. *Ecotoxicology*, 20 (1):226–233, 2011.

[25] Barua, S., Konwarh, R., Mandal, M., Gopalakrishnan, R., Kumar, D., and Karak, N. Biomimetically prepared antibacterial, free radical scavenging poly (ethylene glycol) supported silver nanoparticles as *Aedes albopictus* larvicide. *Advanced Science, Engineering and Medicine*, 5:291–298, 2013

[26] Goswami, L., Patel, A. K., Dutta, G., Bhattacharyya, P., Gogoi, N., and Bhattacharya, S. S. Hazard remediation and recycling of tea industry and paper mill bottom ash through vermiconversion. *Chemosphere*, 92:708–713, 2013.

[27] Page, A. L., Miller, R. H., and Keeney, D. R. *Methods of Soil Analysis*. Part 2. Soil Science Society of America, Madison, Wisconsin, USA, 1982.

[28] Subbiah, B. V. and Asija, G. L. A Rapid Procedure for Estimation of Available Nitrogen in Soil. *Current Science*, 25 (8):259-260, 1956.

[29] Tabatabai, M. A. and Bremner, J. M. Assay of urease activity in soils. *Soil Science Society of America*, 41: 350–352, 1972.

[30] Tabatabai, M. A. and Bremner, J. M. Use of p-nitrophenol phosphate for the assay of soil phosphatase activity. *Soil Biology and Biochemistry*, 1:301–307, 1969.

[31] Brady, N. C. and Weil, R. R. *The nature and properties of soils.* Prentice-Hall Inc., New Jersey, USA, 13th edition, 2002.

[32] Sahariah, B., Goswami, L., Farooqui, I. U., Raul, P., Bhattacharyya, P., and Bhattacharya, S. S. Solubility, hydrogeochemical impact, and health assessment of toxic metals in municipal wastes of two differently populated cities. *Journal of Geochemical Exploration*, 157:100–10, 2015.

[33] Tandon, H. L. S. *Methods of analysis of soils, plants, waters and fertilizers*. Fertilizer Development and Consultation Organization, New Delhi, 1995.

[34] Reddy, T.Y., and Reddi, G. H. S. *Principles of Agronomy*. Kalyani Publishers, Noida, India, 1992.

[35] Anderson, J. M. and Boardman, N. K. Studies on the greening of dark-grown bean plants. *Australian Journal of Biological Sciences*, 17:93–101, 1964.

[36] Radin, J. W. Distribution and development of nitrate reductase activity in germinating cotton seedlings. *Plant Physiology*, 53:458–463, 1974.

[37] Bates, L. S., Waldren, R. P., and Teare, I. D. Rapid determination of free proline for water-stress studies. *Plant and Soil*, 39 (1):205–207, 1973.

[38] Mao, L., Zhang, L., Zhao, X., Liu, S., Werf, W. V. D., Zhang, S., and Spiertz, H. Crop growth, light utilization and yield of relay intercropped cotton as affected by plant density and a plant growth regulator. *Field Crops Research*, 155:67–76, 2014.

[39] Zhang, L., van der Werf, W., Bastiaans, L., Zhang, S., Li, B., and Spiertz, J. H. J., Light interception and utilization in relay strip intercrops of wheat and cotton. *Field Crops Research*, 107:29–42, 2008.

[40] Ignat, T., Schmilovitch, Z., Fefoldi, J., Bernstein, N., Steiner, B., Egozi, H., and Hoffman, A. Nonlinear methods for estimation of maturity stage, total chlorophyll, and carotenoid content in intact bell peppers. *Biosystems Engineering*, 114 (4):414–425, 2013.

[41] Vishniac, W. Methods for study of the Hill reaction. In Colowick, S. P., Kaplan, N.O. editors, *Methods Enzymol*, pages 342–343. Academic Press, New York, 1957.

[42] Chance, B. and Maehly, A. C. Assay of catalases and peroxidases. *Methods in Enzymology*, 2:764–775, 1955.

[43] Dhindsa, R. S., Plumb-Dhindsa, P., and Thorpe, T. A. Leaf Senescence: Correlated with Increased Levels of Membrane Permeability and Lipid

Peroxidation, and Decreased Levels of Superoxide Dismutase and Catalase. *Journal of Experimental Botany*, 32:93–101, 1981.

[44] Kwinta, J. and Cal, K. Effects of salinity stress on the activity of glutamine Synthetase and glutamate dehydrogenase in triticale seedlings. *Polish Journal of Environmental Studies*, 14 (1):125–130, 2005.

[45] Esposito, S., Guerriero, G., Vona, V., Di Martino Rigano, V., Carfagna, S., and Rigano, C. Glutamate synthase activities and protein changes in relation to nitrogen nutrition in barley: the dependence on different plastidic glucose-6P dehydrogenase isoforms. *Journal of Experimental Botany,* 56 (409):55–64, 2005.

[46] Parmer, D. and Schmidt, E. L. *Experimental Soil Microbiology*. Burgess Publication, Minneapolis, 1964.

[47] Vance, E. D., Brookes, P. C., and Jenkinson, D. S. An extraction method for measuring soil microbial biomass C. *Soil Biology and Biochemistry,* 19:703–707, 1987.

[48] Kim, D. J., Chung, S. G., Lee, S. H., and Choi, J. W. Relation of microbial biomass to counting units for *Pseudomonas aeruginosa*. *African Journal of Microbiology Research*, 6 (21):4620–4622, 2012.

[49] Lindsay, W. L. and Norvell, W. A. Development of a DTPA Soil Test for Zinc, Iron, Manganese, and Copper1. *Soil Science Society of America Journal*, 42:421–428, 1978, 2012.

[50] Tessier, A., Campbell, P. G. C., and Bisson, M. Sequential extraction procedure for the speciation of particulate trace metals. *Analytical Chemistry*, 51 (7):844–851, 1979.

[51] Jones, D. L. and Willett, V. B. Experimental evaluation of methods to quantify dissolved organic nitrogen (DON) and dissolved organic carbon (DOC) in soil. *Soil Biology and Biochemistry*, 38 (5):991–999, 2006.

[52] Das, P., Sarmah, K., Hussain, N., Pratihar, S., Das, S., Bhattacharyya, P., Patil, S. A., Kim, H. S., Iqbal, M., Khazie, A., and Bhattacharya, S. S. Novel synthesis of an iron oxalate capped iron oxide nanomaterial: a unique soil conditioner and slow release ecofriendly source of iron sustenance in plants. *RSC Advances*, 6 (105):103012–103025, 2016

[53] Berman, E. Toxic metals and their analysis. In: Thomas, D.C., editors, *International Topics in Science Series*. Hayden, London, 1980.

[54] Sharma, V. J. and Satyanarayan, S. Effect of selected heavy metals on the histopathology of different tissues of earthworm *Eudrillus eugeniae*. *Environmental Monitoring and Assessment*, 180:257–267, 2011.

[55] Aebi, H., Wyss, S. R., Scherz, B., and Skvaril, F. Heterogeneity of erythrocyte catalase II. Isolation and characterization of normal and variant erythrocyte catalase and their subunits. *European Journal of Biochemistry*, 48:137–145, 1974.

[56] Ellman, G. L. Tissue sulphydryl groups. *Archives of Biochemistry*, 82:70–77, 1959.

[57] Clair, D. K. S. and Chow, C. K. Glutathione peroxidase: activity and steadystate level of mRNA. In Neville, A. P., and Frank, J. K., editors, *Free Radicals: A Practical Approach*, pages 227–238. Oxford University Press, New York, 1996.

[58] Nimmo, I. A., Clapp, J. B., and Strange, R. C. A Comparison of the Glutathione S-Transferases of Trout and Rat Liver. *Comparative Biochemistry and Physiology B.,* 63:423–427, 1979.

[59] Lowry, O. H., Rosebrough, N. J., Farr, A. L., and Randall, R. J. Protein measurement with the folin phenol reagent. *Journal of Biological Chemistry*, 193:265–275, 1951.

[60] Habig, W. H., Pabst, M. J., and Jakoby, W. B. Glutathione S-transferases. The first enzymatic step in mercapturic acid formation. *Journal of Biological Chemistry*, 249 (22):7130-9, 1974.

[61] Panse, V. G. and Sukhatme, P. V. *Statistical Methods for Agricultural Workers*. Indian council of Agricultural research, New Delhi, 1954.

[62] Ahamed, M., Karns, M., Goodson, M., Rowe, J., Hussain, S. M., Schlager, J. J., and Hong, Y. DNA damage response to different surface chemistry of silver nanoparticles in mammalian cells. *Toxicology and Applied Pharmacology*, 233:404–410, 2008.

[63] Kawata, K., Osawa, M., and Okabe, S. In vitro toxicity of silver nanoparticles at noncytotoxic doses to HepG2 human hepatoma cells. *Environmental Science & Technology*, 43:6046–6051, 2009.

[64] El Badawy, A. M., Silva, R. G., Morris, B., Scheckel, K. G., Suidan, M. T., and Tolaymat, T. M. Surface charge-dependent toxicity of silver nanoparticles. *Environmental Science & Technology*, 45:283–287, 2011.

[65] Ma, X., Geiser-Lee, J., Deng, Y., and Kolmakov, A. Interactions between engineered nanoparticles (ENPs) and plants: phytotoxicity, uptake and accumulation, *Science of the Total Environment*, 408:3053–3061, 2010.

[66] Lombi, E., Donner, E., Taheri, S., Tavakkoli, E., Jamting, A. K., McClure, S., Naidu, R., Miller, B. W., Scheckel, K. G., and Vasilev, K. Transformation of four silver/silver chloride nanoparticles during anaerobic treatment of wastewater and post-processing of sewage sludge. *Environmental Pollution*, 176:193–197, 2013.

[67] Zhang, H. and Zhang, C. Transport of silver nanoparticles capped with different stabilizers in water saturated porous media. *Journal of Materials and Environmental Science*, 5:231–236, 2014.

[68] Brinkman, R. Clay transformations: aspects of equilibrium and kinetics. In Bolt, G. H., editors, *Soil Chemistry. B. Physicochemical Models. Developments in Soil Science 5B*, 2nd edition, pages 433–458. Elsevier, Amsterdam, 1982.

[69] Bandyopadhyay A., Banerjee P. P., Shaw P., Mondal M. K., Das V. K., Chowdhury P., Karak N., Bhattacharya S., Chattopadhyay A. Cytotoxic and Mutagenic Effects of Thuja occidentalis Mediated Silver Nanoparticles on Human Peripheral Blood Lymphocytes. *Materials Focus*, 6(3):290-6, 2017.

[70] Barua, S., Banerjee, P. P., Sadhu, A., Sengupta, A., Chatterjee, S., Sarkar, S., Barman, S., Chattpadhyay, A., Bhattahcharya, S., Mondal, N. C., and Karak, N. Silver nanoparticles as antibacterial and anticancer materials against human breast, cervical and oral cancer cells. *Journal of Nanoscience and Nanotechnology*, 17 (2):968-76, 2017.

[71] Chen, K. L. and Elimelech, M. Aggregation and deposition kinetics of fullerene (C60) nanoparticles. *Langmuir*, 22 (26):10994–11001, 2006.

[72] El Badawy, A. M., Luxton, T. P., Silva, R. G., Scheckel, K. G., Suidan, M. T., and Tolaymat, T.M. Impact of environmental conditions (pH, ionic strength, and electrolyte type) on the surface charge and aggregation of silver nanoparticles suspensions. *Environmental Science & Technology*, 44 (4):1260–1266, 2010.

[73] Mulvaney, P., Linnert, T., and Henglein, A. Surface chemistry of colloidal silver in aqueous solution: observations on chemisorption and reactivity. *The Journal of Physical Chemistry*, 95 (20):7843–7846, 1991.

[74] Brady, N. C. *The Nature and Property of Soils*. Macmillan Publishing Company, Inc., New York, N.Y, 8th edition, 1974.

[75] Basak, R. K. *Soil Testing and Recommendation*, Kalyani Publishers, Ludhiana, India, 2000.

[76] Chunjaturas, W., Ferguson, J. A., Rattanapichai, W., Sadowsky, M., and Sajjaphan, K. Shift of bacterial community structure in two Thai soil series affected by silver nanoparticles using ARISA. *World Journal of Microbiology and Biotechnology*, 30:2119–2124, 2014.

[77] Calder, A. J., Dimkpa, C. O., Mclean, J. E., Britt, D. W., Johnson, W., and Anderson, A. J. Soil components mitigate the antimicrobial effects of silver nanoparticles towards a beneficial soil bacterium, *Pseudomonas chlororaphis* O6. *Science of the Total Environment*, 429:215–222, 2012.

[78] Sondi, I., and Salopek-Sondi, B. Silver nanoparticles as antimicrobial agent: a case study on *E-coli* as a model for Gram-negative bacteria. *Journal of Colloid and Interface Science*, 275 (1):177–182, 2004.

[79] Lok, C. N., Ho, C. M., Chen, R., He, Q. Y., Yu, W.Y., Sun, H. Z, Tam, P. K. H., Chiu, J. F., and Che, C. M. Proteomic analysis of the mode of antibacterial action of silver nanoparticles. *Journal of Proteome Research*, 5(4):916–924, 2006.

[80] Prabhu, S. and Poulose, E. K. Silver nanoparticles: mechanism of antimicrobial action, synthesis, medical applications, and toxicity effects. *International Nano Letters*, 2 (1):32, 2012.

[81] Schlich, K. and Hund-Rinke, K. Influence of soil properties on the effect of silver nanomaterials on microbial activity in five soils. *Environmental Pollution*, 196:321–330, 2015.

[82] Klitzke, S., Metreveli, G., Peters, A., Schaumann, G. E., and Lang, F. The fate of silver nanoparticles in soil solution — sorption of solutes and aggregation. *Science of The Total Environment*, 535:54–60, 2015.

[83] Levard, C., Hotze, E. M., Lowry, G. V., and Brown, G. E. Environmental transformations of silver nanoparticles: impact on stability and toxicity. *Environmental Science & Technology*, 46 (13):6900–6914, 2012.

[84] Mitrano, D. M., Rimmele, E., Wichser, A., Erni, R., Height, M., and Nowack, B. Presence of nanoparticles in wash water from conventional silver and nano-silver textiles. *ACS Nano*, 8 (7):7208–7219, 2014.

[85] Kim, H. Corrosion process of silver in environments containing 0.1 ppm H_2S and 1.2 ppm NO_2. *Materials and Corrosion*, 54(4):243–250, 2003.

[86] Rosicka, D. and Sembera, J. Assessment of influence of magnetic forces on aggregation of zero-valent iron nanoparticles. *Nanoscale Research Letters*, 6 (1):10, 2011.

[87] Hayat, S., Hayat, Q., Alyemeni, M. N., Wani, A. S., Pichtel, J., and Ahemd, A. Role of proline under changing environments A review. *Plant Signaling & Behavior*, 7 (11):1456–1466, 2012.

[88] Doshi, R., Braida, W., Christodoulatos, C., Wazne, M., and O'Connor, G. Nano-aluminum: transport through sand columns and environmental effects on plants and soil communities. *Environmental Research*, 106 (3):296–303, 2008.

[89] Salama, H. M. H. Effects of silver nanoparticles in some crop plants, common bean (*Phaseolus vulgaris* L.) and corn (*Zea mays* L.). *International Journal of Biotechnology*, 3:190–197, 2012.

[90] Chen, Q. and Silflow, C. D. Ioslation and characterization of glutamine synthetase genes in *Chlamydomonas reinhardtii*. *Plant Physiology*, 112:987–996, 1996.

[91] Zuverza-Mena, N., Armendariz, R., Peralta-Videa, J. R., and Gardea-Torresdey, J. L. Effects of silver nanoparticles on radish sprouts: root growth reduction and modifications in the nutritional value. *Frontiers in Plant Science*, 7:90, 2016.

[92] Mcteer, J., Dean, A. P., White, K. N., and Pittman, J. K. Bioaccumulation of silver nanoparticles into Daphnia magna from a freshwater algal diet and the impact of phosphate availability. *Nanotoxicology*, 8 (3):305–316, 2014.

[93] Goswami, L., Sarkar, S., Mukherjee, S., Das, S., Barman, S., Raul, P., Bhattacharya, P., Mandal, N. C., Bhattacharya, S., and Bhattacharya, S. S. Vermicomposting of tea factory coal ash: metal accumulation and metallothionein response in *Eisenia fetida* (Savigny) and *Lampito mauritii* (Kinberg). *Bioresource Technology*, 166:96–102, 2014.

[94] Goswami, L., Pratihar, S., Dasgupta, S., Bhattacharyya, P., Mudoi, P., Bora, J., Bhattacharya, S. S., and Kim, K. H. Exploring metal detoxification and accumulation potential during vermicomposting of tea factory coal ash: sequential extraction and fluorescence probe analysis. *Scientific Reports*, 6: 30402, 2016.

[95] Das, S., Bora, J., Goswami, L., Bhattacharyya, P., Raul, P., Kumar, M., and Bhattacharya, S. S. Vermiremediation of water treatment plant sludge employing metaphire posthuma: a soil quality and metal solubility prediction approach. *Ecological Engineering*, 81:200–206, 2015.

[96] Nannoni, F., Protano, G., and Riccobono, F. Uptake and bioaccumulation of heavy elements by two earthworm species from a smelter contaminated area in northern Kosovo. *Soil Biology and Biochemistry*, 43 (12):2359–2367, 2011.